PAN-AFRICAN UNIVERSITY

INSTITUTE FOR WATER AND ENERGY SCIENCES

(Including CLIMATE CHANGE)

Master Dissertation

Submitted in partial fulfillment of the requirements for the Master degree in

ENERGY ENGINEERING

Presented by

Adel MOKRANE

MODELLING AND OPTIMIZATION OF STAND-ALONE PV-DIESEL HYBRID SYSTEM WITH HYDROGEN STORAGE: CASE OF ALGERIA

Defended on 04/08/2018 Before the Following Committee:

Chair	Francis Kemausuor	Dr.	KNUST, Ghana
Supervisor	Abdelatif ZERGA	Prof.	PAUWES, University of Tlemcen
Co-Supervisor	Ismail JUMARE	Ph.D.	PAUWES, University of Tlemcen
External Examiner	Venkatta Ramayya	Prof.	Jimma Institute of Technology
Internal Examiner	Abdelhalim Benmansour	Prof.	University of Tlemcen

I Adel MOKRANE, hereby declare that this thesis represents my personal work, realized to the best of my knowledge. I also declare that all information, material and results from other works presented here, have been fully cited and referenced in accordance with the academic rules and ethics.

September 17th, 2018.

I declare that this is from the student's own effort and that it has been submitted this day with my approval.

Signature 

September 17th, 2018

Prof. A. ZERGA
(Supervisor)

- To my God Almighty;
- To my lovely parents who did and still do everything to make my life better;
- To my brothers and sisters who encourage me every time;
- To my family individuals wherever they are;
- To all my friends wherever they are and
- To all persons who helped me to achieve this work.

I dedicate this work.

I would like to express my gratitude and appreciation to all those who gave me the possibility to complete this report. I take this opportunity to express my deepest and sincere gratitude to the African Union Commission for offering me the opportunity to be a part of the Pan African University Scholarships Programme. I would like also to express my gratitude to my supervisor Prof. A. ZERGA and co-supervisor I.A. JUMARE for their help, encouragement and support in successful completion of this project. I would like also to convey my thanks to the teaching and non teaching staff of the Pan African University of Water and Energy Sciences PAUWES for their invaluable help and support throughout the period of Master studies.

Renewable energy-based off-grid systems have been considerably growing in popularity in last few years. This kind of systems is referred to as decentralized electricity supply system that can provide power to meet the needs of individual households or small communities in rural populations, mainly in regions where the national grid is not economical to be extended due to the remoteness of the region. A hybrid system comprises one or several renewable energy technologies as primary energy sources and a conventional fossil fueled-based technology. Therefore, several system configurations can be used to meet the need of the power load.

The aim of this study is to find the optimum system configuration of a hybrid power system that can supply electricity to a rural community in south of Algeria. A rural village from the region of Adrar containing 15 households is selected with a daily electricity demand of 145.44 kWh and a day-time peak of 39.80 kW. In addition, the optimum hybrid power system can also produce hydrogen using the electrolysis of water process. The region of Adrar receives abundant solar radiation with an annual average of 6.26 kWh/m^2/day. Therefore, solar PV technology is the only used renewable energy generation system. In this study, HOMER Pro. (Hybrid Optimization Model for Electrical Renewables) computer modeling software was used to model the power system, its physical behavior and its life cycle cost. Sensitivity analysis with minimum renewable fraction and solar radiation variations was also done.

It has been found that the combination of PV system, three diesel generators, an electrolyzer and a hydrogen tank yields the optimum hybrid system type. The hybrid system configuration has been found to be 21.7kW-PV, three 10kW-diesel genset, 20.0kW-electrolyzer and 380kg-hydrogen tank. The PV system generates 51.24% of the total system energy generation. The remaining 48.76% is generated by the diesel generators resulting a total hours of operation of 7,044 hrs/yr. The total Net Present Cost NPC of this hybrid power system was found to equal $823.744 and electricity can be supplied at an approximate cost of energy LCOE of 0.60 $/kWh despite the variation in the annual average solar radiation in the range of 4.10-6.26 kWh/m^2/day. However, with an increase in the minimum renewable fraction to 40%, both the NPC and the LCOE would increase significantly. Moreover, the hydrogen gas that can be generated using electrolysis of water was found to be 353 kg/yr with an energy capacity of approximately 11,750 kWh.

Key words

Electricity, off-grid, optimum system configuration, hybrid power system, HOMER Pro, PV, diesel generator, electrolyzer, hydrogen, Net Present Cost, cost of energy.

Les systèmes hors réseau basés sur l'énergie renouvelable ont connu une popularité croissante au cours des dernières années. Ce type de système est appelé système décentralisé d'approvisionnement en électricité qui peut fournir de l'énergie pour répondre aux besoins des ménages individuels ou des petites communautés rurales, principalement dans les régions où le réseau national n'est pas rentable en raison de l'éloignement de la région. . Un système hybride comprend une ou plusieurs technologies d'énergie renouvelable en tant que sources d'énergie primaire et une technologie conventionnelle basée sur les combustibles fossiles. Par conséquent, plusieurs configurations de système peuvent être utilisées pour répondre aux besoins de la charge d'alimentation.

Le but de cette étude est de trouver la configuration optimale d'un système d'énergie hybride capable de fournir de l'électricité à une communauté rurale du sud de l'Algérie. Un village rural de la région d'Adrar contenant 15 ménages est sélectionné avec une demande journalière en électricité de 145,44 kWh et un pic de jour de 39,80 kW. En outre, le système de puissance hybride optimal peut également produire de l'hydrogène en utilisant l'électrolyse de l'eau. La région d'Adrar reçoit un rayonnement solaire abondant avec une moyenne annuelle de 6,26 kWh/m^2/jour. Par conséquent, la technologie solaire PV est le seul système de production d'énergie renouvelable utilisé. Dans cette étude, HOMER Pro. (Hybrid Optimization Model for Electrical Renewables) un logiciel de modélisation informatique a été utilisé pour modéliser le système d'alimentation, son comportement physique et son coût du cycle de vie. Une analyse de sensibilité avec une fraction renouvelable minimale et des variations du rayonnement solaire a également été effectuée.

Il a été constaté que la combinaison du système PV, de trois générateurs diesel, d'un électrolyseur et d'un réservoir d'hydrogène donne le type de système hybride optimal. La configuration du système hybride s'est révélée être de 21,7 kW-PV, trois groupes électrogènes diesel de 10 kW, un électrolyseur de 20 kW et un réservoir d'hydrogène de 380 kg. Le système PV génère 51,24% de la production d'énergie totale du système. Les 48,76% restants sont générés par les générateurs diesel, ce qui donne un total d'heures d'opération de 7 044 heures/an. Le coût total net CTN total de ce système d'alimentation hybride s'est avéré égal à 823 744$ et l'électricité peut être fournie à un coût énergétique CE approximatif de 0,60 $/kWh malgré la variation du rayonnement solaire annuel moyen de l'ordre de 4,10 à 6,26 kWh/m^2/jour. Cependant, avec une augmentation de la fraction renouvelable minimale à 40%, le CTN et le CE augmenteraient considérablement. De plus, l'hydrogène qui peut être généré par électrolyse de l'eau est de 353 kg/an avec une capacité énergétique d'environ 11 750 kWh.

Mots Clés

Électricité, hors réseau, configuration optimale du système, système d'alimentation hybride, HOMER Pro, PV, générateur diesel, électrolyseur, hydrogène, coût total net, coût énergétique .

Table of Contents

AC	Alternating Current
APRUE	Agency for the Promotion and Rationalization of the Use of Energy
BWh	Bust Waist Hip
CDER	Renewable Energies Development Center
CRF	Capital Recovery Factor
DLR	Deutsches Zentrum für Luft- und Raumfahrt (German Space Center)
DC	Direct Current
EF	Emission Factor
FF	Fill Factor
GDP	Gross Domestic Product
GHG	Greenhouse Gases
GW	Giga Watt
HDKR	Hay, Davies, Klucher, Reindl
HHV	High Heating Value
HOMER	Hybrid Optimization Model for Electric Renewables
HPS	Hybrid Power System
HRES	Hybrid Renewable Energy Systems
IEA	International Energy Agency
ICE	Internal Combustion Engine
IG	Isolated Grids
kJ	Kilo Joule
km	Kilo Meter
Ktoe	Kilo Tonnes Of Oil Equivalent
kV	Kilo Volt
kW	Kilo Watt
kWh	Kilo Watt hour

LCOE	Levelized Cost of Energy
LPG	Liquefied Petroleum Gas
LVH	Low Heating Value
MEM	Ministry of Energy and Mines
MPPT	Maximum Power Point Tracking
Mtoe	Million Tonnes Of Oil Equivalent
MW	Mega Watt
NEAL	New Energy Algeria
Nm^3	Normal Cubic Meter
NPC	Net Present Cost
NPV	Net Present Value
NREL	National Renewable Energy Laboratory
PEM	Proton Exchange Membrane
P&O	Perturb and Observe
PV	Photovoltaic
RCREEE	Regional Center of Renewable Energy and Energy Efficiency
REEEP	Renewable Energy and Energy Efficiency Partnership
RES	Renewable Energy Sources
SFF	Sinking Fund Factor
SOE	Solid Oxide Electrolyser
STC	Standard Conditions
TPES	Total Primary Energy Supply
TWh	Tera Watt Hour
USD	United States Dollar

1.1. Background to the study

According to the Energy Access Outlook 2017 [1], about 1.1 billion people (14% of the global population) did not have access to electricity. A considerable portion of this population suffers from a supply that is of poor quality. 84% of populations without access to electricity live in rural regions and 95% of them are in Sub-Saharan Africa and Developing Asia. The report defines the energy access as the "golden thread" that makes up the economic growth, the human development and the environmental sustainability. One of the major global challenges that face the world nowadays is the challenge of providing affordable, efficient and cost-effective electricity. Despite grid extension has been always preferred for rural electrification [2], but the unavailability of finance and the infeasibility of extending the utility grid to geographically remote and dispersed populated regions are known as the main problems. Off-grid solutions are suitable in such cases.

Access to electricity is a prerequisite for human development as well as wealthy economic development and job creation. Africa has vital needs to focus on "access to energy" through the expansion of both electricity production capacity (on-grid and off-grid) and the supply of other energy forms [3]. Africa is abundant with substantial renewable energy sources: biomass, geothermal energy, wind energy, solar energy and large scale and small scale hydro power. Due to the restrict policies and unviable finance for investment, these renewable energy resources have not been exploited [4]. The African continent is endowed with huge energy resources both conventional and renewable. Despite the huge energy resources and potential endowment that exceed the current needs Africa, most of its population and economic sectors do not have access to energy mainly electricity: about two thirds of the continent's population does not have access to electricity. Furthermore, wide parts of the rural Africa are not electrified and power generation capacity is not able to satisfy the rapidly growing demand in the urban and pre-urban areas. However, countries in the Northern Africa have higher levels of electricity access but also ought to significantly change their energy systems to meet the future need with low to zero carbon emission transition [3].

Algeria is the largest country in Africa, about 80% of its area is a desert or Sahara. Its geographic location has many advantages for massive use of most of renewable energy sources (solar and wind). The crucial economical changes, which have been experienced these last years on both levels national and international, have led Algeria to get on structural amendments that aim to adapt progressively to these changes especially in the energy sector (fossil and renewable energies) [5]. Algeria has gone through reforms in the sustainable development context by promoting the use of renewable energy technologies for power generation. Among the renewable energy technologies, the photovoltaic or PV energy has been widely used in Algeria for low power application.

Photovoltaic (PV) generators, which convert the solar radiation directly into electricity, have a set of major advantages like being silent, inexhaustible, pollution free and size-independent electric conversion efficiency [6]. PV generators are substituting electricity produced by fossil fuels thanks to their harmless environmental effect. However, PV power generation suffers from large variations in its output power due to weather conditions intermittency. Therefore, the nature fluctuation of the solar radiation imposes the use of purely PV power generators for off-grid applications in large scale. Consequently, these kinds of applications are very expensive. In order to solve this problem, one way is to combine the PV plant with other sources of power such as diesel, battery back-up or fuel cell [7]. The diesel generator can provide a continuous 24-hours power generation but noise and exhaust gases pollution are considered two major drawbacks of such system. In addition, in order to mitigate the

effects of climate change and reduce the toxic pollutants, fuel cells powered by hydrogen provide very efficient energy conversion.

Although hydrogen is not a primary energy source like oil and gas, it has the ability to turn into one of the main energy carriers in the near future. In stand-alone hybrid power systems [8], PV systems and electrolysers can be combined with hydrogen storage and a diesel generator. Unlike batteries, which are considered as flexible and fast response back up storage but very costly, the diesel genset can generate electricity for limitless time to support the PV generator. Hence, combining all of the PV generator, the diesel generator and the hydrogen storage will assure a continuous supply of high quality power generation and an effective storage of energy in form of gas. The combination of the listed power sources is referred to as hybrid power system HPS.

Hybrid power systems are commonly used for both on-grid and off-grid power generation applications indicated by the rising number of publications and a growing interest by governments and organizations to implement these projects.

1.2. Problem Statement

Algeria relies on fossil fuels (natural gas) to satisfy the national demand of electricity. Fossil fuels account 99% of the electricity generation with the remainder generated by hydropower [9]. Algeria has realized the importance of its energy mix diversification although the heavy dependence on fossil fuels. The country has ambitious renewable energy programs for promoting the use of renewable energy resources for power generation. One example of these programs is the "Renewable Energy and Energy Efficiency Program" that focuses on developing and expanding the use of renewable resources to generate 22,000 MW between 2011 and 2030 [10].

According to the Renewable Energy and Energy Efficiency Partnership (REEEP), the average annual solar radiation ranges between 2,000 and 3,900 hours and an average solar energy of 6.57 $kWh/m^2/day$. The German Space Center (DLR) assessed the potential power of 169,440 TWh/year and 13.9 TWh/year [11]. Therefore, it is thought that solar has the greatest potential in Algeria. Unfortunately, this potential is not exploited. On the other hand, few solar energy projects were realized in the past few years. One example is the mini grid solar power plant, which has the capacity of 28 kW, was installed on the rooftop of a reaserch division in Wilaya of Adrar [10].

In order to increase the exploitation of the solar energy potential in Algeria while mitigating the climate changes effect and reducing the toxic pollutants, the installation of hybrid systems represents an excellent option especially in remote areas where the national grid is not available. Coupling a PV generator with a diesel genset is one of the best combinations for night and day electricity generation. In most cases, PV systems electricity generation may lead to an excess. This excess can be stored in different forms using several technological storage systems. Hydrogen gas is one of these forms. Electricity can be converted to hydrogen gas by the use of an electrolyser and stored in hydrogen tank.

1.3. Aim and Objectives

It has been proven that PV power generation source should be coupled with other power sources, mostly used in off-grid or stand-alone system mode. Off-grid power systems are popular and very suitable for remote areas. The focus of this project is on modeling and designing a PV/diesel hybrid power system associated with hydrogen storage to fulfill the electricity demand of fifteen (15) households in Boukazine, Adrar in affordable, reliable and sustainable way with cost-effective solution.
To achieve the main goal mentioned above, the accomplishment of the following objectives should be required:

1- Estimate the energy demand of these households and investigate the resource assessment in the region;
2- Model the different physical components that build up the hybrid power systems;
3- Simulate and optimize the hybrid system with sensitivity analysis;
4- Assess the sustainability of the hybrid system economically and environmentally;

1.4. Methodology

In order to design a hybrid power system for 15 households' facility, the first thing to be done is to collect the different meteorological data such as solar radiation and temperature data, and also decide on the load profile of this facility; the energy consumption of the household should be satisfied. However, in case of a household which is not electrified, the estimation of the energy demand can be done through extensive research of previous works and literature survey. The next step is to use the data collected and the household load profile to design the hybrid power system. This latter consists of solar PV panels which are used to produce electricity using the energy of the sun to meet the load demand of the 15 households, a diesel generator as a back-up power system, an electrolyser that uses the excess of energy from the PV system to produce hydrogen gas using the electrolysis process and hydrogen storage to store the gas produces. To simulate the system, each subsystem is modeled independently at the beginning before integrating all the subsystems into a single system-level simulation. The process of simulation is carried out in the Hybrid Optimization Model for Electric Renewables HOMER Pro. resulting in a techno-economically optimized system. HOMER performs multiple optimizations under a range of inputs assumptions to test the effect of uncertainties in the model input such as solar radiation and minimum renewable fraction; thus the sensitivity analysis is conducted at the end.

1.5. Justification

A hybrid power system, which uses solar energy in combination with diesel generator, a hydrogen-based energy storage system, will be a reliable solution for providing power in remote areas of Algeria. However, this research will bring benefit for all remote areas around the world, optimistically.

This work is of supreme importance to the country of Algeria; owing to the fact that it will reduce the heavy reliance on the conventional energy sources (mainly gas); and will support to boost energy supply at low costs and in an environmentally friendly way.

Finally, this research work is of central importance since it studies a way to generate hydrogen. This study gives a very efficient, reliable and clean manner for producing and storing hydrogen. The exploitation of such energy carrier will help Algeria to diversify its energy mix, improve its energy efficiency and ensure its energy security.

1.6. Scope and Limitations

All the features of the hybrid power systems' complexity cannot be studied in a single research; therefore this Master thesis is limiting its scope to a defined target case study: Modeling and Optimization of Off-grid PV-Diesel Hybrid System with Hydrogen Storage using HOMER. Although HOMER could be time consuming and, but it leads onerous to very detailed results for analysis and evaluation.

Photovoltaic power has been selected over wind power because solar energy is abundant in the location where the case study is considered. In Addition to this, solar is better suited for this specific case study as well as most of the previous research about renewable hybrid power systems has coped with wind power. Moreover, a lot of recent projects and investments are conducted in the solar energy domain.

Diesel generators are the most familiar conventional energy generator used in remote sites. Since the system is designed for 15 households, the application of three genset is considered in this thesis.

Hydrogen is renewable, emission-free and non-toxic fuel that can be used for power generation. However, it is not the absolute preferable, cheap and clean energy for most countries. Therefore, the deployment of this source of energy under the African context may not feasible.

2.1. Introduction

Algeria is the largest country in Africa. It is one of the biggest producers and exporters of oil and gas in Africa. Its hydrocarbon industry is the key of its economy. Fossil fuels (mainly gas) are the sources of the Algeria's electricity generation. The global energy consumption has been increasing rapidly during the last decades where the household sector represents more than one third of the energy consumption. On the other hand, Algeria is endowed with several renewable energy resources especially solar. The deployment of such resources of energy will decrease the heavyweight dependence on fossil fuels for power production and also diversify the energy mix of the country. Therefore, the government of Algeria has committed to renewable energies through the launch of an ambitious program for the development such energies.

This chapter focuses in its first part on reviewing the Algeria's profile, its energy situation and the renewable energy resources available in the country. The second part is dedicated to the technical aspects of this project.

2.2. Algeria Country Overview

Algeria is situated in the northwest of Africa bordered by the Mediterranean Sea to the north, Mali Chad to the south, Tunisia and Libya to the east and Morocco and Western Sahara to the west. Spanning nearly 2.4 million km^2 with a population around 40.9 million (in July 2017), Algeria is the 10th largest country worldwide and the largest in the continent. The Sahara occupies over two million km2, or 84% of the country's area [12]. Its capital, the most populous city, is Algiers located in the north of the country. Administratively, Algeria is divided into 48 provinces called Wilayas.

The geographic location of Algeria is denoted as a key position to play a crucial strategic role for implementing the renewable energy technologies in north Africa, as well as affording enough energy to satisfy its own need and even exporting this energy to other neighboring countries and Europe [5].

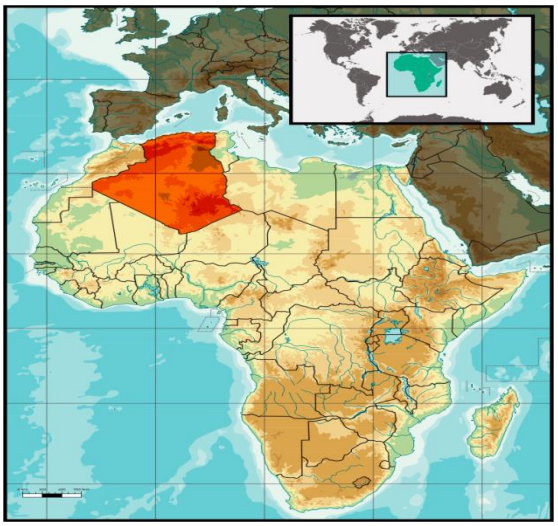

Source: [98]

Figure 2.1: The location of Algeria.

Figure 2.2: The Algeria's map.

2.3. Energy Situation in Algeria

Since its independence in 1962, Algeria had gone for the development of the energy sector, as part of a national policy for developing the electric and gas infrastructures. This policy's aim is to make access to electricity and natural gas for the population as a top priority for improving the quality of life of the citizen and the economic situation of the country. The national charter of 1976 announced the will of generalizing the electrification of households throughout the national territory [13].

In recent years, energy demand in Algeria has experienced a significant evolution, reaching important peaks of consumption. This sharp increase in demand is a direct result of improving the consumers' quality of life and changing their habits, as well as the development happening in the economic, transport and industrial sectors.

2.3.1. Energy-Related Economy

The economy of Algeria shows a heavy reliance on hydrocarbon sector. According to the Regional Center of Renewable Energy and Energy Efficiency RCREEE, the economy has revenues that account around 30% of the country's Gross Domestic Product GDP. This latter has gone, according to the World Bank, from 214 billion US Dollars in 2014 to 156.08 billion US dollars making the GDP value of Algeria to stand for 0.25 % of the world economy. The drop of the GDP value can be explained by the steep decline in oil prices in summer 2014, reaching an average of 40.68 US dollars per barrel in 2016.
Figure 2.3 depicts the comparison between the imports and the exports of Algeria. It shows clearly the dominance of hydrocarbons in the Algerian exportations since the country has a significant amounts of these resources.

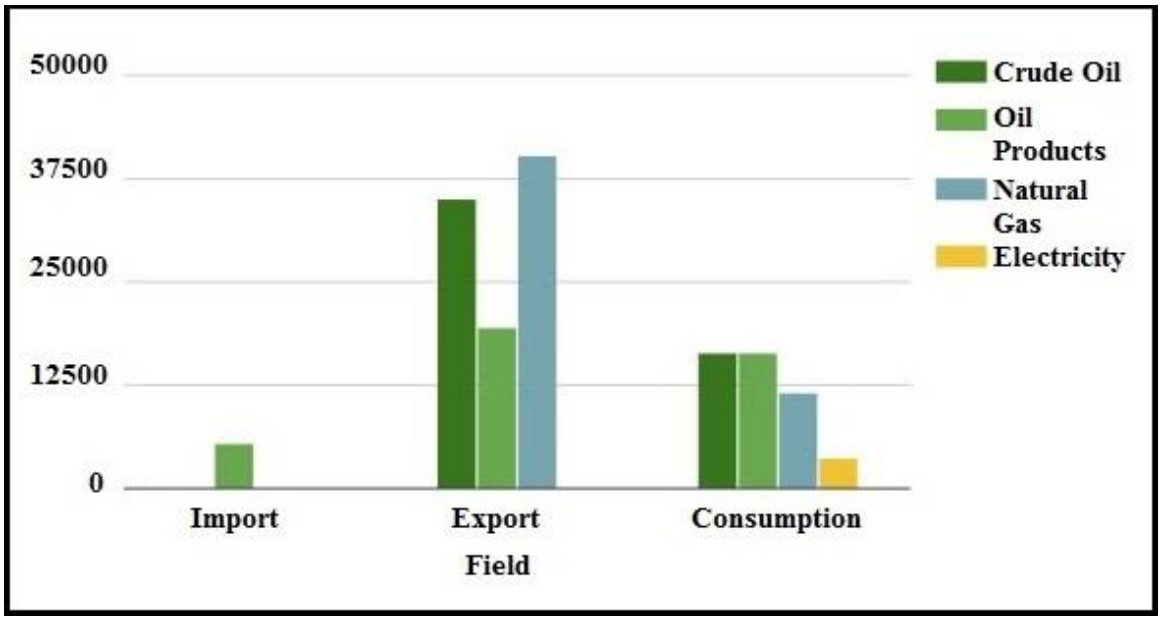

Source: [14]

Figure 2.3: Imports and exports comparison and local consumption in Algeria in ktoe.

2.3.2. Total Primary Energy Supply in Algeria

The Total Primary Energy Supply or TPES comprises the imported energy, the exported energy that is subtracted off and the energy produced from natural resources of a given country. TPES represents the total amount of energy to satisfy the basic utility needs of that country. In 2015 [14], the TPES in Algeria reached 54.01 Mtoe where crude oil and natural gas represent largely the biggest portion of this total reaching a percentage of 99.8. However, renewable energies share was almost nonexistent.

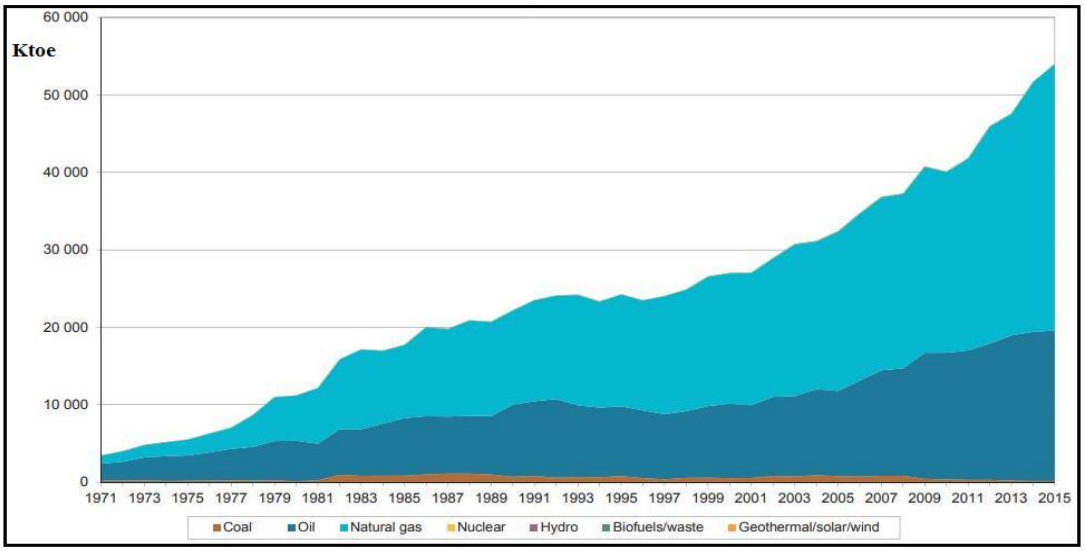

Source: [14]

Figure 2.4: The Total Primary Energy Supply in Algeria (1971-2015).

2.3.3. Primary Energy Production

Commercial production of primary energy in Algeria returned to growing trend in 2016, ending the downward trend observed over several years. It considerably increased (+ 7.3%) compared to 2015 achievements, reaching 166.2 Mtoe. This growth was led by natural gas, followed by crude oil, which offset the drop in condensate and Liquefied Petroleum Gas or LPG, as shown in the table below [15]:

Table 1: Algeria primary energy production in ktoe.

Product	2015	2016	Evolution	
			Quantity	%
Natural Gas	79,931	89,731	9,800	+12.3
Crude oil	54,250	56,193	1,943	+3.6
Condensate	10,885	10,449	-436	-4.0
GPL	9,753	9,726	-27	-0.3
Electricity	53	80	+27	+51.1
Solid Combustible: wood	6	6	-0.19	-3.1
Total	154,878	166,184	+11,306	+7.3

Source: [15].

2.3.4. Final Energy Consumption

The final energy consumption in Algeria increased from 42.5 Mtoe in 2015 to 42.9 Mtoe in 2016, reflecting a slight increase of 1.0% [15]. This increase can be explained by the reduction of 2.8% in consumption of petroleum products to 15.5 Mtoe, the increase of 3.3% in natural gas demand to reach 12.7 Mtoe, the growth in electricity consumption by 4.3% to reach 12.5 Mtoe due to the increase in customer demand for low voltage, and the slight decline in final LPG consumption by -0.8% to attain 2.2 Mtoe.

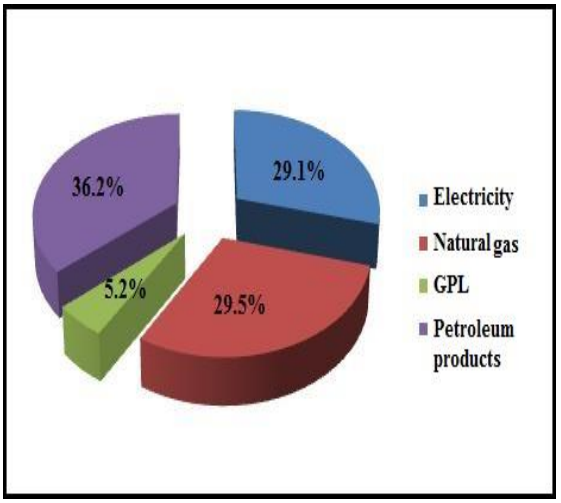

Source: [15].

Figure 2.5: Final energy consumption by product.

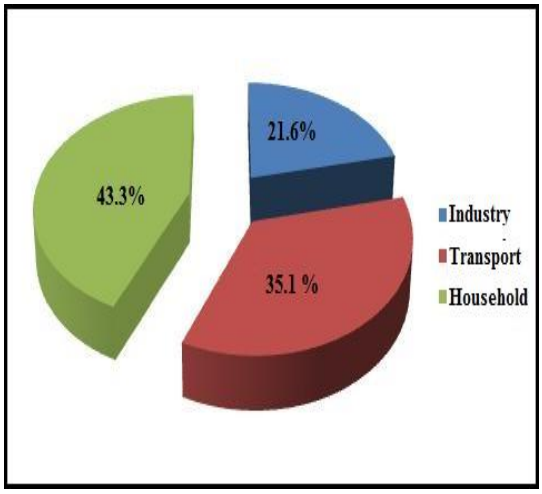

Figure 2.6: Final energy consumption by sector.

2.3.5. Electricity Situation in Algeria

More than 99% of the electricity is generated from fossil fuels (mainly natural gas) in Algeria; the rest is produced from hydropower [9] (Figure 2.7). Sonelgaz, the national company established in1969, held the monopoly on the production, transport, the distribution of electricity as well as the transport and distribution of gas. Many efforts have been made by this company and its subsidiaries to reinforce the production capacities [13], which have experienced in recent years a significant evolution of installed power generation. The installed capacity reached 17.2 GW in 2015. The total length of the national electricity transmission network, all levels of voltages combined (60 to 400 kV) was 27,274 km at the end of 2015. Knowing that, the Algerian electricity transmission network is connected to two other networks: Moroccan and Tunisian via several power lines; the most recent of which are 400 kV realized in 2014. However, the total length of the national distribution network of average and low voltage electricity was 303,463 km.

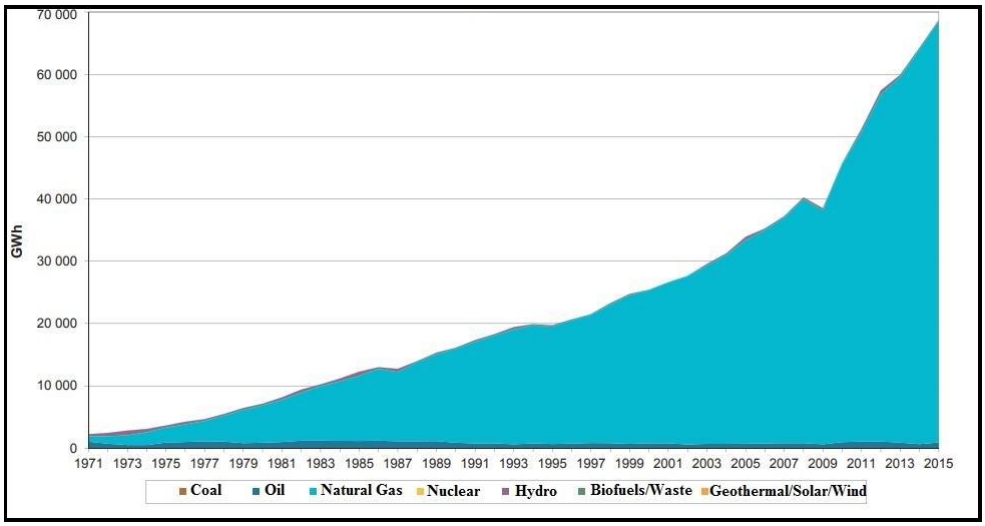

Source: [14].

Figure 2.7: Electricity generation by fuel in Algeria (1971-2015).

Figure 2.8 shows the different technologies used for electricity generation and their shares. It can be seen easily that the production is widely done using gas turbines followed by combined cycles.

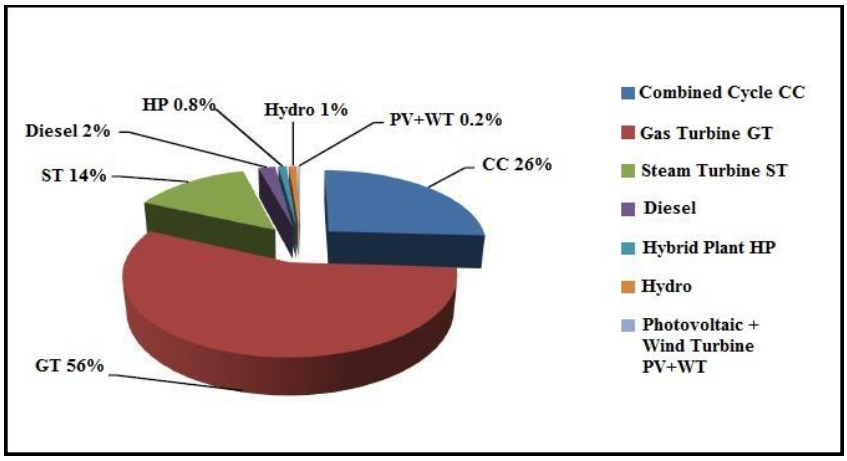

Source: [15].

Figure 2.8: Electricity installed by technology.

2.4. Renewable Energy in Algeria

As mentioned before, the production of energy in Algeria is widely dependent on fossil fuels which are considered as non-renewable energy sources. The heavy utilization of such energy sources may lead to some challenges such as their depletion in rapid rate and the deterioration of the environment by increasing the amount of the Greenhouse Gases (GHG) in the air. Therefore, renewable energy sources offer the perfect solution to alleviate these challenges. The renewable energy projects are means to manage the other energy sources reserves and also a key for sustainable development in the country.

The Algerian government has stated new policies to encourage the production and the use of renewable energies. Because of the high solar radiation in Algeria, solar energy has been given particular attention (See Table 2). The size of the Algerian Sahara could capture enough solar energy to satisfy the need of the world's electricity [16]. Algeria has a huge solar energy potential; the

International Energy Agency estimates the production of electricity to be 162 TWh in the country's land [17]. This source of energy is a blessing for Algeria which considers it as an opportunity for the social and economic development by establishing wealthy and job-creating industries. Despite wind, biomass, geothermal and hydropower energies potentials are comparatively small, this does not meant exclude the launch of several wind projects and the realization of biomass and geothermal experimental projects [18].

Table 2: Energy resources of different regions of Algeria.

Regions	Coastal	Hauts Plateaux	Sahara
Surface (%)	4	10	86
Average Sunshine (Hours/year)	2650	3000	3500
Average Energy Received (kWh/m^2/year)	1700	1900	2650
Average recoverable wind energy (TWh/year)	1	4.5	31.5
Mineable quantity of groundwater (m^3/year)	-	0.12 billion	0.88 billion

Source: [17].

Nowadays, the development of adequate energy infrastructures, which can attain higher economic development, is a necessity in Algeria. This would let its population access to quality and adequate energy supply [16]. In this context, important goals are targeted at significant increasing and promoting the use of renewable energies for power production. Therefore, Algeria has invented a green momentum by creating an ambitious program to develop the contribution of renewable energies in the energy mix and promote energy efficiency. The renewable energy development program was adopted by the Algerian government in 2011 and it was updated in February 2015. This program aim is to develop mainly large-scale photovoltaic and wind projects over 15 years (2015-2020-2030) (See Table 3) [19]. The program focuses on the generation of 22,000 MW of which 12,000 MW would meet the national domestic need and 10,000 MW destined for export to Europe. The share of renewable energy sources in primary energy supply would achieve 40% (See Figure 2.9).

Table 3: Algerian program of renewable energy (2015-2030).

Technology	First Phase [2015-2020] (MW)	Second Phase [2021-2030] (MW)	Total (MW)
Photovoltaic	3,000	10,575	13,575
Wind	1,010	4,000	5,010
CSP	-	2,000	2,000
Cogeneration	150	250	400
Biomass	360	640	1,000
Geothermal	5	10	15
Total	4,525	17,475	22,000

Source: [11]

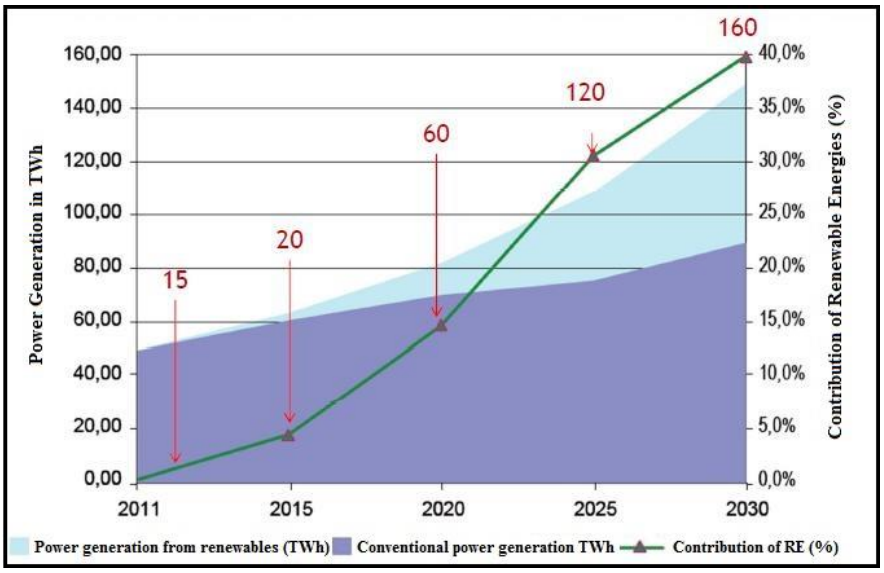

Source: [11].

Figure 2.9: Contribution of renewable energies in power generation in TWh.

2.4.1. Photovoltaic Solar Energy in Algeria

Photovoltaic is an elegant process of generating power on site; it is a technology of converting sunlight energy into electricity using photovoltaic cells. This kind of energy does not have a concern for fuel supply or environmental impact. Electricity is produced silently with no pollution, no depletion of resources and with low cost maintenance. One of the main advantages of such energy is that it is suitable for decentralized or stand-alone applications especially for providing power for isolated people living in remote areas to satisfy their basic energy needs: light, water pumping, refrigeration, television, radio [20].

Algeria endows one of the largest solar potentials in the world (See Figure 2.10). Due to the abundant sunshine throughout the year, the implementation of photovoltaic solar energy projects is the best solution for electricity production.

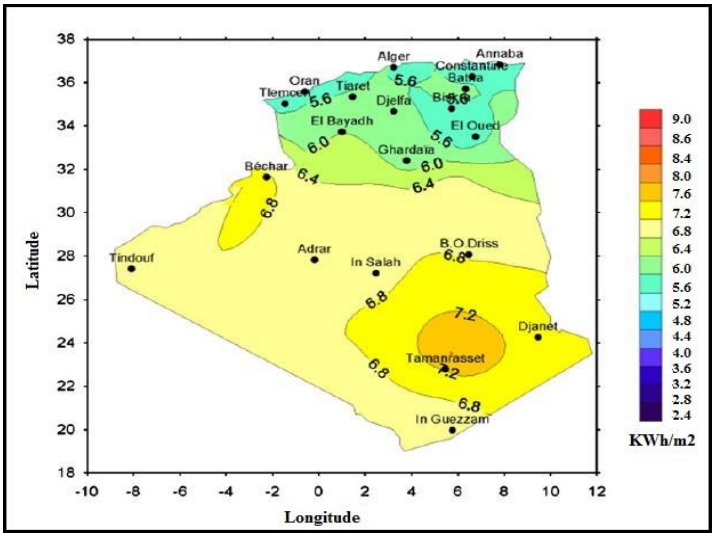

Source: [16].

Figure 2.10: The daily global irradiation received on inclined plane in summer in Algeria.

The national renewable energy program adopted involves the implementation of 27 photovoltaic power plants which will be connected to the Interconnected Northern Network. The most important plant (48 MW) will be installed in the Wilaya of Djelfa, followed by that of M'sila (44 MW). The other plants will be located in Ouargla, Tolga, El-Bayadh, Mghair, Ain Beida, Naama and Saida [21]. However, several photovoltaic power plants have been already installed [22]:

- ✓ Ain El Melh photovoltaic power plant: realized in 2014 with capacity of 20 MW.
- ✓ Dhaya (Sidi Bel Abbas) power plant: achieved in 2014 with capacity of 15 MW.
- ✓ Ras El Oued (Bordj Bou Arreridj) photovoltaic power plant: installed by a Chinese company with capacity of 20 MW in 2014.
- ✓ Ghardaia experimental photovoltaic power plant with capacity of 1.1 MW.

In addition to this program, Algeria has adopted another ambition program called rural electrification program. The program targets around 906 households in eighteen (18) different villages in the four southern provinces: Illizi, Adrar, Tindouf and Tamenrasset. These villages were selected according to their geographical locations; they are characterized by their remoteness from any communication network [16]. The rural electrification program is financed by the Special Funds for the Development of the South Area. It consists of providing photovoltaic kits for each house. In the second phase of the program, sixteen (16) other villages in Tamenrasset, El Oued, M'sila, Ghardaia and Illizi will be concerned with electrification.

In order to promote the use of photovoltaic solar energy as a means for electricity production, Algeria relies on Feed-In Tariffs which are brought in the new renewable energy law. This will help spreading out the deployment of this kind of energy [20].

2.4.2. Solar Hydrogen Energy in Algeria

Hydrogen is another kind of clean energy which is a crucial material in the chemical industry. Hydrogen is not considered as an energy source. It is not even a primary energy but a secondary form of energy that has to be transformed to other kind of energy like electricity. It has been proven that hydrogen is safer than other flammable fuels such as natural gas or gasoline. The importance of such fuel is in its production; it can be generated using one of the abundant energy which is solar.
Algerian Sahara is a strategic site for solar hydrogen production due to its endowment with huge solar potential, the existence of sufficient water and space for the installation of solar hydrogen systems [23]. Such systems could not only expand the existence of fossil fuels in Algeria and alleviate pollution, but they would provide the country with a clean, efficient and permanent energy and enhance its Gross Domestic Product by exporting such energy to other countries [16]. A technological cooperation in developing the solar hydrogen economy was agreed by the International Energy Agency and Algeria [24]. In addition to this cooperation, an Algerian Hydrogen Association was founded in June 2005 following the Algiers Declaration on hydrogen from renewable sources. The New Energy Algeria NEAL, which is a national company created by Sonatrach and Sonelgaz, has set up goals on increasing energy generation and solar hydrogen production. Several works have been launched in the field of using solar energy for hydrogen production for fuel cells in the Renewable Energies Development Center CDER. However, these initiations are in their primary stages and have not yet yield in electricity generation [16]. Today, hydrogen in Algeria comes from steam reforming of natural gas. Industrial Gas (GI) of Algeria has achieved 300 m^3/h production of hydrogen.

2.5. Hybrid Power Systems

In remote areas, where the electric power grid cannot be accessed physically or economically, the demand for electricity is provided by isolated diesel generators. However, these diesel generators have higher operating and maintenance costs. In these circumstances, the diesel generator can be combined with renewable energy sources forming a hybrid power system. It has been proven that hybrid power systems can provide reliable and efficient electricity while reducing the total lifecycle cost of the stand-alone power systems [25]. Hybrid power systems HPS or hybrid renewable energy systems HRES consist of two or more energy sources, energy storage and a distribution system. The aim of the hybrid system is to convert all of the energy sources into one form (mainly electricity). It can combine renewable energy sources RES with fossil fuel powered diesel/petrol generator to generate electricity. It may or may not be tied to the electric power grid. The use of renewable energy sources in hybrid power systems decreases the dependence on fossil fuels and allows a cleaner production of electricity [26]. Generally, a hybrid power system comprises: RES, Alternating Current (AC) diesel generators, an AC distribution system, a Direct Current (DC) distribution system, energy storage, power convertors loads and an optional Energy Management Unit [27]. A schematic diagram of a hybrid power system is shown in the Figure 2. 11.

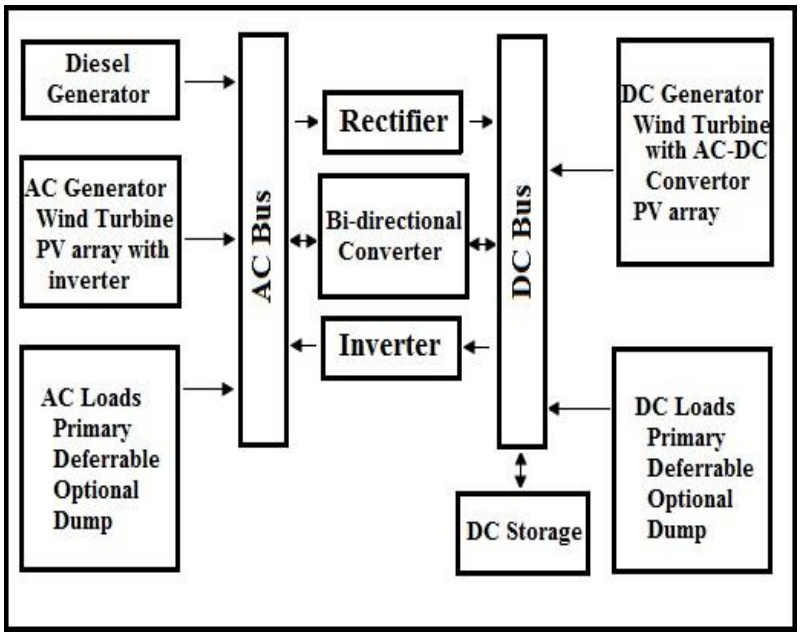

Figure 2.11: Hybrid Power System schematic diagram [27].

2.5.1. Classification of Hybrid Power Systems

Hybrid power systems can be designed according to different classifications in order to harness the available renewable and non-renewable energy sources and to meet the need of the required power load. Hence, hybrid power systems can be classified according to [28]:

a. The presence of conventional energy sources

Hybrid systems that utilize conventional sources for power generation are very powerful and responsible. On the other hand, hybrid systems without conventional sources are likely irresponsible and comparatively low-power. However, if such systems were designed properly with energy storage, they would be able to provide sustainable energy.

b. The number of energy sources

Hybrid power systems are characterized by their sustainability, efficiency and complexity. These characteristics have a relationship with the number of the energy sources used in the system. The larger the number of energy sources leads to construct a complex system, but at the same time makes it more sustainable and energy efficient.

c. The type of energy produced

The produced energy by hybrid systems can be in different types depending on the renewable energy technology used. Wind turbine produces mechanical energy that can be converted to electrical one or consumed directly such as pumping water. PV panels generate electrical energy that can be stored or consumed. It can be also distributed or converted to another form. Solar thermal collectors can be used to produce thermal energy as in systems that use geothermal energy. Fuel production also is a type of energy generated using hybrid systems such as hydrogen production by means of electrolysis.

d. The energy storage

Hybrid power systems are not profitable without storage since the needs do not match with the energy availability. Hence, on a hand energy can be available but remains unused, on the other hand, the load can be left unpowered. In hybrid systems with storage, the surplus produced electricity can be stored and used when needed. Consequently, not only the problem of intermittency of RES is solved, but the hybrid system becomes more effective. Many storage systems are known; they can be electrical (batteries), mechanical (flywheel), thermal (boilers), potential (dam) and fuel conversion (hydrogen).

e. The rated power

Hybrid power systems are used to provide electricity depending on the utility needed to be powered. Meteorological, telecommunication and different stations are supplied with low power (less than 1 kW). Remote houses can be supplied with middle power (more than 1 kW and less than 10 kW). Isles, towns and villages which are far from the power electric grid, however, use high power (more than 10 kW).

f. The connection to the power grid

Stand-alone power systems are mainly used to satisfy the need of remote sites for electricity. They produce electricity independently of the power electric grid. As a result, storage systems are mostly needed to store electricity during off-peak demand times. In contrast, grid connected or grid-tied systems are independent power systems that are connected to an electricity transmission and distribution systems. This kind of systems must be synchronized with the distribution ones. When the hybrid system produces surplus electricity, this latter will fed into the utility grid. When there is a shortage, electricity is drawn from the utility grid.

2.5.2. Hybrid Power System Components

Hybrid power systems using renewable energy and low carbon power sources are becoming increasingly desired for electricity production mainly in remote sites. Several components are combined to build up the system. These components depend on the type of energy sources needed to be harnessed. For the scope of this thesis, hybrid renewable energy systems consisting of PV panels, diesel generator, electrolyzer and hydrogen storage are considered.

2.5.2.1. PV panels

Solar energy is the greatest and most promising of the renewable energy sources because of its abundance and indefinite potential. The electromagnetic radiations emitted by the Sun are transmitted and can be used by photovoltaic modules to produce electricity. The use of photovoltaic panels for power productions has been increasing in the last decade. The use of PV panels in photovoltaic systems applications are mainly in grid-tied, distributed systems providing few kilowatts of electricity. Nevertheless, the development of new technologies, new methods of Maximum Power Point Tracking MPPT and implementing systems, the applications of photovoltaic systems is estimated to grow [29]. The efficiency of the photovoltaic panels has been enhanced significantly from 4% from first model developed by Pearson, Fuller and Chaplin in 1954 to around 40% recently [30].

Photovoltaic panels are the most well-known means used within electricity generation systems to convert the light energy coming from the Sun into electrical energy. In typical power generation systems, panels are connected in series, in parallel or in series-parallel forming a PV array to produce enough power to supply the load correctly. These panels are formed using semiconductors cells, which are the basic element level, connected together in series resulting an increase in the output voltage of the system. For instance, the solar panel KC200GT is build up from 54 PV cells connected in series to produce an open circuit voltage of 32.9V [31].

Today's photovoltaic cells are fabricated from semiconductor materials mainly crystalline silicon. In a PV cell, there are two doped semiconductor materials: N-type material (electron) and P-type material (hole). Hence, a PV cell is a p-n junction (see Figure 2.12). The direction of the current flowing across this p-n junction is defined by a spontaneous electric potential field applied at its boundary.

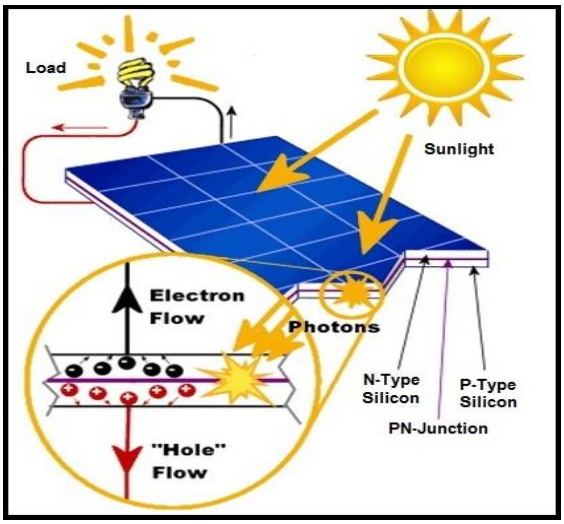

Source: [99].

Figure 2.12: Basic operating principle of a solar cell.

Different materials are used to manufacturer solar PV cells. The main material is known as silicon which is available in the Earth's crust and can be obtained from sand. In market, there are different types of technologies used for the PV cells production: monocrystalline, polycrystalline and thin film [32]. PV cells of silicon material are classified into:

a. Mono-crystalline PV cells

Such PC cells are fabricated from uncontaminated silicon single crystals. They are characterized by their dark color and trimmed corners. The production of mono-crystalline silicon cells requires an absolutely pure semiconductor material. Since this type of cells is made from one crystal, it is very efficient but very expensive. The mono-crystalline silicon cell works efficiently in an environment where low energy sources are present. However, the drawback of such technology is that it consumes more time to be manufactured. It involves heating the pure silicon material to reach its super saturated state, then introducing seed crystal into the molten silicon. The crystal is sliced to form cells after pulling the seed crystal out of the melted mono-crystalline slowly to obtain silicon ingot [33]. This type of cells has a conversion efficiency from 13% to 17% and a lifespan of 25 to 30 years [32].

b. Polycrystalline PV cells

The manufacture of this type of cells is economically more efficient comparing to the previous type. Molten silicon is poured to form blocks which are then sliced into slabs. It is made from the combination of many silicon crystals [33]. Consequently, the conversion efficiency is lower than the mono-crystalline silicon technology. In PV cell area of one meter square (1 m^2), t is able to convert a solar radiation of 1000 W/m^2 to 130 W of electricity. Hence, polycrystalline silicon cells has an efficiency ranging from 10% to 14% and a lifespan between 20 and 25 years [32].

c. Thin-film PV cells

The production of this type of cells is based on piling thin film layers of photosensitive materials on low-cost substrate such as stainless steel, glass or plastic. The manufacturing processes of thin-film have lead to lower production costs compared to the two other technologies above. However, the price advantage of such technology is counterbalanced by lower efficiency which ranges from 5% to 13% and a lifespan of 15-20 years [33]. Depending on the active material, there exist three commercial types of thin-film PV cells: amorphous silicon (a-Si), Cadmium-Tellurium (CdTe) and Copper Indium Gallium Selenide (CIS, CIGS) [32].

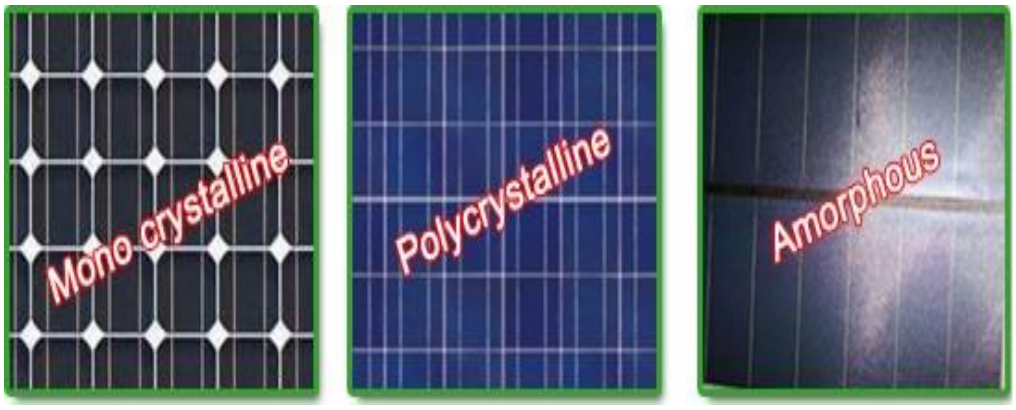

Figure 2.13: Typical first generation solar cells technologies [100].

All of mono-crystalline, polycrystalline and amorphous silicon cells belong to the first generation of PV technologies, but thin-film photovoltaic cells are considered as the second generation of PV technologies. A new solar cell generation has emerged known as the third generation of PV technologies. The solar cells under this generation do not obey the p-n junction design like the other generations, but they are fabricated from different new materials in addition to silicon including organic dyes, conductive plastics and nano-materials. This generation comprises Dye Sensitized Solar Cells (DSSC), Perovskite and Organic Photovoltaic (OPV) [34].

Among the renewable energy technologies, solar photovoltaic is low-cost today and it will become the cheapest in many regions in the world. The electricity produced by photovoltaic panels is nowadays cost competitive with both wind onshore and electricity generated using fossil fuels [34]. This can be explained by the benefits that solar energy has [35]. It is environmentally friendly and emission free, minimum maintenance and low running cost are required, it has a longer lifespan, and it does not use of water and fuels.

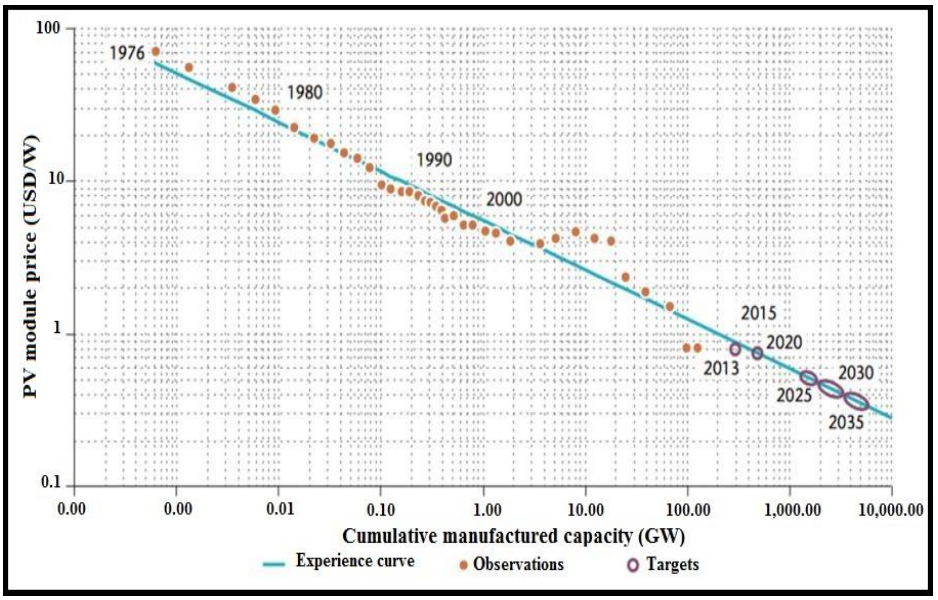

Figure 2.14: Past modules prices and projection to 2035 [14].

2.5.2.2. Diesel Generator

A generator is one of crucial elements that build up a hybrid power system. It provides power for the load in case the supply is less than the demand. In most cases, generators are used to optimize the output of a renewable power, enhance frequent deficit of energy when power interruption occurs in renewable sources and the battery is not able to provide the energy required. Power generators are machines used to produce electricity by transforming the kinetic energy of motion of the combustion engines into electricity by the means of different sources of energy [33]. They are chosen depending on their sizes, their types, types of the load to be fed and type of the fuels they use to operate.

A diesel generator is a diesel engine coupled with an electric generator called alternator via a shaft to produce electric energy. The diesel generator uses the chemical energy available in the fuel and converts it into mechanical energy. The mechanical energy, by its turn, drives the engine shaft that is connected to the alternator. Diesel generator sets (gensets) are mostly used: in places where the electric power grid is unavailable, as an uninterruptible emergency supply, as well as in different

complex applications like peak-chopping, power grid export and support from the grid [36]. Basically, there are two types of diesel generators: AC generators and DC generators.

Diesel generators function most efficiently when operating near its full load. Figure 2.15 depicts a typical generator set efficiency curve. It can be seen clearly that the efficiency decreases significantly when the load decreases. Furthermore, when the load increases from 20% to 80%, the efficiency of the generator doubles. Hence, the consumption of fuel per kWh is cut by two.

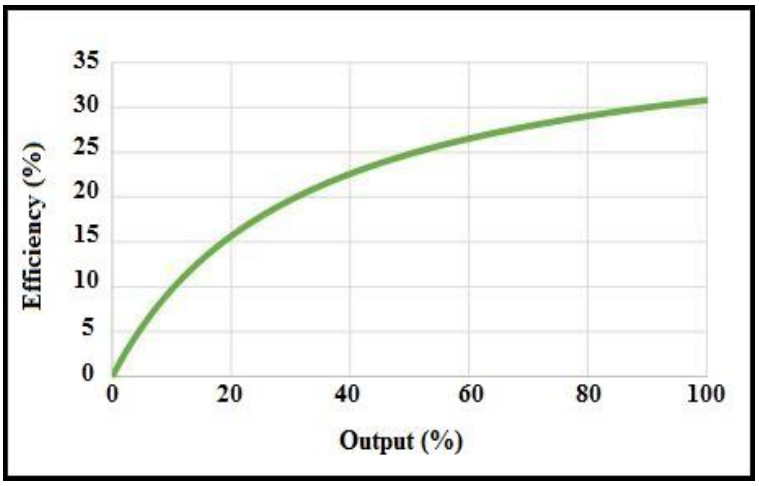

Figure 2.15: Typical generator set efficiency curve [37].

The initial investment of diesel generators is small comparing with the initial investments of PV power plant, wind power plant and hydro power plant. Nevertheless, the maintenance and the operating costs of diesel generators are relatively high. They require a continuous supply of fuel (diesel), inspection of the engine and recurrent maintenance. These costs play an important role not only to minimize repairs, maximize reliability and reduce long term costs but to maximize the lifetime of the generator and assure its start and operation when needed [38].

2.5.2.3. Power Conditioning Tools

Power conditioners are equipments that can convert a DC power to an AC power, and/or vice versa. They can function as DC-DC converters. Power conditioners can extract the maximum energy available in the PV generator by using subsystems that implement algorithms to pursuit the Maximum Power Point MPP of the PV system.

Hybrid power system needs a DC-AC converter to convert the voltage coming from the solar panels and/or batteries into AC voltage needed by the load. This type of converter is called inverters, however; the AC-DC type of converters that operates as an inverse of the power inverter is referred to as rectifier [33]. In general, the inverters that are used in renewable energy applications are grouped into two: grid connected inverters and off-grid inverters. To insure better performance of these renewable applications, a Maximum Power Point Trackers are integrated with some inverters. Some other inverters, however, are integrated with charge controllers. There are also bi-directional inverters operating in both inverting and rectifying modes. Therefore, the choice of a specific inverter for the power system must be done properly. The efficiency of an inverter changes depending on the load. The inverter efficiency curve is usually provided by the manufacturer. [39].

Inverters can be classified also according to the produced waveform. Generally, there are three common waveforms which are the square wave, the modified square wave and sine wave. Square wave inverters has little voltage output and significant harmonic distortion. They are not costly and used only in small appliances. The modified sine wave inverters are much better than the square wave ones since they have an output with less distortion. The main drawback of sine wave inverters is that they are very costly. They can produce a voltage that is as the grid voltage. This is why they are mostly found in grid-tied power systems [39]. The Figure 2.16 below shows a simple square wave inverter operation. When the switches 1 and 2 are closed, the AC output is positive in the left terminal. However, when the switches 3 and 4 are closed, the AC output is positive at the right terminal. Hence, switching from opening to closing generates the square waveform [40].

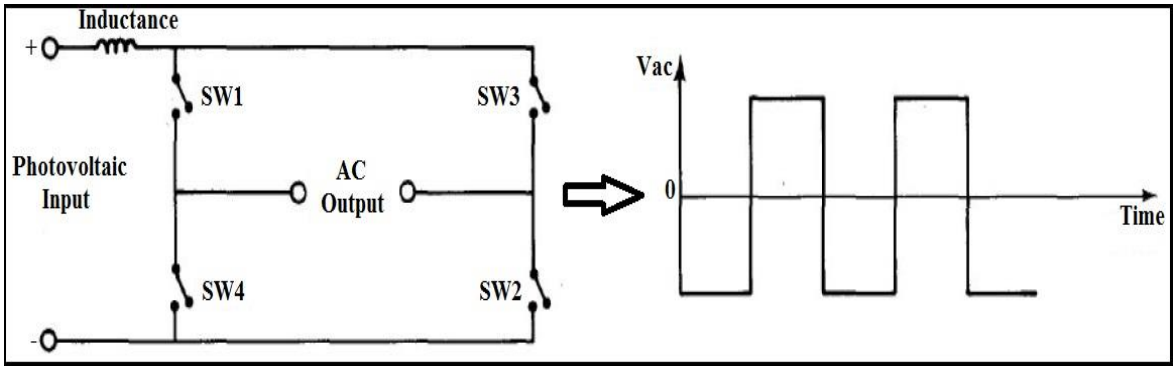

Figure 2.16: Simple square wave operation [40].

2.5.2.4. Maximum Power Point Tracking MPPT Methods

Photovoltaic power systems are promising methods for generating clean energy. The amount of the power generated by these systems is mainly dependent on temperature and solar irradiance. On the other hand, such systems are characterized by their low efficiency and high cost. Therefore, PV systems should operate at the maximum power point (MPP) which varies with solar irradiance variations [56]. Maximum Power Point Tracking MPPT controller is used to deliver continuously the maximum output power of the PV system to the utility regardless the temperature and the irradiance variations. Generally, MPPT controllers are embedded in the power conditioner systems.
Maximum Power Point Tracking controller is a very high efficiency electronic device which can be also inserted between the PV modules to reach optimal matching. Its function is to adjust the PV module operating point, which enables the PV module to deliver the available maximum power at any moment. Several control algorithm methods are reported in literature for MPP searching: Perturb and Observe (P&O) method, the open voltage method, the short current pulse method, the incremental conductance method and the temperature method. The most commonly used methods are the P&O method and the incremental conductance method which can be explained below [57].

a- Perturb and Observe (P&O) Method

The Perturb and Observe method forces the tracking direction toward the maximum power point based on creating a perturbation in the PV operating point. In other words, it is based on the perturbation of the system by increasing or decreasing a reference voltage V_{ref} (or reference current I_{ref}), then the observation the effect on the output power (P=V*I where V is the voltage and I is the current) for possible correction of cyclical report. The P&O algorithm can be explained using V_{ref} below:
For a given step k:

If $dP = (P_k - P_{k-1}) < 0$ and if $dV_{ref} = (V_{ref,k} - V_{ref,k-1}) < 0$, we increase V_{ref}; if $dV_{ref} > 0$, we decrease V_{ref}.

If $dP = (P_k - P_{k-1}) > 0$ and if $dV_{ref} = (V_{ref,k} - V_{ref,k-1}) < 0$, we decrease V_{ref}; if $dV_{ref} > 0$, we increase V_{ref}.

Perturb and Observe method is the commonly used MPPT controller owing to its simplicity and fewer measured parameters. However, this method fails under rapidly changing environmental conditions and partially shading.

b- Incremental Conductance Method

The incremental conductance method is based on the fact that the slope of the curve of the PV module is positive on the left of the MPP ($\frac{dP}{dV} > 0$), zero at the MPP ($\frac{dP}{dV} = 0$) and negative on the right of the MPP ($\frac{dP}{dV} < 0$).

Since: $$\frac{dP}{dV} = \frac{d(V*I)}{dV} = I + V * \frac{dI}{dV} \approx I + V * \frac{\Delta I}{\Delta V} \quad (2.1)$$

Thus:
$$\begin{cases} \frac{\Delta I}{\Delta V} > \frac{-I}{V} & \text{left of the MPP} \\ \frac{\Delta I}{\Delta V} = \frac{-I}{V} & \text{at the MPP} \\ \frac{\Delta I}{\Delta V} < \frac{-I}{V} & \text{right of the MPP} \end{cases}$$

In the incremental conductance algorithm, the MPP is tracked by comparing the incremental conductance $\frac{\Delta I}{\Delta V}$ to the instantaneous conductance $\frac{I}{V}$. The PV module is forced to operate at a given reference voltage V_{ref} where $V_{ref} = V_{MPP}$ at the MPP (V_{MPP} the voltage at the MPP). The PV module is maintained at the MPP once it is reached unless a variation in ΔI occurs which implies a change in the environmental conditions and the MPP. Hence, the algorithm increments or decrements the reference voltage for the new MPP tracking.

c- Constant Duty Cycle

This method is the simplest one among the MPPT methods discussed in this section. It is based on selecting a constant duty cycle to control the solar module and drive it to its close enough MPP. In this way, the duty cycle does not change; hence, there is nothing to vary. Such MPPT method assumes that changing in the irradiance and temperature are irrelevant and can be ignored [58]. The advantage of the constant duty cycle method is its simplicity. It may prove to do better in low irradiance conditions. However, it does not track the MPP but gives an output power close enough to the MPP.

d- Short-Circuit Current or Open-Circuit Voltage Method

Another method to control the solar module power is to measure either the short-circuit current or the open-circuit voltage, or both. The current at the MPP is approximately 78 to 92% of the short-circuit current. The voltage at the MPP is around 70 to 80% of the open-circuit voltage as well. Therefore, by having both the short-circuit current and the open-circuit voltage; an algorithm can be implemented to approximate the MPP. This method is known by its simplicity and inaccuracy [59].

e- Temperature and Irradiance Models

This method is based on implementing mathematical models that determine the voltage at the MPP using some useful temperature and irradiance data measured by the system. To illustrate this, one has to know that the voltage at the MPP changes when the temperature varies as it is given in the following model:

$$V_{MPP}(T) = V_{MPP,ref} + K_{V/T}(T-T_{ref}) \quad (2.2)$$

Where: $K_{V/T}$ is the the coefficient of change in voltage over temperature,
V_{MPP} is the MPP voltage at temperature T,
$V_{MPP,ref}$ is the MPP voltage at the reference temperature T_{ref}.

The model (2.2) utilizes the temperature only. Another model can be added to this model using solar irradiance. As a result, the new model becomes very robust. In this way, models can be built to describe how both irradiation and temperature affect the voltage at the MPP [60]. Alternatively, a table can summarize different V_{MPP} measurements for different solar irradiation and temperature data. Based on these collected data, a control algorithm can be implemented to sort the desired V_{MPP}. An interpolation can be used to approximate the V_{MPP} in case the measured data do not match up.

f- Current Sweep Method

The current sweep method consists of adjusting the current from the solar module at certain intervals. Consequently, the control unit obtains several current and voltage measurements to decide on the voltage that produces the MPP. By doing this, the control unit drives the solar module's voltage to V_{MPP} [59]. The current sweeps is similar to the open-circuit voltage and short-circuit current methods since they do not converge exactly to the MPP but close enough to it.

2.5.2.5. Electrolyzer

An electrolyser consumes electrical energy and converts it into chemical energy to produce hydrogen via the electrolysis of water (electrochemical water dissociation). It contains two electrodes: a cathode (negatively charged) and anode (positively charged). Water is decomposed into its gaseous components using electricity, oxygen at the anode and hydrogen at the cathode. The electrodes are separated by a membrane called diaphragm which prevents the two gases to blend and form water again. The produced hydrogen can be extracted and stored then for instance in pressure tanks or metal hydrides. The electrolysis process generates high-purity hydrogen without polluting or causing any harmful effects on the environment [6]. The total chemical reaction that happens inside an electrolyser is given by:

$$2H_2O(l) + \text{Electrical Energy} \rightarrow 2H_2(g) + O_2(g) \quad (2.3)$$

The process must be input by an electrical energy which can be generated by renewable energy sources such solar or wind. There exist three types of electrolysers' technologies.

a. Alkaline water electrolyser

This type of technology is well proven and has been used widely in hydrogen production. It covers the majority of the market. The electrolyte, which is a chemical that conducts electricity when mixed with water, used in this technology has an aqueous solution of potassium hydroxide KOH. The solution of water and potassium hydroxide is referred to as the fluid operating medium and it has a concentration of 20 to 30 wt.% . The alkaline water electrolyser has an operating temperature raging from 70°C to 100°C, a pressure of 1 bar to 30 bar and operates with DC power [41].
An alkaline electrolyser consists of an anode, cathode, cell frame, electrolyte and a separating diaphragm. It can be uni-polar or bi-polar designed. The electrodes in the uni-polar design are alternatively suspended with parallel electrical link of the individual cells. This design is very simple to manufacture and repair, but it operates at low temperature and current densities. In the bi-polar design, the individual cells are electrically connected in series. The advantage of the bi-polar design is its compactness which increases the design efficiency. However, the main disadvantage of such design is that it is hard to repair.

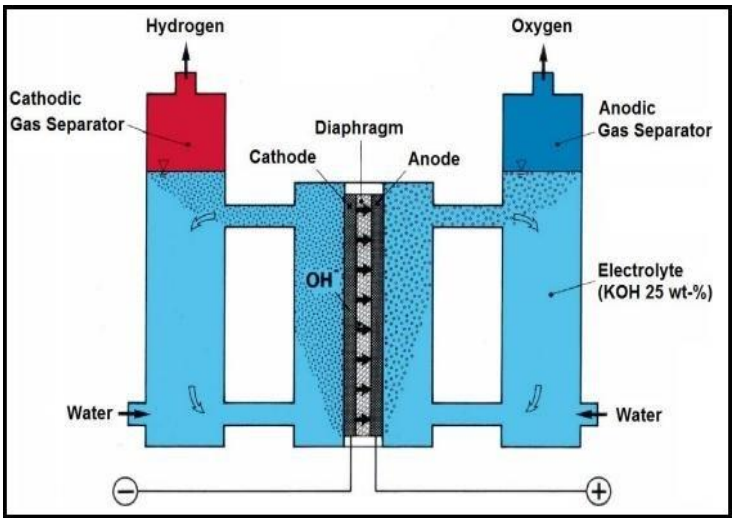

Figure 2.17: Alkaline electrolyser schematic construction [42].

The chemical reactions that happen in the alkaline water electrolyser are:

At the cathode:

$$4H_2O(l) + 4e^- \rightarrow 2H_2(g) + 4OH^-(aq) \quad (2.4)$$

At the anode:

$$4OH^-(aq) \rightarrow O_2(g) + 4e^- + 2H_2O(l) \quad (2.5)$$

Hence, the overall reaction can be derived by combining the two chemical equations above and is given by the chemical equation (2.3).

b. Proton Exchange Membrane (PEM) electrolyser

This technology depends on the use of solid polymeric electrolytes and expensive metals such as platinum. This type of electrolysers does not require the compression of hydrogen after the electrolysis process as in alkaline type since PEM electrolysers operates at high pressures (up to 200 bar). In addition, PEM electrolysers are more efficient than alkaline electrolysers and have less parasitic losses

but they are more expensive. Moreover, they are not only environmentally clean because of the absence of any chemical electrolyte (KOH), but they produce hydrogen with high purity. Generally, their sizes are small and light [43]. More advantages of PEM electrolysers over alkaline electrolysers [44], they consume much lower power, they are safer, and they operate at a high current density and also with transient variations in the electrical energy input. This is why they are excellent in renewable energy sources applications. Figure 2.19 shows the schematic construction of a PEM electrolyser. The splitting of water molecules into hydrogen and oxygen ions occurs at the anode. Then, the hydrogen ions (protons) move across the PEM which is a porous material and the electrons flow through an external circuit. At the cathode, hydrogen ions combine with electrons to form hydrogen gas [34].

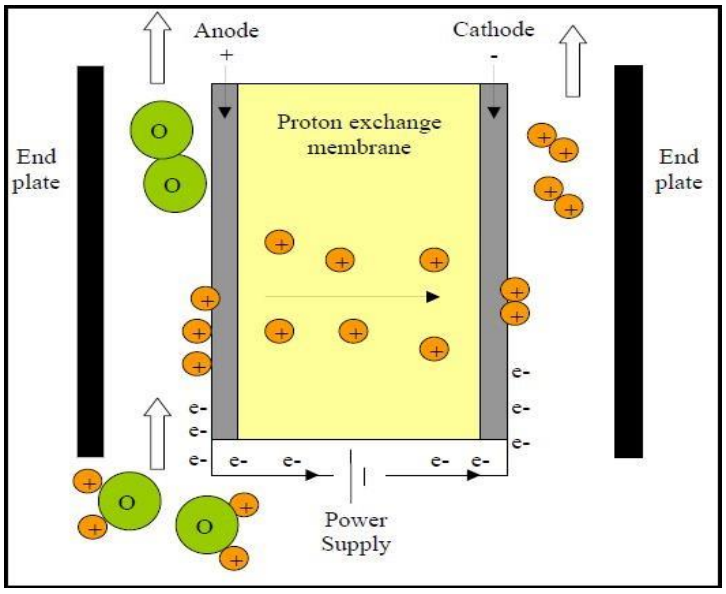

Figure 2.18: PEM electrolyser schematic construction [43].

The chemical reactions that happen in the PEM electrolyser are:

At the anode:

$$2H_2O(l) \rightarrow O_2(g) + 4H^+(aq) + 4e^- \quad (2.6)$$

At the cathode:

$$4H^+(aq) + 4e^- \rightarrow 2H_2(g) \quad (2.7)$$

c. *Solid Oxide Electrolyser SOE or High Temperature Electrolyser*

This is a promising technology which is based on the production of massive hydrogen gas using heat and electric power from steam at high temperature (1000°C). Since the water is in its steam form, SOE requires less energy for splitting it to produce hydrogen. Solid ceramic electrolytes are use in SOE because of their high resistance to high temperatures and their better ion conductivity. This type of electrolysers is highly efficient but it is still under development and it is not commercialized yet because of its high temperature that limits its operation [45].

2.5.2.6. Hydrogen Storage

As all fuels, hydrogen fuel needs to be stored in order to be transported and consumed afterwards. The properties of hydrogen must be known before designing and developing any technology for hydrogen storage. Hydrogen is a chemical element that can be found abundantly in the universe. Hydrogen gas has no color, no taste and no odor. Hydrogen gas is the lightest molecule with molecular weight of 2.016 g/mol and its density is 14 times less than the air. It can be liquefied at a temperature below 20.3°K at atmospheric pressure. Its density becomes then 70.8 kg/m^3. Environmentally, it is not toxic and not poisonous. It is a very efficient fuel for power production since has the highest energy per unit mass among all fuels; its High Heating Value HHV is 141.9 MJ/kg (11.89 MJ/m^3) and Low Heating Value LHV is 119.9 MJ/kg (10.043 MJ/m^3). Hydrogen is characterized by its small molecular size that makes it to leak easily through porous medium. Yet, it is not corrosive and it does not react with typical container materials. Therefore, hydrogen storage technologies have recently received great attention owing to the long life storage as fuel [46].

In case of hybrid renewable energy systems with hydrogen storage, the intermittency of the renewable sources can be solved. Hydrogen storage can be put between the power generation and the load to solve the problem that may arise when the demand gets bigger than the supply. Hydrogen has low density in normal conditions; hence it is difficult to be stored. It can be stored as compressed or pressurized hydrogen gas, as liquid hydrogen or as metal hydrides.

a. Compressed gaseous hydrogen storage CGH_2

Compressing the hydrogen gas is considered as the simplest solution to store it. It requires only a compressor and a pressure vessel. The disadvantage of this type of storage is that it has a low storage density which depends of course on the pressure of storage. Consequently, the capital and operating costs becomes higher [47]. Compressed gaseous hydrogen storage operates at ambient temperature but with a pressure of 250 bar to 350 bar (the pressure can reach 750 bar but in this case the use of carbon fibers is a must; thus resulting a very expensive storage system). The storage tanks can be made from material coated aluminum or steel [46].

b. Liquid hydrogen storage LH_2:

Liquefaction of hydrogen gas is performed in order to reduce the volume of this gas needed to be stored. It is the most efficient way of storage for commercial purposes. The drawback of such systems is the short time storage; it is only 4 days storage. In order to keep the low temperature of the hydrogen liquid, 1%/day of the hydrogen stored should be evaporate. The liquid hydrogen tanks are manufactured with multi layers insulation double walls (70 to 100 layers, 25 mm) and can operate at a temperature of 20.4 °K (253°C) and a pressure of 1 bar to 10 bar [46]. Cylindrical tanks are most of the time preferable since they are easy and cheaper to construct than spherical tanks. Moreover, their volume/surface ratio is approximately the same [48].

c. Metal hydride hydrogen storage MHH_2

This technology is based on binding chemically the hydrogen with a metal or an alloy called metal hydride. An exothermic process occurs when a hydride is formed with a metal/alloy (heat is generated). In contrast, an endothermic process happens when hydrogen releases from the metal (heat is provided) as shown by the chemical reactions (2.8) and (2.9) [49]. Metal hydride storage has a

higher volumetric energy storage density (0.4 to 5.2 MJ/l). Nonetheless, it has a low mass/energy density value and the metals used are relatively costly [46].

Charging or absorption: $A + xH2 \rightarrow AH2x + Heat$ (2.8)

Discharging or desorption: $AH2x + Heat \rightarrow A + xH2$ (2.9)

Where: A is the alloy or metal, AH is the hydride and x is the ratio of the number of hydrogen atoms to the number of hydrating substance atoms.

2.5.3. Hybrid Power System Configuration

In order to harness the renewable energy resources availability and meet the demand of the power load, HPS are designed in such a way they have different configurations (topologies). Ideally, the energy sources (renewable and conventional), energy storage system and the power load are able to be integrated and work independently as a unit. However, a hybrid system should be capable to integrate any number of devices without re-configuring of the system [49]. There are several ways to combine the subsystems that build up the hybrid system. Among them, three are the most common: DC-coupled, AC-coupled and mixed coupled or hybrid-coupled.

2.5.3.1. DC-coupled topology

In a DC-coupled system configuration, all of the energy sources and the storage units are connected to the DC bus-bar before connected to the AC power load (see Figure 2.19). Converters are used to convert all the AC power sources into DC power sources and add their DC outputs to the main DC bus-bar. The DC bus-bar, by its turn, can be connected to a DC load by the means of a DC-DC converter, AC load using DC-AC converter or electric power grid through a bi-directional converter. Referring to the Figure 2.19, each power system is tied to the DC bus-bar by its own DC-DC converter. In case of batteries and hydrogen storage, they are tied through a bi-directional converter to permit the charge and the discharge of both energy storages.

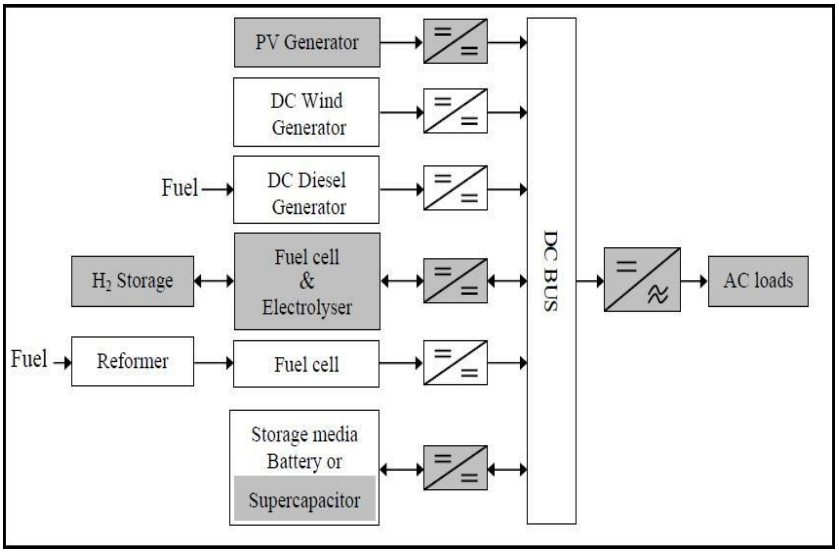

Figure 2.19: DC-coupled hybrid system block diagram [6].

The DC-coupled configuration is simple to implement. The load demand is met without any interruption even when the storage units are charged by the power sources. In contrast, this configuration is disadvantageous in terms of low efficiency conversion. Moreover, adding power sources as well as expanding the system is difficult since the DC-AC power inverter has a limited nominal capacity [6].

2.5.3.2. AC-coupled topology

In AC-coupled hybrid systems, all the system sub-units are tied to the AC bus-bar before connecting them to the AC power load (see Figure 2.20). In such configuration, the inverters are synchronized to their power generators in such a way each of them can provide power to the load either independently or simultaneously with other inverters. Thus, the system is flexible to satisfy the required consumer's load. In off-peak demand, all of the power generation and storage units may work in parallel to satisfy this demand. This configuration has advantages over the previous one: its efficiency is relatively higher, the energy availability is kept at its high level and the operating time of diesel generator is reduced and thus its maintenance costs can be reduced.

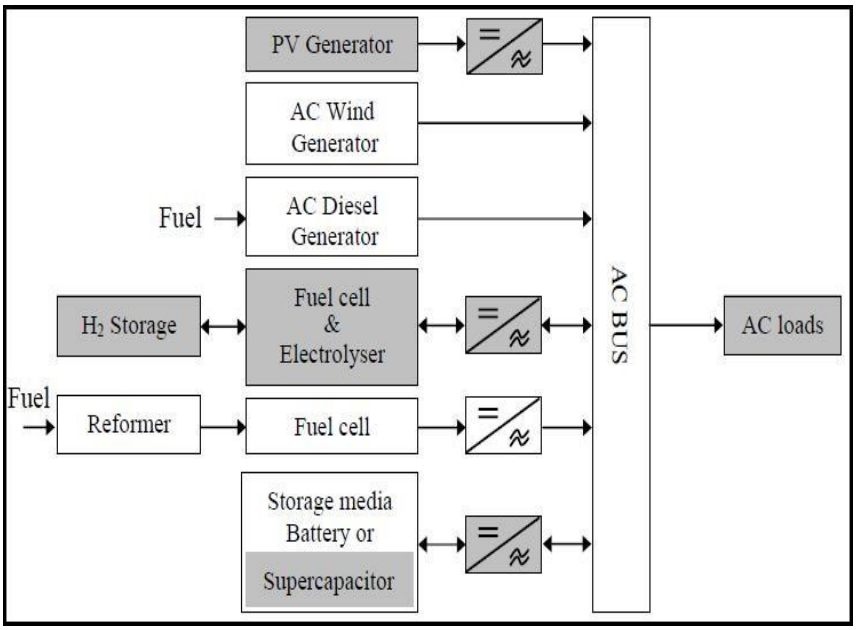

Figure 2.20: AC-coupled hybrid system block diagram [6].

2.5.3.3. Hybrid-coupled topology

In such topology, several energy generation units are connected to the DC or AC bar buses. Some of these units may be combined to the system without any power electronic interfacing circuit. Therefore, the resulting system can achieve a higher frequency with low capital cost capital. Nevertheless, the energy management and control unit can be more complex compared to the AC-coupled and DC-coupled hybrid power systems [50].

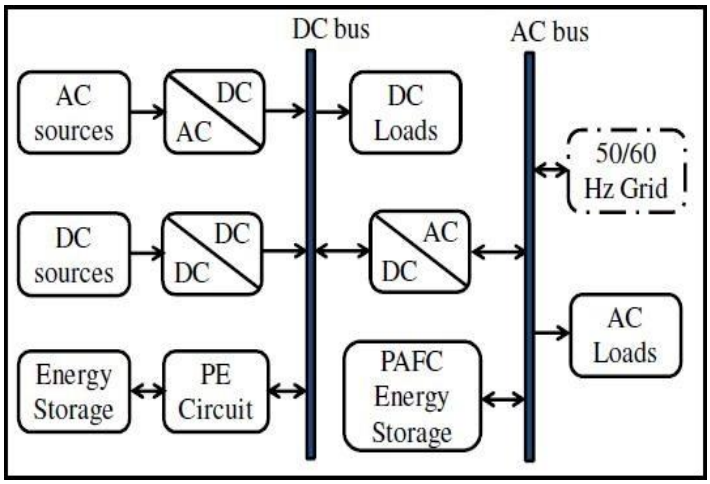

Figure 2.21: Hybrid-coupled hybrid system block diagram [50]

2.6. Hydrogen Production Methods

Because of the high quality of storing energy, hydrogen is becoming one of the most efficient alternative fuels. Hydrogen exists in several chemical compounds in nature. Thus, several production and extraction methods have been created. Many process technologies can be used to produce hydrogen from diverse domestic feedstocks. All of steam reforming, partial oxidation and gasification are conversion techniques for hydrogen production. Steam reforming, which provides 90% of the world hydrogen, is currently the cheapest hydrogen production technique. It is based on chemical process where water and natural gas (methane) are mixed at very high temperature (1100 to 1300 °K), and then passed over a nickel-alumina catalyst. At the end of the chemical process, hydrogen and carbon dioxide are formed, according the overall reforming reaction equation (2.10) [51]:

$$CH_4(g) + 2H_2O(g) + 165\ kJ/kg \rightarrow CO_2(g) + 4H_2(g) \quad (2.10)$$

In partial oxidation, hydrocarbons in liquid or gaseous form are combined with oxygen in a high pressure reactor. The final products of this process are the same compared with the steam reforming (see equations (2.11) and (2.12)). Theoretically, both processes have same efficiencies even though partial requires less water. The gasification technique is used mainly with coal. This coal is partially oxidized with oxygen in a reactor at high pressure to decrease forming of nitrogen oxides in the chemical process [51].

$$CH_4(g) + 1/2O_2(g) \rightarrow CO(g) + 2H_2(g) \quad (2.11)$$
$$CO(g) + H_2O(g) \rightarrow CO_2(g) + H_2(g) \quad (2.12)$$

The chemical conversion techniques described before have common advantages and disadvantages. All of them use fossil fuels as feedstocks which are abundant in many parts of the world. However, the main byproduct is carbon dioxide which makes these processes not sustainable and environmentally unfriendly.

There exist other process techniques for hydrogen production. Thermolysis of water is one of them. In order to split water into oxygen and hydrogen, this process needs a significant amount of thermal energy. Thermolysis system is a promising technology that may be integrated in nuclear power plants. Photolysis is another process used from hydrogen production in which biomass processing, wastes and algae are the main feedstocks. Both thermolysis and photolysis are in experimental and development stages [51].

2.6.1. Electrolysis

Electrolysis is known as the best technology for hydrogen production for some applications. Electrolysis of water offers a more economical way than the other techniques especially when undersized quantities of hydrogen are needed. Since this technique is reliable, clean and can be related to renewable power production, it is becoming more important in hydrogen production commercial technologies. Electrolysis is based on passing a DC between two electrodes (cathode and anode) which are immersed in an electrolyte. As a result, hydrogen gas is formed at the cathode and oxygen gas at the anode (see equation (2.3)).

During the process of water electrolysis, the electrical and the thermal energies are converted to a chemical energy stored in hydrogen. The energy required for decomposing water into hydrogen and oxygen gases is the enthalphy of formation of water ΔH where only free energy of the electrolysis reaction or Gibbs free energy must be provided as electricity, and the remaining is a thermal energy TΔS as shown by the equation below [52]:

$$\Delta H = \Delta G + T\Delta S = zF\left[T\left(\frac{\partial Vrev}{\partial T}\right)_p - V_{rev}\right] \quad (2.13)$$

Where: z: the number of moles of electrons transferred (for hydrogen z = 2),
F: Faraday's constant F = 96485.3365 C/mol,
V_{rev}: the lowest voltage required for the electrolysis to happen.

In case where no heat is generated or absorbed (no thermal energy), the minimum voltage that decomposes water is referred to as thermoneutral voltage V_{tn}. At standard condition (T= 25°C and p= 1 bar), the reversible and the thermoneutral voltages are calculated to be 1.23V and 1.48V, respectively (ΔG = 237.21 kJ/mol, ΔS = 0.16 kJ/mol.K and ΔH = 285.84 kJ/mol). Hydrogen production is impossible when the potential is under the reversible voltage. The thermoneutral voltage is the minimum potential that has to be provided to split the water molecule; above this voltage the electrolysis is exothermic thus heat is produced and wasted, below it is endothermic. Therefore, if the reaction took place in the shaded area (Figure 2.22), it would result an efficiency of 100% [52].

As the temperature of the electrolyte increases, the ideal voltage needed to split the water molecule decreases, thus the ideal efficiency decreases. Hence when the operating voltage is above the thermoneutral one, the ideal efficiency is inversely proportional to the voltage [53].

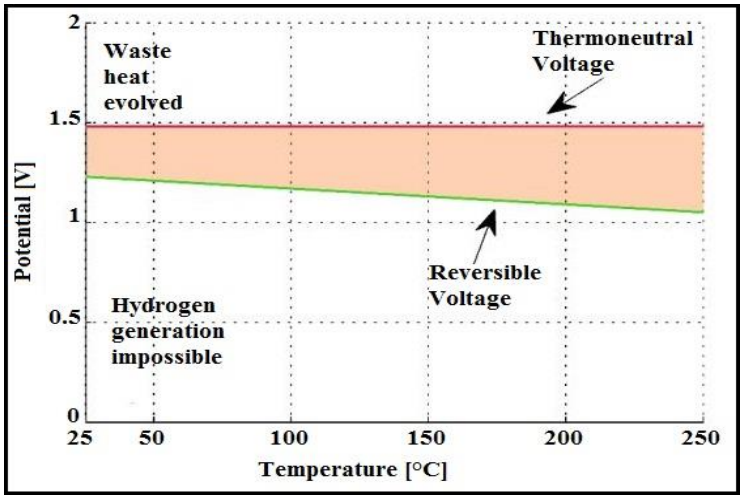

Figure 2.22: Ideal operating hydrogen production potential vs. temperature [52].

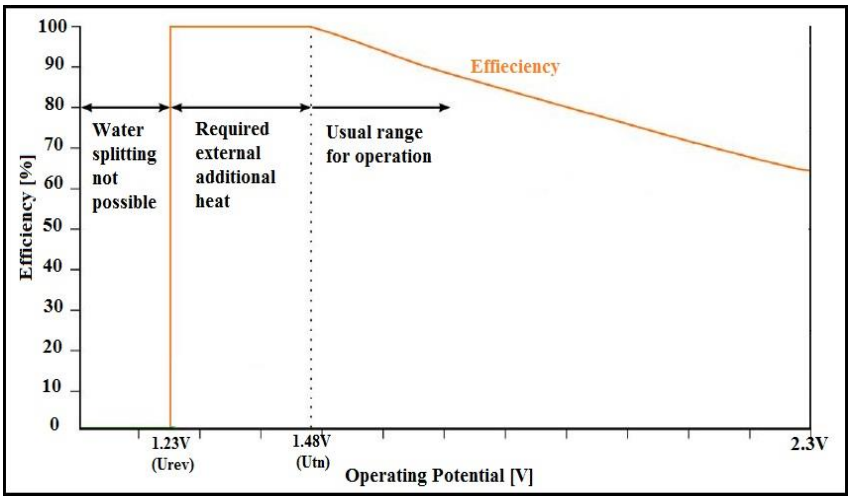

Figure 2.23: Efficiency as a function of the voltage cell [53].

2.7. System Sizing Optimization

When designing a hybrid power system, several objectives must be taken in consideration to ensure the supply of power for the load at all time. Cost minimization is one of these objectives. The total costs, which enclose both the capital costs and the recurring costs or the operational costs, can be calculated either by using the Net Present Cost NPC or the Levelized Cost of Energy LCOE. Maximizing the system reliability is another objective. This objective can be achieved by minimizing the probability of losing power in the supply and ensuring its continuity. On the other hand, maximizing the system efficiency is another objective while designing a hybrid system that can be attained by selecting efficient components that made up the whole system. Besides, power line losses minimization can be realized through the use of appropriate types and sizes of the hybrid power system.

The hybrid system optimum design can be either single objective or multi objectives design. This latter can be designed by selecting either two consistent objectives such as maximizing the system reliability and efficiency or two contradictory objectives such as maximizing the system reliability and minimizing the cost.

2.7.1. Software Based Approach

Simulation and optimization programs are the most common tools for assessing the performance of renewable power systems. In computer simulation, the performance and energy production cost of different system configurations are firstly compared in order to reach an optimum configuration. Some of the famous software programs are: HOMER, HYBRID2, HOGA, HYBRIDS, TRNSYS, HYDROGEMS, etc.

Table 4: Comparison among the famous software programs [54].

	HOMER	HYBRID2	HOGA	HYDROGEMS + TRNSYS	HYBRIDS	INSEL	ARES	RAPSIM
Free download and use	X	X	X					
PV, Diesel, Batteries	X	X	X	X	X	X	X	X
Wind	X	X	X	X	X	X		X
Mini-hydro	X	X	X	X				
Fuel cell, electrolyser, hydrogen tank	X	X	X	X				
Hydrogen load	X	X	X	X				
Thermal load	X			X				
Control strategies	X	X	X					
Simulation	X	X	X	X	X	X	X	X
Economic optimization	X		X	X				
Multi-Objective optimization			X					

HOMER

HOMER, which stands for Hybrid Optimization Model for Electric Renewable, is a computer modeling software developed by National Renewable Energy Laboratory NREL. HOMER is one of the well-known and popular programs that are used for modeling off-grid and grid-tied power systems for remote, stand-alone and distributed generation. HOMER is commonly used for optimizing and preparing prefeasibility studies of hybrid systems. It has many energy generating components (both conventional and renewable energy technologies). To begin the system design, the package requires different inputs like resources data, component types, storage technologies, and economical constraints. This software is a time-step simulator from one minute to several hours [55].

Because of the large combination of design solutions and the presence of uncertainties, system analysis and design becomes a challenging task. The complexity and uncertainty of the design increase when dealing with renewable sources of energy since these sources are intermittent by nature and non-dispatchable [33]. HOMER performs mainly three tasks shown in the following figure.

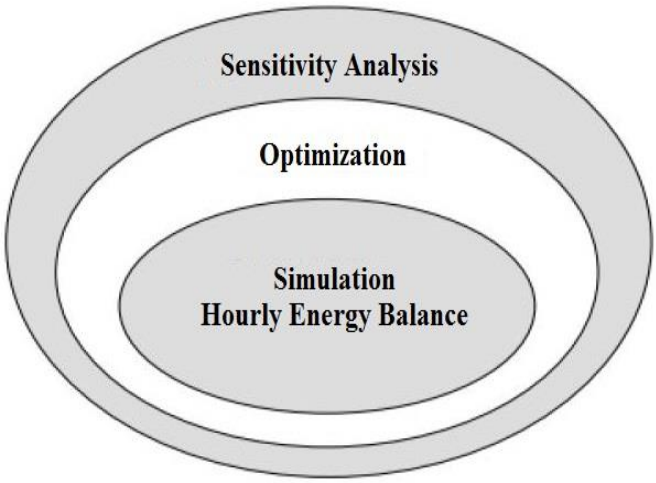

Source: NREL, 2009.

Figure 2.24: Simulation, optimization and sensitivity analysis interactions.

The simulation compares the load demand and the energy supplied by the hybrid system in a given precise time. During this time, it decides whether to use load following or dispatch strategy to drive generator and storage bank, generators, etc. The dispatch strategy is an aspect of control strategy that can be used to control generator and storage bank functioning whenever the demand is higher than the supply. Nevertheless, the load following strategy is by itself a dispatch strategy whereby whenever a generator runs; it generates only enough power to achieve the higher-priority objective which is satisfying the power load. The other lower-priority objectives such as storage charging are reached by the renewable sources.

In the process of optimization, different system configurations are simulated in search for the lowest Net Present Cost NPC and a list the hybrid power systems that satisfy the power load is sorted. The objective of this process is to find the optimal system based on decision variables defined by the designer. These decision variables can be: size of the PV array, size of generator, converter size, wind turbines quantities, batteries quantity, dispatch strategy, etc. Looking for the optimal system takes into account the power components mix such as size, quantity and dispatch strategy at the same time. On the other hand, the sensitivity analysis studies the effect of external parameters called sensitivity parametric variables and performs optimization for each variable. These variables must be input into the software at the beginning. Hence after defining the sensitivity parametric variables as inputs into the software, the process of optimization must be recurred. HOMER's sensitivity variables may include components cost, fuel cost, climatic data variations, interest rate, and etc. At the end, the sensitivity results are shown in graphical and tabular forms [33].

HOMER is widely used in literature for optimal designing of hybrid power systems. However, this software only performs single objective optimization in minimizing the cost; HOMER cannot formulate multi-objective optimization.

3. 1. Introduction

Modeling of hybrid power system components is an essential step in both design and operation process of power systems. The purpose of this step is to investigate the performance of each component separately in such a way all the models can be integrated together so as to meet the need of the power load. The supply reliability, safety in operation and financial viability can be ensured when the hybrid system is well modeled. This chapter describes modeling components of the PV-Diesel-Hydrogen storage hybrid power system. Various models for such system have been reported in literature. Brief modeling descriptions for PV-Diesel-Hydrogen storage are shown in this chapter's subsections.

3. 1. Hybrid Power System Components modeling

3.2.1. PV Model Development

As explained in the previous chapter, a PV module consists of certain number of interconnected solar PV cells (typically 36 connected in series), put into single, stable and long-lasting component unit. This unit protects the interconnecting solar cells and wires from harsh environment in which they are installed. The solar PV cell is a semiconductor device constructed from a p-n junction. When illuminated, the imbalance of the electrical charge in the two layers (p layer and n layer) causes the charge to move through the junction thereby producing electricity. Modeling a PV module relies mainly on the characteristic of the solar cell. It is therefore crucial to have a good knowledge of how it works. On the other hand, the relationship between the electrical parameters of the PV module and the environmental parameters (mainly temperature and solar irradiance) must be understood [61].

3.2.1.1. Electrical Characteristics of Solar Cell

The I-V characteristic of a solar cell is the superposition of that of a diode under darkness and photo-generated current. The illumination of the structure has the effect of moving the curve I (V) of the diode towards the reverse currents. Since the PV cell is considered as a generator, the convention is to reverse the axis of currents. Note that the photovoltaic cell imposes neither the current nor the operating voltage; only the curve I (V) is fixed. It is the value of the impedance of the load at the terminals of the cell that will impose the operating point [62]. The electrical characteristic of a PV cell showing its different operating modes is shown in Figure 3.1 below. In this figure, two important operating points can be distinguished: short-circuit current I_{sc} and open-circuit voltage V_{oc}. When there is no resistance in the circuit, a PV cell generates its maximum current known as the short-circuit current I_{sc}. The voltage in this case is zero. The open-circuit voltage is the voltage across the cell when there is no current. Its value is of the order of 0.6 V for the crystalline solar cells. These two points delimit the operation of the cell in three different zones [63].

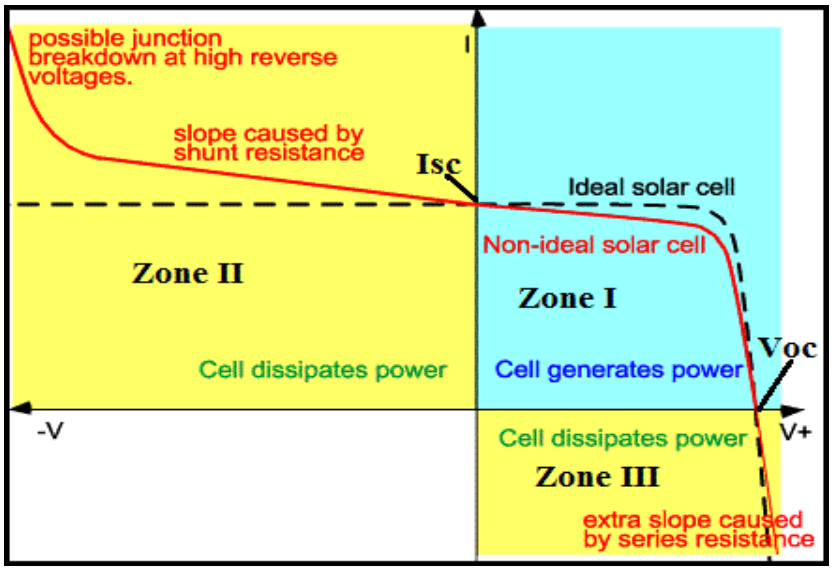

Source: [101]

Figure 3.1: I-V characteristics of a PV solar cell.

Zone I in Figure 3.1 corresponds to the generator operation of the solar cell with the current $0 < I < I_{sc}$ and the voltage $0 < V < V_{oc}$. This is the so-called normal operation of the cell in which it delivers the power produced to the load.

In Zone II where $I > I_{sc}$ and $V < 0$, the solar cell dissipates power by absorbing energy which is delivered by other cells. When the current flowing through the solar cell is forced by an external circuit to surpass its short circuit current, the cell generates a negative voltage across its terminals. The current increase will cause damage to the cell if the voltage at its terminals reaches a certain limit called breakdown voltage. Some experiments on different crystalline solar cells have shown that the breakdown voltage varies between -30V and -10V [64].

In Zone III, the solar cells dissipates power as in Zone II but this time with ($I < 0$, $V > V_{oc}$). A reverse current flows in the cell when the voltage at the cell's terminals exceeds its open-circuit voltage. Similarly, if this reverse current surpasses a certain limit, the solar cell will be irreparably damaged.

3.2.1.2. Solar PV module Model

Modeling of PV module entails the estimation of the non-linear I-V curves. In order to do so, circuit topologies of the module have been utilized by researchers to model its characteristics when subjected to environmental variations mainly temperature and solar irradiance. Generally, there are two circuit models in use: the one-diode model (See Figure 3.2 (a)) and the two-diode model (See Figure 3.2 (b)) [65].

At the early beginnings, the one-diode circuit was the simplest model; it was built up by a current source in parallel to a diode (Figure 3.2). In this case, the current source output is directly proportional to the light that falls on the solar cell. However, several improvements of this circuit model have been done since it does not show an adequate behavior of the solar cell that is subjected to the environmental variations, in particular at low voltage. The first improvement of the one-diode model was the insertion of a series resistance R_s. The series resistance represents the resistivity of the material in which the cell is manufactured; the contact resistance between the semiconductor and the metal; the resistance of the top and rear metal contacts. This model is widely used thanks to its simplicity and computational efficiency. However, its accuracy decreases when the solar cell is

subjected to high temperature [66]. Therefore, the one-diode circuit model has been improved by adding a shunt resistance R_p (parallel resistance) resulting a more practical model. The parallel resistance represents all the paths traversed by the leakage current, whether in parallel with the solar cell or at the edge of itself [67]. The one-diode model represents a relatively normal solar cell in normal operation. Nevertheless, it does not take into consideration the avalanche effect of the PV cell. The avalanche breakdown occurs when the solar cell is partially shaded; this cell is said to be reverse biased in shading and it behaves like a load in the circuit. Hence, this effect is considered in the Bishop model by the inclusion of a nonlinear multiplier M (V1) in series with the shunt resistor (See Figure 3.3) [68].
The main drawback of the one-diode model of the solar cell is that it does not consider the presence of the recombination loss in the depletion region which represents a substantial in real solar cells in particular at low voltages. The recombination effect cannot be modeled using the one-diode model.

The two-diode model represents a more accurate model even when the solar cell is subjected to weather variations. It shows similar results as the one-diode model under the standard conditions STC but more accurately under lower irradiance. This model needs the computation of seven (7) parameters instead of (5) as in the previous model. Consequently, the complexity of this model is known as its main drawback. In addition, the computation of the model parameters is time consuming since it requires iterative approaches to do so [69].

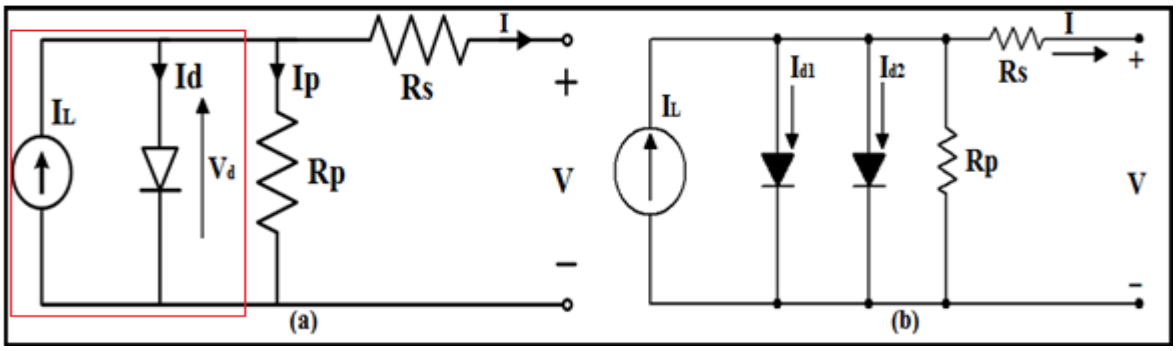

Source: [102].

Figure 3.2: Solar cell circuit models: (a) one-diode circuit model, (b) two-diode circuit model.

In this work, the one-diode circuit model is considered due to its simplicity, viability and widely usage.

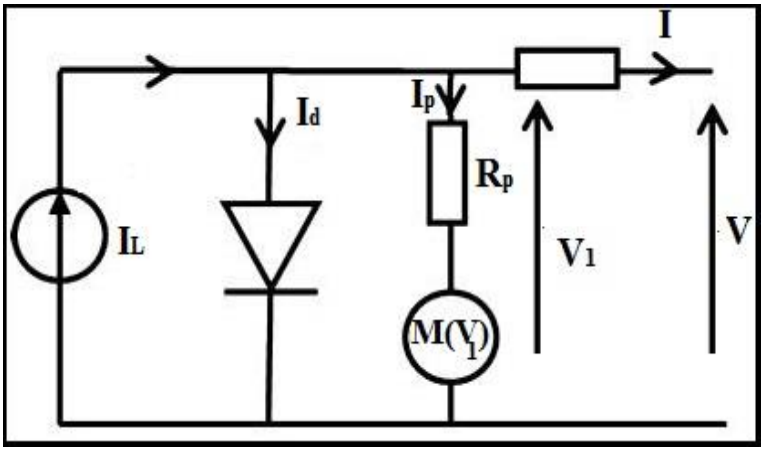

Figure 3.3: Solar cell Bishop Model [70].

Based on the model shown in Figure 3.2 (a) and according to Kirchoff's Current Law, the current that flows through the load is given by:

$$I = I_L - I_d - I_p \quad (3.1)$$

Where: I_L is the light generated current, I_d is the diode current losses and I_p is the shunt current. The diode current is given by the expression below:

$$I_d = I_0 [\ \exp(\frac{qVd}{nkT}) - 1\ ] \quad (3.2)$$

Where: I_0 is the saturation current of the diode in Ampere (A),
q is the elementary charge of an electron $-1.6*10^{-19}$ Coulombs,
n is the ideality factor (1 or 2),
k is a Boltzmann's constant $1.381*10^{-23}$ J/K,
T is the temperature in Kelvin (°K) and
V_d is the voltage across the diode in Volts (V) and it is given by $V_d = V + IR_s$.

According to Kirchoff's Voltage Law, the shunt current is given by the expression:

$$I_p = \frac{V+IRs}{Rp} \quad (3.3)$$

Therefore, the overall expression of the load current I generated by a single solar cell is given by (3.4) below:

$$I = I_L - I_0 [\ \exp(\frac{q(V + IRs)}{nkT}) - 1\ ] - \frac{V+IRs}{Rp} \quad (3.4)$$

However, the I-V characteristics of a PV panel containing N_s series solar cells and N_p parallel solar cells are given by the following equation [71]:

$$I\ (1 + \frac{R_s}{R_p}) = N_p I_L - N_p I_0\ [\ \exp(\{\ \frac{q}{nkT}\ (\frac{V}{N_s} + IR_s)\ \}) - 1\ ] - \frac{V - N_s}{R_p} \quad (3.5)$$

Due to the large value of the parallel resistance R_p, it is usually neglected to simplify the model. R_p can be assumed to be equal to an infinity resistance. Hence, the equation (3.5) becomes:

$$I = N_p I_L - N_p I_0\ [\ \exp(\{\ \frac{q}{nkT}\ (\frac{V}{N_s} + IR_s)\ \}) - 1\ ] \quad (3.6)$$

The light generated current is proportional to the solar radiation and is assumed to be linearly based on the solar cell surface temperature T. It is given by [71]:

$$I_L = \{\ I_{SC} + k_i\ (T - T_{STC})\ \}\ \frac{G}{G_{STC}} \quad (3.7)$$

Where: I_{SC} is the short-circuit current in Ampere,
k_i is the short-circuit current temperature coefficient (Ampere/°K),
T_{STC} is the reference temperature 298 °K,
G is the solar radiation (W/m^2) and
G_{STC} is the reference solar radiation 1000 W/m^2.

The saturation current I_0 varies with the variation of the solar cell surface temperature T. It is given by [71]:

$$I_0 = I_{STC} \left(\frac{T}{T_{STC}}\right)^3 \exp\left\{\frac{q\,E_{gap}}{nk}\left(\frac{1}{T_{STC}} - \frac{1}{T}\right)\right\} \quad (3.8)$$

Where: I_{STC} is the reverse saturation current at temperature T_{STC} and solar radiation G_{STC},
E_{gap} is the energy band gap. For silicon it is $E_{gap} \approx 1.1$ eV.

Given the equation (3.4), the I-V characteristics can be represented graphically as shown in the following figure.

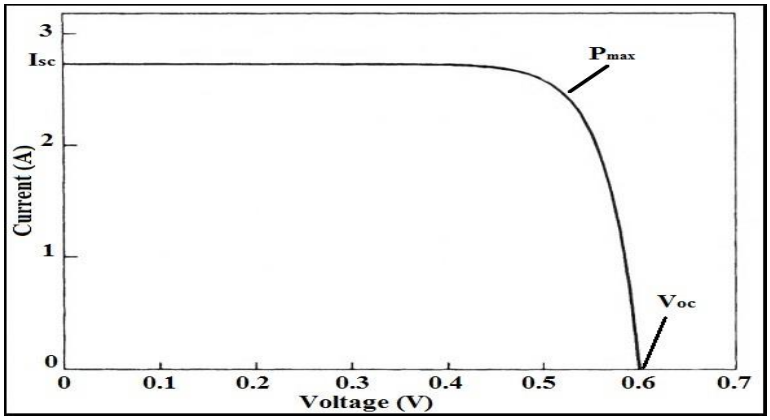

Source: [103].

Figure 3.4: Typical I-V curve for a solar PV cell.

From the I-V characteristics of the PV cell, the specific electrical parameters of the cell are deduced:
- ***The open-circuit voltage V_{oc}:*** occurs when there is no current that passes through the solar cell V (I = 0). It is the maximum voltage available between the cell's terminals.
- ***The short-circuit current I_{sc}:*** this is the maximum current that the solar cell can generate. It occurs when the cell is short circuited I (V = 0).
- ***The output power P_{out}:*** it is given by the multiplication of the current and the voltage.

$$P_{out} = V * I = V * \left\{ I_L - I_0 \left[\exp\left(\frac{q(V + IR_S)}{nkT}\right) - 1 \right] - \frac{V + IR_S}{R_p} \right\} \quad (3.9)$$

The output power reaches its maximum at P_{max} called the Maximum Power Point. The corresponding current and voltage are designated as I_m and V_m, respectively.
- ***The Maximum Power Point P_m:*** it is the point in the I-V curve at which maximum power is being generated by the solar cell. This point occurs on the "knee" of the I-V curve. Mathematically, this point can be found by differentiating the equation of the output power (3.8) with respect to the voltage and equating to zero. After solving the equation, this yields:

$$P_m = V_m * I_m \quad (3.10)$$

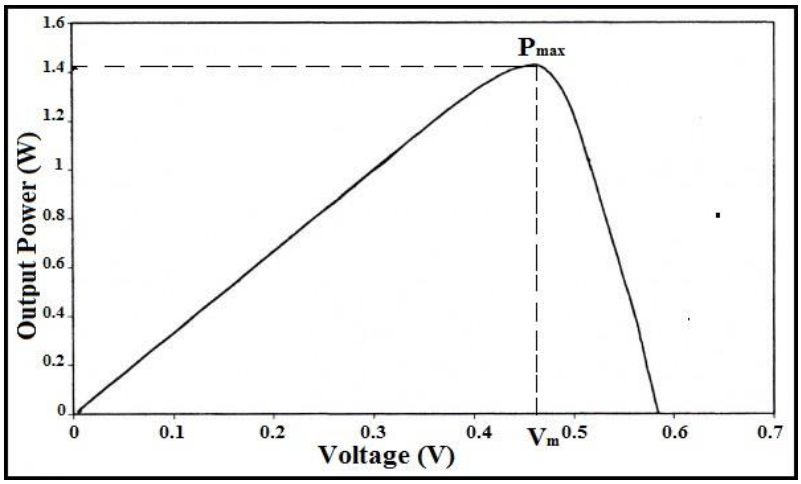

Source: [103]

Figure 3.5: Typical output power vs. Voltage for a PV cell.

- ***The Fill Factor FF:*** It measures the rectangular character of the I-V curve; it determines the quality electrical cell. A bigger fill factor is desirable. It is given by:

$$FF = \frac{V_m * I_m}{V_{oc} * I_{sc}} \quad (3.11)$$

- ***The efficiency η:*** it is the ratio of the output power P_{out} and the input power to the solar cell P_{in}. Pout in this case is Pmax since the PV cell can operate till its maximum power output to have a maximum efficiency.

$$\eta_{max} = \frac{P_m}{P_{in}} = \frac{FF * V_{oc} * I_{sc}}{P_{in}} \quad (3.12)$$

3.2.1.3. PV Module Output Power Modeling

Due to the changing in the meteorological conditions, the output power of a PV module varies for different days in different seasons. In order to have better understanding of the PV system performance, sufficient information on the daily and seasonal pattern must be known before. The power output of a single PV module can be obtained from equation (3.9), however there exists another model that takes in into account the effect of both solar radiation and temperature. This model is explained below.

The PV module voltage V_{mod} and current I_{mod} are obtained using the equation (3.13) and equation (3.14) below:

$$V_{mod} = N_s * V \quad (3.13)$$

$$I_{mod} = N_p * I \quad (3.14)$$

Where: I and V are obtained from the I-V characteristics equation (3.4).
Therefore, the power output of a single PV module is given by:

$$P_{pv,mod} = V_{mod} * I_{mod} \quad (3.15)$$

However, the output power of PV module while considering the temperature and solar radiation fluctuations is given by the equation below [72]:

$$P_{pv,mod} = P_{pv,STC} * f_{PV} * \frac{G_T}{G_{STC}} * [\, 1 + \alpha_p \, (T_{cell} - T_{cell,STC}) \,] \quad (3.16)$$

Where: $P_{pv,STC}$ is the module rated power at Standard Test Conditions STC,

f_{PV} is PV derating factor that applies to the PV module power output to show the drop of the power in real operating conditions,

α_p is the module power temperature coefficient,

$T_{cell,STC}$ is the cell temperature at STC,

GT is the hourly solar radiation and

T_{cell} is the cell temperature and is given by [72]:

$$T_{cell} = T_{amb} + [\, \frac{(NOCT-20)}{800} \,] * G_T \quad (3.17)$$

Where: T_{amb} is the ambient temperature in °C,

NOCT is the normal cell temperature in °C usually specified by the manufacturer.

In equation (3.16), G_T represents the total hourly radiation on a fixed inclined surface. When computing the hourly output of a PV module, the hourly solar radiation G which can be obtained from weather stations, has to be converted to that on the solar PV module G_T. The total hourly radiation G_T is assumed to be the combination of the beam radiation, the diffuse radiation and ground-reflected radiation (See Figure 3.6) [73].

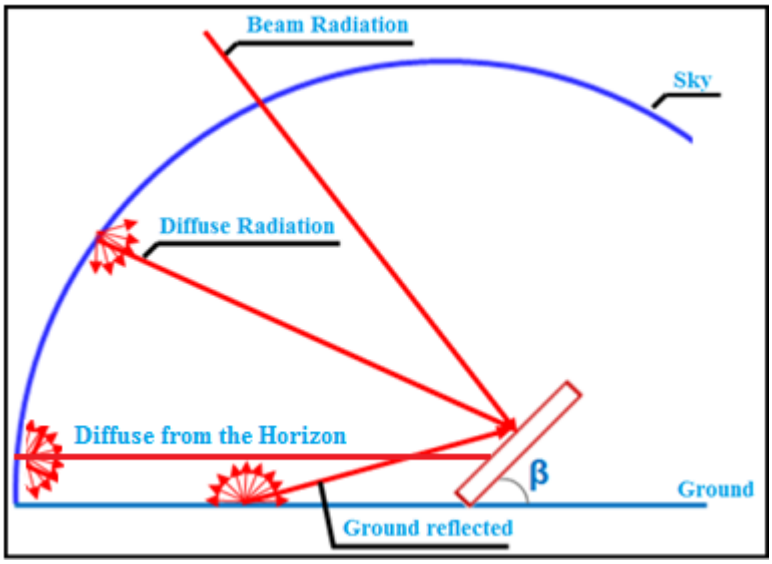

Figure 3.6: Beam, diffuse and ground-reflected radiation on an inclined surface [73].

Therefore, the total hourly solar radiation on the titled surface with an angle β at latitude φ is given by the HDKR model (the Hay, Davies, Klucher, Reindl model) [73]:

$$G_T = (G_b + G_d * A_i)\, R_b + G_d\, (1 - A_i)\, (\frac{1+\cos\beta}{2})\, [1 + f_{PV} * \sin^3 (\frac{\beta}{2})] + G * \rho_g * (\frac{1-\cos\beta}{2}) \quad (3.18)$$

Where R_b is the ration of the beam radiation to that on a horizontal surface and it is given by:

$$R_b = \frac{\cos\theta}{\cos\theta_z} = \frac{\cos(\varphi - \beta)\cos\delta\sin\omega + \sin(\varphi - \beta)\sin\delta}{\cos\varphi\ cos\ \delta\sin\omega + \sin\varphi\ \sin\delta} \quad (3.19)$$

Where: θ is the angle of incidence between the beam radiation on the surface and the normal to that surface, θz is the zenith angle between the vertical and line to the sun.

δ is the solar declination angle in n the number of the day when January 1st is aqual to 1. It is given by the following equation:

$$\delta = 23.45 * \sin\left(360 * \frac{284 + n}{365}\right) \quad (3.20)$$

ω is the hour angle which is the sun's angular deviation from the south and it is given by:

$$\omega = 15° * (\text{Solar time} - 12) \quad (3.21)$$

The solar time is the time based on the apparent angular motion of the sun with solar noon (the time when the sun crosses the observer's meridian) [73]. It is given by:

$$\text{Solar time} = \text{standard time} + 4 * (L_{st} - L_{loc}) + E \quad (3.22)$$

Where L_{st} is the standard meridian for the local time zone, L_{loc} is the longitude of the location. E is a parameter in minutes which is calculated from the equation below:

$$E = 229.2 * (0.000075 + 0.001868\cos B - 0.032077\sin B - 0.014615\cos 2B - 0.04089\sin 2B) \quad (3.23)$$

Where B is found from the equation (3.24)

$$B = 360 * \frac{n-1}{365} \quad (3.24)$$

As stated before, f_{PV} is the derating factor and can be calculated using the equation below:

$$f_{PV} = \sqrt{\frac{G_b}{G}} \quad (3.25)$$

In HDKR model, some of the diffuse radiations are taken into account as horizontal diffuse that is to be considered as forward scattered; they are treated to be incident at the same angle as the beam radiation G_b [73]. This explains the presence of the anisotropy index A_i. A_i becomes high under clear conditions and zero when there are no beam radiations. It is given by:

$$A_i = \frac{G_b}{G_0} \quad (3.26)$$

G_0 is the extraterrestrial solar radiation on horizontal surface in one hour between the hour angles ω_1 and ω_2 in [kJ/m^2.h]. G_0 should be calculated first in order to find the beam and the diffuse radiations on the horizontal surface and it is determined by:

$$G_0 = \frac{12*3600*G_{sc}}{\pi} * \left(1 + 0.033 * \cos\left(\frac{360*n}{365} \right) \right) * \left(\cos\varphi * \cos\delta * \left(\sin\omega_1 - \sin\omega_2 \right) + \frac{\pi*(\omega 1 - \omega 2)}{180} * \sin\varphi * \sin\delta \right) \quad (3.27)$$

Where: G_{sc} is the solar constant and equals to 1367 W/m^2.

Once the extraterrestrial solar radiation on horizontal surface G_0 is determined, the hourly clearness index k_T is calculated using equation (3.28) below. The hourly clearness index is the ratio of the hourly solar radiation G and the extraterrestrial solar radiation on horizontal surface G_0.

$$k_T = \frac{G}{G_0} \quad (3.28)$$

Finally, the diffuse radiations G_d can be obtained depending on the value of k_T calculated above.

$$\frac{G_d}{G} = \begin{cases} 1.0 - 0.09 * k_T & \text{for} \quad k_T \leq 0.22 \\ 0.9511 - 0.1604*k_T + 4.388*k_T^2 - 16.638*k_T^3 + 12.336*k_T^4 & \text{for} \quad 0.22 < k_T \leq 0.80 \\ 0.165 & \text{for} \quad k_T > 0.80 \end{cases} \quad (3.29)$$

Hence, the value of the diffuse radiations is:

$$G_d = \frac{G_d}{G} * G \quad (3.30)$$

The value of the beam radiation is just:

$$G_b = G - G_d \quad (3.31)$$

The overall produced power output by an array of N_{pv} number of panels is given by:

$$P_{pv} = N_{pv} * P_{pv,mod} \quad (3.32)$$

The performance of PV module degrades annually because of the moisture presence and the effect of shading. The module type and the manufacturer are the main factors that affect the degradation rate. It has been suggested that the annual degradation of a PV module performance can attain 0.01% [72].

3.2.1.4. Effect of Temperature on PV Module I-V Characteristics

As stated before, the performance of the solar cell and its output parameters (voltage, current, power, Fill Factor) are largely dependent on the environmental conditions. Temperature affects the electricity flow in the electrical circuit. This is can be done by changing the speed at which the electrons move. Mainly, the voltage parameters are affected by the module temperature. Both the open-circuit voltage V_{oc} and the maximum voltage V_m decrease when the module temperature decreases. This can be explained by the increase in the circuit resistance. The short-circuit current I_{sc} increases slightly which

can be ignored. The decrease in the silicon solar cell is around 2 mV/°C and the temperature effect on the Maximum Power Output P_{max} is -0.005 mW/°C [74].

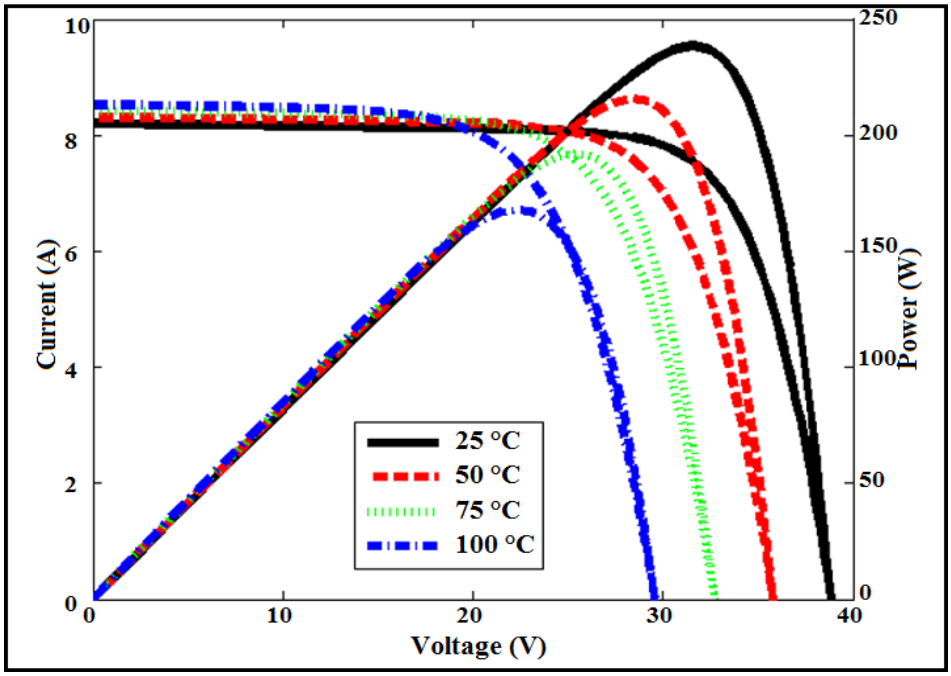

Figure 3.7: Temperature effect on the P-V and I-V curves of a PV module [76].

3.2.1.5. *Effect of Irradiance on PV Module I-V Characteristics*

The solar irradiation, which is the measure of the sun's energy, has an influence on the PV cell performance due to its variation time to time. The amount of irradiance decreases in hazy days and becomes smaller on over cast days. The solar cell current, which is directly proportional to the solar irradiance as shown by the equation (3.7), is the most affected parameter. In contrast, the voltage varies slightly and is usually ignored.

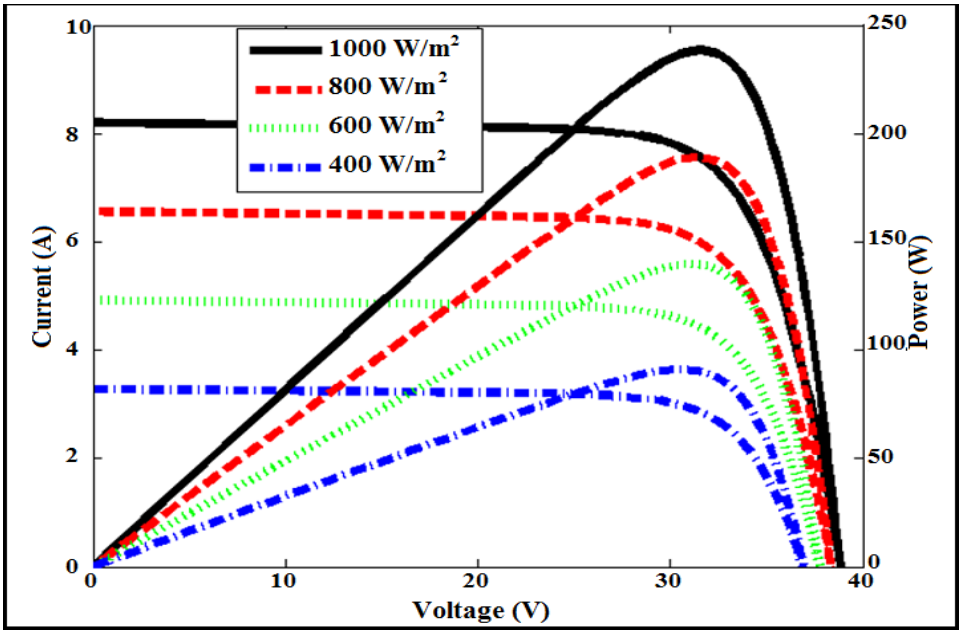

Figure 3.8: Irradiance effect on the P-V and I-V curves of a PV module [76].

3.2.1.6. *Effect of Connection Type on PV Module I-V Characteristics*

There are three types of PV cell connection: a simple serial configuration block, a parallel configuration block, and a serial connection of series-parallel configuration blocks [75]. The desired configuration of the cell interconnection circuit for producing the energy required for a given application is obtained by calculating the number of cells in series to generate the requested voltage, and the number of rows in parallel to produce the requested current.
The following figure is a representation of the I-V characteristic of a single cell, two cells in series and two cells in parallel.

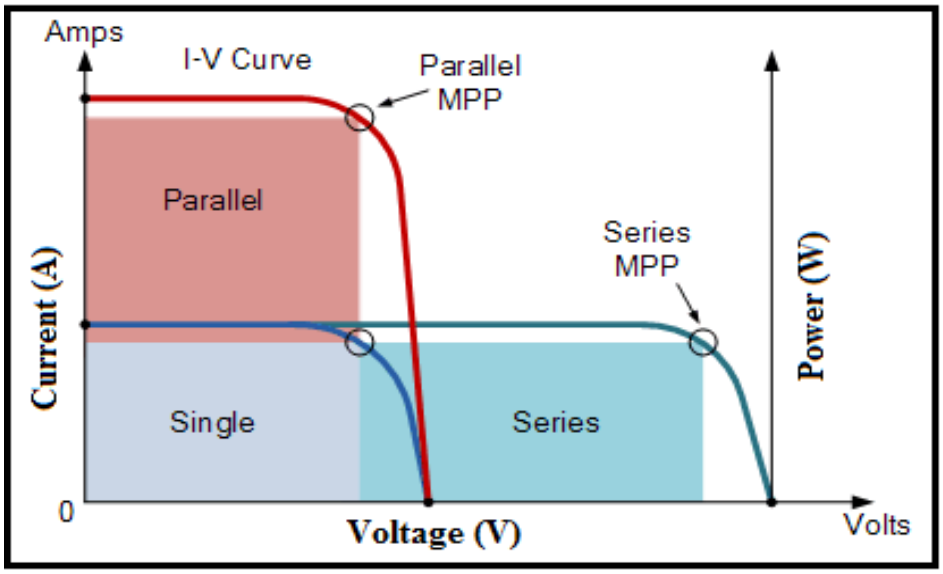

Source: [104].

Figure 3.9: Connection effect on the I-V curve of a PV module.

3.2.1.7. *Effect of Series Resistance on PV Module I-V Characteristics*

In general, the typical value of a PV cell series resistance R_s is very low. In order to see the effect of this resistance, the author in [77] performed a simulation using three different values of R_s which are 1 mΩ, 5 mΩ and 10 mΩ, respectively. The simulation was done under STC. As a result, the variation of the series resistance affects the deviation of the maximum power output of the solar cell and the module as well. However, all of the open-circuit voltage V_{oc} and the shot-circuit current I_{sc} did not change.

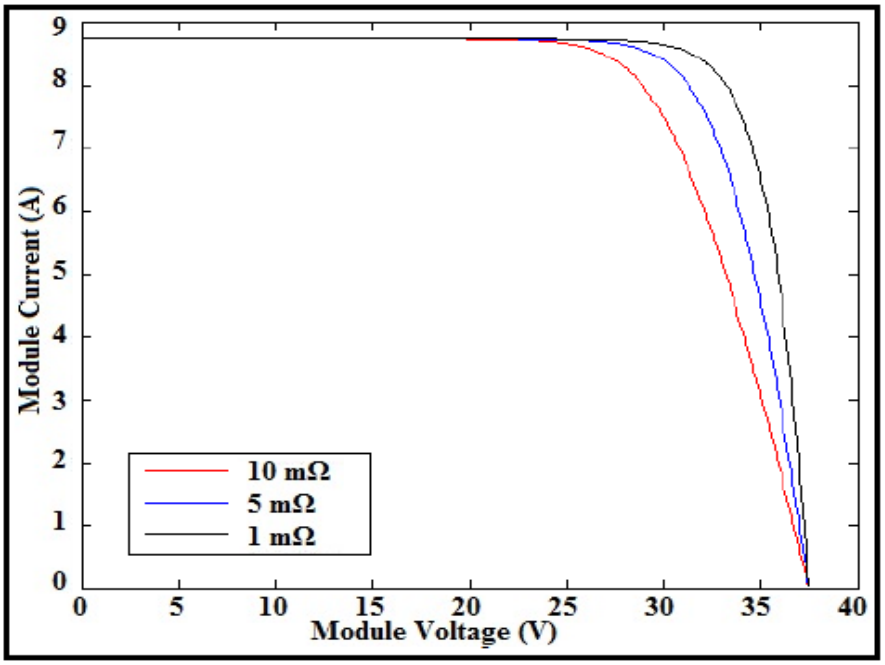

Figure 3.10: Series Resistance variation effect on the I-V curve of a PV module [77].

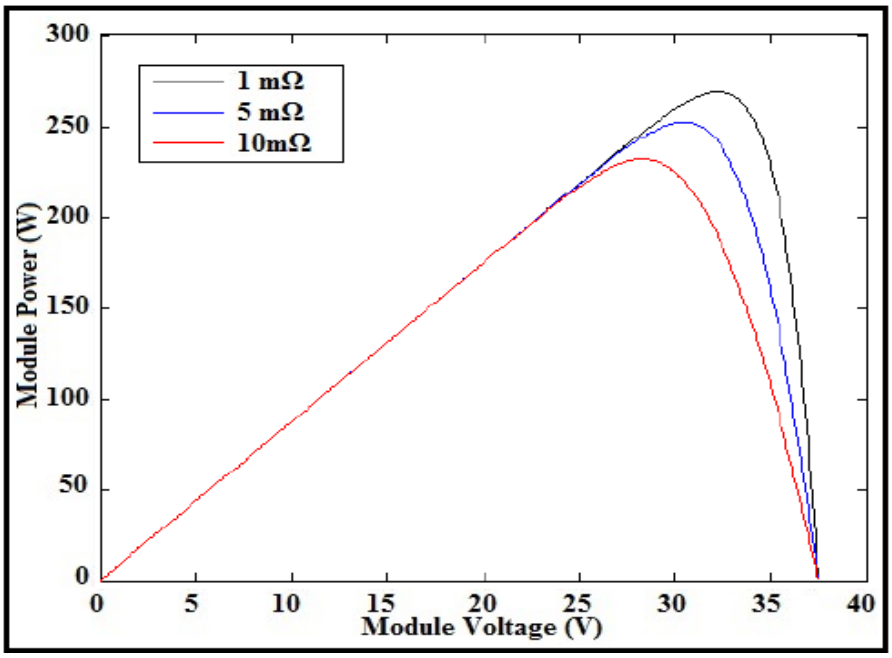

Figure 3.11: Series Resistance variation effect on the P-V curve of a PV module [77].

3.2.1.8. Effect of Parallel Resistance on PV Module I-V Characteristics

Generally, the value of the solar cell parallel resistance R_p should be large enough to reach the maximum power output from the PV module. Again the effect of the parallel resistance is studied in [77] where three different values of such resistance were used: 1Ω, 10Ω and 1000Ω. The results are shown in Figure 3.12 and Figure 3.13 below. It can be seen clearly that the output current decreases when R_p decreases. As a result, a high power loss is caused. In addition, The R_p variation affects the deviation of the maximum power output of the solar cell and the module as well.

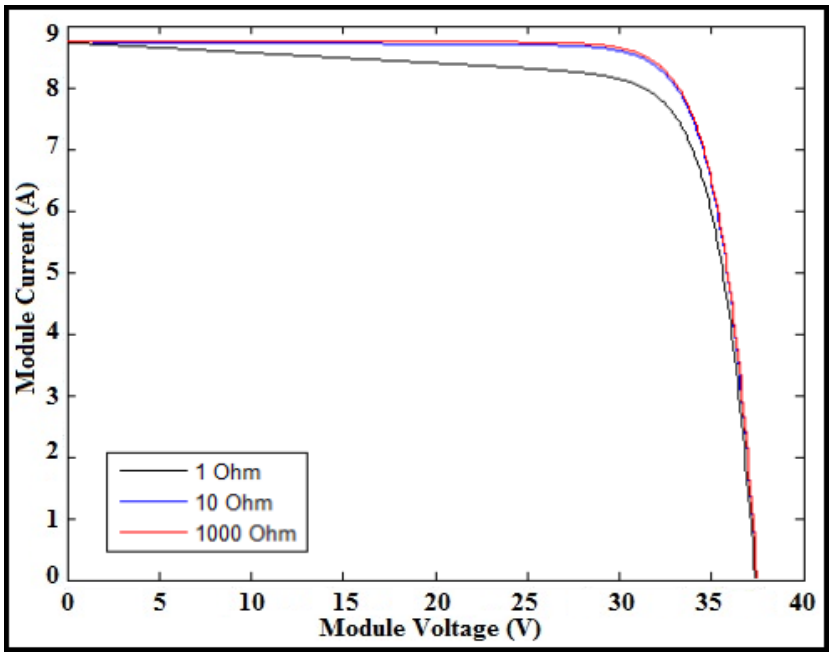

Figure 3.12: Parallel Resistance variation effect on the I-V curve of a PV module [77].

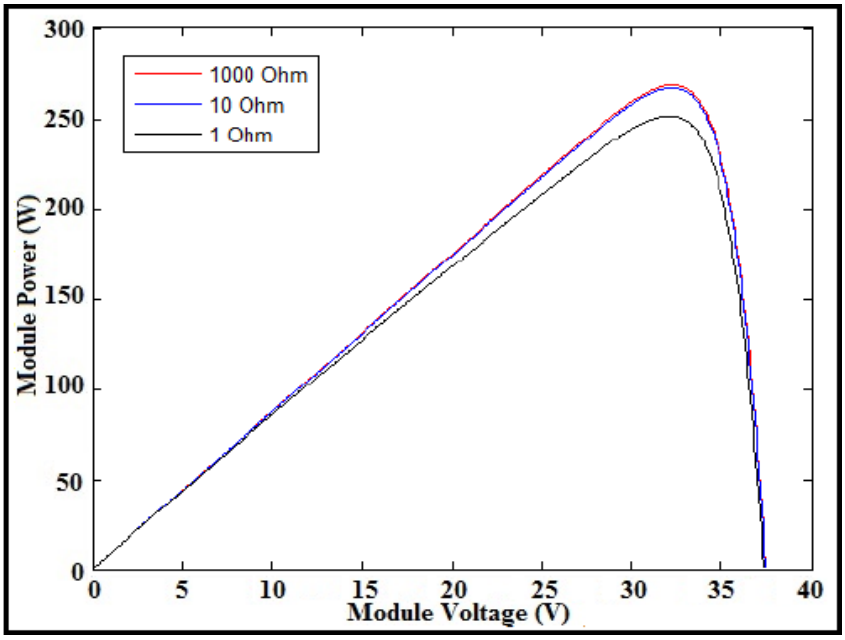

Figure 3.13: Parallel Resistance variation effect on the P-V curve of a PV module [77].

3.2.2. Diesel Generator Model Development

Diesel generators can be modeled mathematically in two (2) ways either by using dynamic model when smaller time-steps (seconds) are considered or linear model when dealing with bigger time-steps (hours). In our work, the second model is used since this model describes the performance of a diesel generator with enough accuracy [78]. Since the time-step of one (1) hour is commonly used when analyzing the techno-economical performance of a hybrid power system, the most familiar model used to express the fuel consumed with respect to the output electrical power of the diesel generator is linear. In most cases, this linear relationship, which helps to calculate the fuel consumption at any load supplied by generator, can be provided by the generator manufacturer. In linear model, it is usually assumed that the response provided by the diesel generator is instantaneous [78].

The diesel generator fuel consumption depends on the generator size and the load at which it operates. The linear equation that gives the fuel consumption $fuel_{cons}$ in [units/h] vs. the output power $P_{a\text{-}DG}$ in [kW] is described by the equation below [79]. The unit of the fuel consumption can be kg/h, l/h or m^3/h.

$$fuel_{cons} = \alpha_{DG} P_{n\text{-}DG} + \beta_{DG} P_{a\text{-}DG} \quad (3.33)$$

Where: α_{DG} and β_{DG} are the coefficients of fuel consumption curve in [units/h*kW],
$P_{n\text{-}DG}$ is the nominal capacity of the diesel generator [kW].

The efficiency of the diesel generator η_{DG} is defined as the ratio of the power output and the heating value of the fuel consumption [79].

$$\eta_{DG} = \frac{P_{a\_DG}}{Fuel_{cons} * LHV_{fuel}} \quad (3.34)$$

Where: LHV_{fuel} is the Lower Heating Value (or Lower Calorific Value) of the fuel used in [kWh/units].

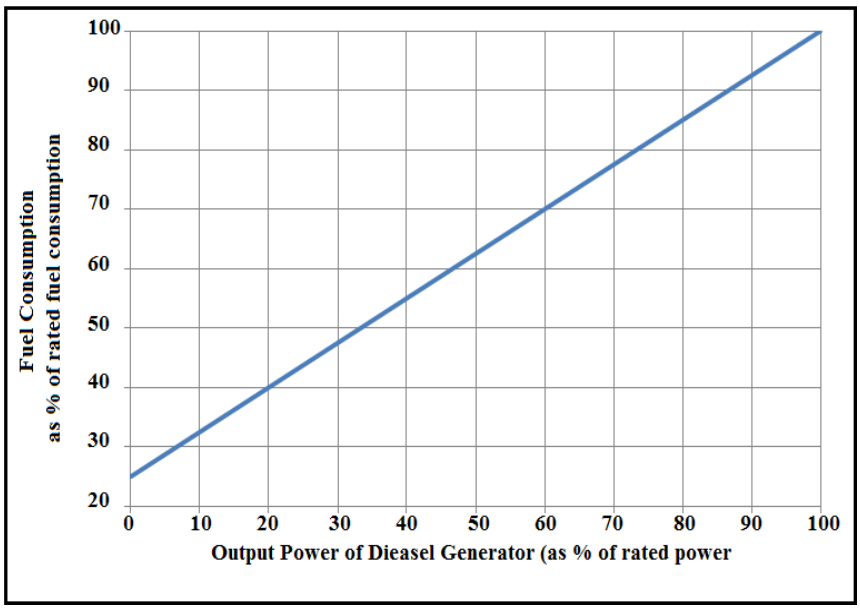

Figure 3.14: Fuel consumption vs. output power of a diesel generator [79].

The Figure 3.14 shows the fuel consumption plotted versus the power output as described by the equation (3.33). The plot is a straight line where the y-intercept shows no-load fuel consumption of the generator, and the slope reflects the marginal consumption of that generator. The coefficient of fuel consumption α_{DG} and β_{DG} can be obtained from the plot.

$$\alpha_{DG} = \frac{y\text{-}intercept}{P_{n\_DG}} \quad (3.35)$$

$$\beta_{DG} = \text{slope of the straight line} \quad (3.36)$$

3.2.3. CO_2 Emission Mathematical Model

Since diesel generator is used in our hybrid power system, hence CO_2 is the most exhausted gas by the system. In this study, the number of kilograms produced by the diesel generator is taken in consideration to denote the pollutant emission. For each time period during a year, the emission of CO_2 is calculated using the equation below:

$$CO2_{emission} = \sum_{t=1}^{8760} fuel_{cons}\,(t) * EF \tag{3.37}$$

Where: EF is the diesel generator emission factor that depends on the diesel engine characteristics and the type of the fuel used.

3.2.4. Electrolyser Development Model

As stated in the previous chapter, there are mainly two commercialized electrolyser technologies: the alkaline water electrolyser and the Proton Exchange Membrane PEM electrolyser. The alkaline electrolyser, which will be used in this work for hydrogen production, is the most widely used technology for water electrolysis. This type of electrolysers is advantageous; it can be made of abundant and inexpensive materials like nickel and iron.

The performance of the alkaline electrolyser can be studied using its V-I characteristics (polarization curve) which can be obtained by plotting the cell voltage V_{cell} versus the current density J_{cell}. The hydrogen production in the electrolyser is impossible under the reversible voltage; the cell voltage should be always larger than the reversible voltage ($V_{cell} > V_{rev}$). Hence, there are some primary sources that increase the cell voltage since the electrolysis process is considered irreversible [80]. The primary sources are:

- ✓ The electrolyte ohmic loss,
- ✓ Overvoltage associated with oxygen,
- ✓ Overvoltage associated with hydrogen,
- ✓ The electrodes and circuitry ohmic loss.

As a result, the cell voltage can be obtained as the sum of the overvoltages that appear in the cell and the reversible voltage.

$$V_{cell} = V_{rev} + V_{act} + V_{ohm} \tag{3.38}$$

Where V_{act} is the activation overvoltage and V_{ohm} is the ohmic loss overvoltage.

3.2.4.1. Reversible Cell Voltage

Based on the chemical equation of electrolysis, a minimum electric voltage is applied to both electrodes of the electrolyser. This voltage is referred to as the reversible voltage and can be determined using Gibbs equation [81].

$$\Delta G = zFV_{rev} \tag{3.39}$$

Where ΔG is the Gibbs energy, z is the number of electrons and F is the Faraday's Constant.

The Gibbs equation can be rearranged to get the reversible voltage.

$$V_{rev} = \frac{\Delta G}{zF} \tag{3.40}$$

At standard conditions, the Gibbs energy used for splitting water equals to 237.21 $kJ.mol^{-1}$, the Faraday's constant equals to 96485.37 $C.mol^{-1}$ and z is just 2. Therefore, V_{rev} is found to be:

$$Vrev = \frac{237.21*1000}{2*96485.37} \tag{3.41}$$

$$V_{rev} = 1.229\ V \tag{3.42}$$

3.2.4.2. *Activation Overvoltage*

The activation voltage V_{act} is produced due to the electrochemical kinematics of both the anode and the cathode during the simultaneous half-reactions. Energy is required to transfer electric charges between the electrodes and the chemical species. This transfer of electric charges is highly dependent on the catalytic properties of the electrode materials. The presence of such transfer leads to generate an overvoltage across the electrode which is referred as activation overvoltage. This latter is given by the following equation [81]:

$$V_{act} = (s_1 + s_2 * T + s_3 * T^2) * \log (\frac{t_1 + \frac{t_2}{T} + \frac{t_3}{T^2}}{A} * I + 1) \tag{3.43}$$

Where:

s_1, s_2, s_3, t_1, t_2, t_3 are the coefficient for overvoltage on electrodes,
I is the current density,
T is the cell temperature and
A is the electrode area.

3.2.4.3. *Ohmic Loss Overvoltage*

This kind of overvoltages corresponds to the ohmic losses inside the cell. These losses are due to the elements of the cell such as electrodes, separating diaphragm and the different interconnections. The ohmic loss overvoltage V_{ohm} can be reduced by shortening the distance between the cathode and the anode. It is proportional to the current that flows through the cell and it is given by [81]:

$$V_{ohm} = \frac{r_1 + r_2 * T}{A} * I \tag{3.44}$$

Where: r_1 and r_2 are parameters that have a relationship with the electrolyte ohmic resistance.

Hence, the cell voltage equation (3.38) becomes:

$$V_{cell} = V_{rev} + (s_1 + s_2 * T + s_3 * T^2) * \log (\frac{t_1 + \frac{t_2}{T} + \frac{t_3}{T^2}}{A} * I + 1) + \frac{r_1 + r_2 * T}{A} * I \tag{3.45}$$

The V-I characteristic of an alkaline electrolyser cell is shown in the following figure.

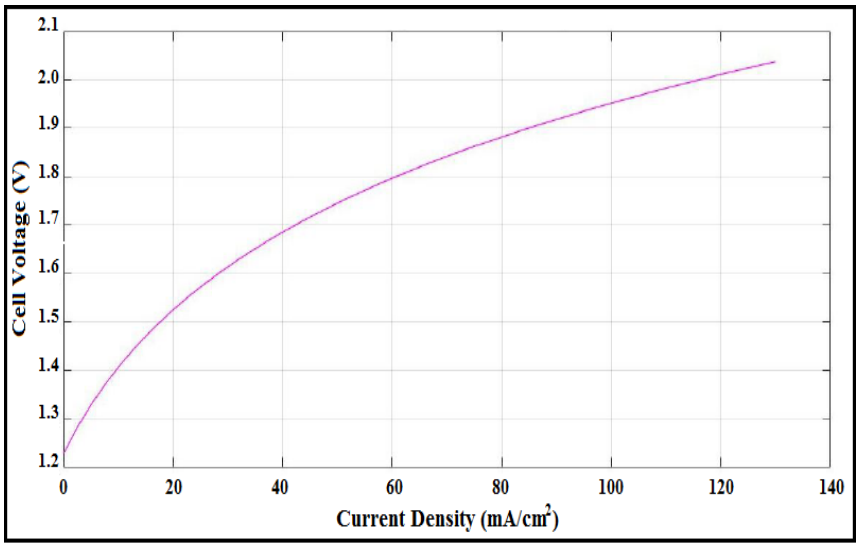

Figure 3.15: The V-I characteristic of an alkaline electrolyser [82].

The P-I characteristic of an alkaline electrolyser cell is shown in the following figure.

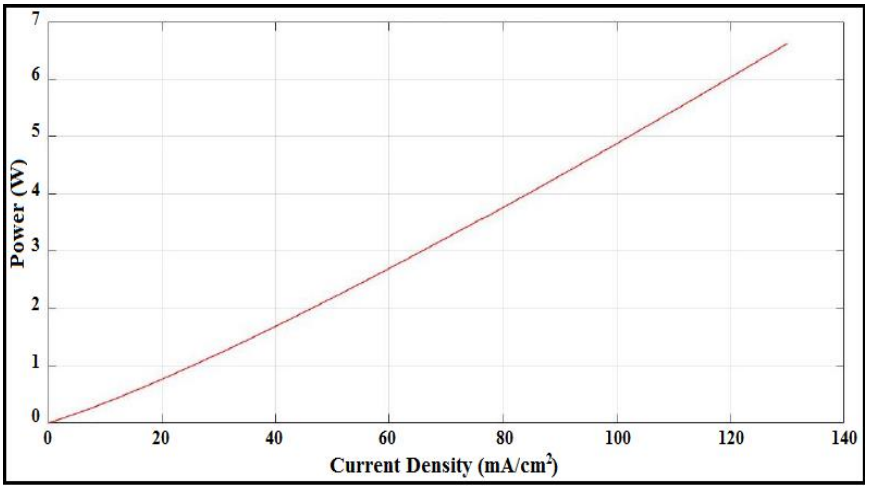

Figure 3.16: The P-I characteristic of an alkaline electrolyser [82].

3.2.4.4. *Hydrogen Production Rate*

The hydrogen production rate inside the alkaline electrolyser is directly proportional to the electrical current I. It can be determined by the following equation [83].

$$\dot{n}_{H2} = \eta_F * \frac{N_c}{zF} * I \quad [mol/s] \tag{3.46}$$

Where N_c is the number of cells inside the electrolyser, η_F is the Faraday's efficiency which is the ratio of the real and the theoretical maximum amount of hydrogen produced by the electrolyser. The Faraday's efficiency decreases when the temperature increases and it is given by the following empirical expression:

$$\eta_F = \left(\frac{I_{density}^2}{a_1 + I_{density}^2} \right) * a_2 \tag{3.47}$$

Where $I_{density}$ is the current density, a_1 and a_2 are empirical parameters.

The flow rate can be expressed in other units as follows:

$$Q_{H2} = \dot{n}_{H2} * 3600 * 0.022414 \ [Nm^3/h] \quad (3.48)$$

$$Q_{H2} = \dot{n}_{H2} * 3600 * 0.022414 * 0.08988 \ [kg/h] \quad (3.49)$$

3.2.4.5. Alkaline Electrolyser Power Consumption

In the alkaline electrolyser, hydrogen and oxygen gases are produced from water using electrical energy. This electrical energy $Elec_{EL}$ [kW] can be modeled as a function of the nominal hydrogen mass flow ($Q_{n\text{-}H2}$) [kg/h] and the actual hydrogen mass flow (Q_{H2}) [kg/h] as shown by the following equation [78]:

$$Elec_{EL} = \alpha_E * Q_{n\text{-}H2} + \beta_E * Q_{H2} \quad (3.50)$$

Where: α_E and β_E are coefficient of electrical consumption curve per hydrogen mass flow in [kW/kg/h].

3.2.4.6. Alkaline Electrolyser Efficiency

The efficiency of the alkaline electrolyser is given by [83]:

$$\eta_{alk} = \eta_F * \eta_e \quad (3.51)$$

Where η_e is the energy efficiency which can be calculated from the thermoneutral voltage V_{tn} and the cell voltage V_{cell}:

$$\eta_e = \frac{V_{tn}}{V_{cell}} \quad (3.52)$$

3.2.5. Hydrogen Storage Development Model

In literature, several hydrogen storage models were proposed. In these models, different state equations have been used to predict the behavior of hydrogen at high pressures. Figure 3.17 shows three different graphs of the hydrogen density versus pressure of three different models: the ideal gas model, the Van Der Waals model and the compressibility factor of hydrogen model. It can be seen clearly that up to 150 bar, the graphs of the three models are identical. However, when the pressure exceeds 150 bar, the ideal gas model deviates the other two models [84].

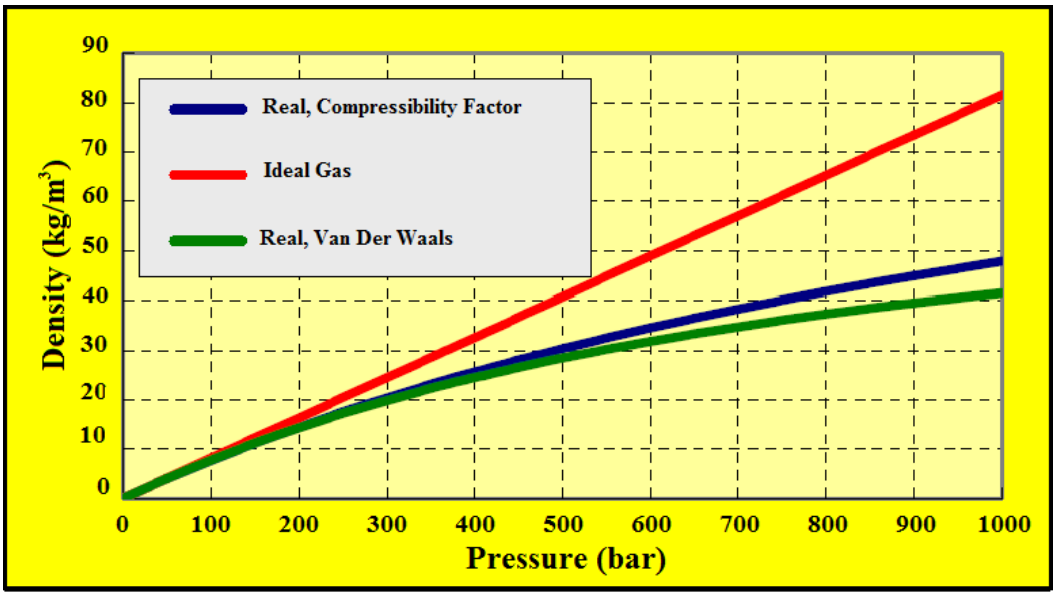

Figure 3.17: Hydrogen density versus pressure for three models [84].

There are mainly two different systems to store hydrogen gas. The first one is to run the electrolyser at high pressure and the hydrogen is already compressed for storing it. Such approach does not need additional energy input to store hydrogen. Nonetheless, high pressures may generate large amount of hydrogen crossover owing to higher gas solubility. As a result, the storage system becomes less efficient. The second approach is to run the electrolyser at ambient pressure and store the hydrogen using a compressor. This system does not show high hydrogen crossover and considers the storage tank as the only high pressure subsystem. However, the compressor consumes energy which can be considered a disadvantageous for this system. Generally for hydrogen storage, systems with low pressure are more favorable than high pressure systems.

In our work, the low pressure hydrogen system is used for modeling. The electrolyser produces an amount of hydrogen which is sent to the storage tank using a compressor. Applying the law of conservation of mass which is the fundamental law that governs the dynamics of the storage tank, the following equation is given [83]:

$$\frac{dm(t)}{dt} = \dot{m}_{H2\_in} - \dot{m}_{H2\_out} \tag{3.53}$$

Where: $\dot{m}_{H2\_in}$ is the input hydrogen mass flow rate [kg/unit of time],
$\dot{m}_{H2\_out}$ is the output hydrogen mass flow rate [kg/unit of time] and
m(t) is the total mass of hydrogen at time t [kg] where:

$$\frac{dm(t)}{dt} = V\frac{d\rho}{dt} \tag{3.54}$$

Where: ρ is the density of the gas [kg/m^3], V is the volume of the storage [m^3].

The relationship between pressure (p) [N/m^2], density and the temperature (T) [K] is given by the ideal gas law:

$$p = \rho * R_{h2} * T \tag{3.56}$$

Where: R_{h2} is the hydrogen gas constant R_{h2} = 4124.18 N.m.K^{-1}.kg^{-1}.

All of the pressure, the density and the temperature are functions of time. Using the Chain Rule of Partial Differentiation:

$$\frac{d\rho}{dt} = \frac{\partial\rho}{\partial p} \cdot \frac{dp}{dt} + \frac{\partial\rho}{\partial T} \cdot \frac{dT}{dt} \tag{3.57}$$

T is constant therefore:

$$\frac{dT}{dt} = 0 \tag{3.58}$$

Using equation (3.56), and by taking the derivative with respect to pressure:

$$\frac{d\rho}{dp} = \frac{1}{R_{h2} * T} \tag{3.59}$$

Replacing all of (3.58) and (3.59) in equation (3.57):

$$\frac{d\rho}{dt} = \frac{1}{R_{h2} * T} \cdot \frac{dp}{dt} \tag{3.60}$$

Replacing (3.60) in the equation of total mass (3.54):

$$\frac{dm(t)}{dt} = V \frac{1}{R_{h2} * T} \cdot \frac{dp}{dt} \tag{3.61}$$

Hence, the mathematical model of the hydrogen storage is given by the equation below:

$$\frac{dp}{dt} = \frac{R_{h2} * T}{V} * (\dot{m}_{H2\_in} - \dot{m}_{H2\_out}) \tag{3.62}$$

The unit of pressure in this case is [N/m^2] or simply [pa].

3.2.6. Hydrogen Compressor Model Development

The aim of the compressor is to fill the hydrogen storage at the desired pressure for sake of increasing the storage capacity. It is difficult to model the mechanical work required for compression since hydrogen does not behave as an ideal gas at high pressures. In addition, the compression process is performed in stages with cooling between these stages. To simplify the model, hydrogen compression is considered as isentropic process; i.e. the process is adiabatic and reversible [85].

Generally, the compressor model is based on an ideal gas in a quasi-equilibrium compression process. It is based also on a two stage polytropic compression with inter-cooling process. A polytropic process describes the pressure-volume relationship during compression and it is expressed as:

$$(pV)^{\gamma} = \text{constant} \tag{3.63}$$

Where: γ is the polytropic coefficient which equals 1.4 in case of hydrogen gas.

The isentropic specific work of the compressor w_{comp} needed for compressing hydrogen gas from pressure p_1 [pa] to pressure p_2 [pa] is:

$$w_{comp}\ (\text{isentropic}) = \frac{R_{h2} * T_1 * \gamma}{\gamma - 1} \left[\left(\frac{P_1}{P_2}\right)^{\wedge}\left(\frac{\gamma - 1}{\gamma}\right) - 1 \right] \quad [\text{J/kg}] \tag{3.64}$$

Where: T_1 is the temperature of the hydrogen in [K] at pressure p_1.

However, since the adiabatic compression of hydrogen is an irreversible process, isentropic efficiency of the compressor ηisentropic, which has a value approximated to 75%-80% can be taken into consideration for deviation from the ideal behavior. So, the actual specific work of the compressor is given by [85]:

$$w_{com}\ (\text{actual}) = \frac{w_{com\ (isentropic)}}{\eta_{isentropic}} \quad [\text{J/kg}] \tag{3.65}$$

Therefore, the power required to drive the compressor P_{comp} in [W]is given by:

$$P_{comp} = \frac{w_{actual}}{3600 * \eta_c} * Q_{H2} \tag{3.66}$$

Where: η_c is the compressor efficiency and,
Q_{H2} is the flow rate of the hydrogen and is given by equation (3.49).

3.2.7. Power Conditioning Equipment Model development

Power conditioners are devices that can function as DC/DC converters, or they can also invert DC power to AC power and/or vice versa. In hybrid power systems, such devises are mostly used either to invert the voltage from DC to AC for AC current applications or transfer DC power from one voltage to another [86].

In power conditioners, the power loss P_{loss} can be modeled. It is mainly dependent on the electrical current flowing through it. The proposed model of the power loss for a power conditioner is given below [86]:

$$P_{loss} = P_{in} - P_{out} = P_0 + \frac{V_s}{V_{out}} * P_{out} + \frac{R_i}{V_{out}^2} * P^2_{out} \tag{3.67}$$

Where: P_{in} and P_{out} are the power input and power output respectively in [W],
P_0 is the power loss when there is a voltage across the power conditioner [W],
V_s is the set point voltage [V],
V_{out} is the voltage output in [V] and,
R_i is the internal resistance [Ω].

By normalizing the equation (3.67) above with respect to the nominal power P_{nom} [W] of the power conditioner, a convenient expression between the input power and the output power can be obtained as shown in the equation below [86]:

$$\frac{P_{in}}{P_{nom}} = \frac{P_0}{P_{nom}} + \left(1 + \frac{V_s}{V_{out}}\right)\frac{P_{out}}{P_{nom}} + P_{nom} * \frac{R_i}{V_{out}^2} * \left(\frac{P_{out}}{P_{nom}}\right)^2 \tag{3.68}$$

The power conditioner can have either the input power P_{in} or the output power P_{out} can be assigned as input. If P_{out} is the input then the equation (3.68) is used straightforward. However, if P_{in} is the input,

then an equation analytically derived from equation (3.68) will be used. Consequently, this makes the model numerically robust.

The efficiency of the power conditioner is given simply

$$\eta_{pc} = \frac{P_{out}}{P_{in}} \tag{3.69}$$

The output current can be expressed as:

$$I_{out} = \frac{P_{out}}{V_{out}} \tag{3.70}$$

3.3. Hybrid Power System Economics Modeling

Hybrid power system economics has an important role in simulation process in HOMER, in which the system is operated so as the total Net Present Cost NPC is minimized. In addition, the economics of HPS are used in the HOMER's optimization process, in which it looks for the system combination that has the lowest total NPC. The technical modeling of any HPS is insufficient. Economical issues are essential when selecting the final choice of the combination of components during the design [87].

Renewable and conventional energy sources have noticeably different cost characteristics. Renewable sources are likely to have high initial capital costs but low operating costs, however, non-renewable sources tend to have low initial capital costs but high operating costs. Therefore, both capital and operating costs should be taken into consideration [87].

HOMER calculates mainly two key economic indicators when running the simulations: the total NPC and the Levelized Cost of Energy LCOE.

3.3.1. Total Net Present Cost Modeling

Total Net Present Cost is defined as the costs' present value minus the revenue' present value during the lifetime of the project. The costs, which are positive values, comprise capital costs, replacement costs, operating and maintenance costs (O&M), fuel costs, emissions penalties, and the cost of purchasing power from the grid. Revenues, which are negative, comprise salvage value and income from selling power to the grid. Therefore, total NPC, in contrast with the Net Present Value NPV, is considered always as a positive value. HOMER utilizes the total NPC to denote the system's life-cycle cost. It is calculated by adding the total discounted cash flows in each year of the lifetime of the project [88].

In HOMER, it is assumed that all prices rise at the same rate over the lifetime of the project. Therefore, the user can factor out the inflation of the analysis by the use of the real interest rate rather than the nominal interest rate. In addition, the user has to specify for each component the initial capital cost at year zero, the replacement cost at the end of the component lifetime and the O&M cost each year of the project lifetime. Moreover, the modeler has to specify also the lifetime of the components [87].

The total NPC is the main economic output of HOMER; it is the value by which the system configurations are ranked in the optimization results. It is given by the equation below:

$$C_{NPC,tot} = \frac{C_{ann,tot}}{CRF(i,R_{proj})} \quad [\$] \tag{3.71}$$

Where: CRF(i, R_{proj}) is the Capital Recovery Factor. It is used to calculate the present value of an annuity (a series of equal annual cash flows) and is given by [88]:

$$CRF\ (\ i, N\ ) = \frac{i\ (1+i\ )^N}{(\ 1+i\ )^N - 1} \tag{3.72}$$

Where: N is the number of years,

i is the annual real interest rate which is the discount rate used for converting between one-time costs and annualized costs in [%]. It is related to the nominal interest rate by:

$$i = \frac{i\prime - f}{1+f} \tag{3.73}$$

Where: *i'* is the nominal interest rate [%]; the rate at which money can be borrowed and,

f is the inflation rate [%].

$C_{ann,tot}$ is the total annualized cost [$/yr]. It is found by summing the annualized costs of each component, along with any miscellaneous costs (like pollutant emissions penalties). The annualized cost of each component $C_{ann,comp}$ [$/yr] is the sum of its annualized capital cost $C_{ann,cap}$ [$/yr], the annualized replacement cost $C_{ann,rep}$ [$/yr], the O&M cost [$/yr] and the annualized fuel cost if applicable [$/yr]. The annualized capital cost $C_{ann,cap}$ of each component is given by [88]:

$$C_{ann,cap} = C_{cap} * CRF(\ i, R_{proj}\ ) \tag{3.74}$$

Where: C_{cap} is the initial capital cost of the component,

- The annualized replacement cost of each component is calculated using the equation below:

$$C_{ann,rep} = C_{tot,rep} * f_{rep} * SFF(\ i, R_{comp}) - S * SFF(i, R_{proj}) \tag{3.75}$$

Where - $C_{tot,rep}$ is the total replacement cost of the component at the end of its lifetime [$],

- R_{comp} is the component lifetime [yr],

- f_{rep} should be introduced because of the project lifetime can be different than the component life time. It is given by:

$$f_{rep} = \frac{CRF\ (\ i,R_{proj}\ )}{CRF\ (\ i,R_{rep}\ )} \text{ if } R_{rep} > 0, \qquad \text{Or, } f_{rep} = 0 \text{ if } R_{rep} = 0 \tag{3.76}$$

Where R_{rep} is the replacement cost duration in [yr] and is determined by:

$$R_{rep} = R_{comp} * INT\ (\frac{R_{proj}}{R_{comp}}\ ) \tag{3.77}$$

INT () is the integer function that returns the integer part of a real value.

- SFF () is the sinking fund factor which can be used to calculate the future value of a series of equal annual cash flows. It is expressed as:

$$SFF(i, N) = \frac{i}{(1+i)^N - 1} \quad (3.78)$$

- S is the salvage value of each component in [$] which is the value remaining in a component at the end of the project. HOMER assumes that the salvage value is directly proportional to the remaining life of the component. It is given by:

$$S = C_{rep} * \frac{R_{rem}}{R_{comp}} \quad (3.79)$$

Where R_{rem} is the component remaining life in [yr] at the end of the project lifetime and it is expressed as:

$$R_{rem} = R_{comp} - (R_{proj} - R_{rep}) \quad (3.80)$$

3.3.2. Levelized Cost of Energy Modeling

The Levelized Cost of Energy LCOE is defined by HOMER as the average cost per kWh of useful electrical energy generated by the system. Therefore, LCOE is referred to as the cost of producing energy for a particular system. It is also known as Levelized Energy Cost LEC, Levelized Unit Energy Cost LUEC and Long-Run Marginal Cost LRMC. LCOE [$/kWh] is simply calculated by dividing the total annualized cost of generating electricity by the total served electric energy load. Its equation is given by [87]:

$$LCOE = \frac{C_{ann,tot}}{E_{prim} + E_{df} + E_{grid,sales}} \quad (3.81)$$

Where: E_{prim} is the annual primary that must be met by the system,

E_{df} is the annual deferrable load, the load that does not need to be met by the system at specific times throughout one year. This type of load needs a certain amount of power within a specific time period. Loads which are associated with storage are deferrable loads.

$E_{grid,sales}$ is the annual electricity which is sold to the grid.

3.4. Control Strategy of the PV-Diesel-Hydrogen Storage Hybrid System

3.4.1. Load Management Strategy

The system configuration is shown in the Figure (3.18) below. The figure depicts the required system controlling for supervising, organizing and managing the PV-Diesel-H_2 hybrid power system (only one generator is considered). The main power generator for the system is the PV generator controlled by an MPPT based on Observe and Perturb algorithm. The power generated using PV system and either one, two or three diesel generators has the priority to meet the power load demand P_{load}, the power of the electrolyser P_{elec} for hydrogen production and the self consumed power for operating system P_{op}. The operating power of the system is the power consumed by the auxiliary system

component for keeping it running such as: inverters, converters, gas compressor and control units. The diesel generators P_{DG} are used as backup power generators and are the last chance for the system to keep running. The power difference or the net power P_{net} between the generation sources and the power load demand is obtained using the equation below (where n is the number of gensets that produce power {0, 1, 2 or 3}:

$$P_{net} = P_{PV} + nP_{DG} - P_{load} - P_{elec} - P_{op} \quad (3.82)$$

The governing control strategy is given as: At any given time, , the power generated by the PV system and the generators is supplied to the load and to the electrolyser to produce hydrogen that is sent to the hydrogen storage through a gas compressor. Hence, the power balance equation can be expressed as:

$$P_{PV} + nP_{DG} = P_{load} + P_{elec} + P_{op}, \text{ when } P_{net} > 0 \quad (3.83)$$

In this case, the excess in the power can be expressed as P_{EX}:

$$P_{EX} = P_{load} - P_{PV} - nP_{DG} = -(P_{elec} + P_{op}) \quad (3.84)$$

In order to understand how the system gets a deficit power, let us consider the case where only one diesel generator runs (n = 1). The power generated by the PV system and that generator does not satisfy the load demand. In this case, the second diesel genset has to turn ON and produces P_{DG} to solve the problem in the power deficit. The hydrogen production system may continue operating. Thus, the power balance equation in this case should be:

$$P_{PV} + 2*P_{DG} = P_{load} + P_{elec} + P_{op} \quad (3.85)$$

The deficit power P_{def} can be expressed as

$$P_{def} = P_{load} - P_{PV} = P_{DG} - P_{op} - P_{elec} \quad (3.86)$$

However, in case where there is any default in the PV system in which it should be turned OFF (emergency), the diesel generator becomes the only source of power generation. The same thing applies when there is no sun (during the night). In such conditions, the genset supplies only the load and the electrolyzer may use some power to produce hydrogen (the hydrogen production occurs for few hours during nighttimes). The purpose of this is to reduce the power demand in order to reduce the diesel generator's hours of operation. In case of defaults in the PV system, some appliances should be

forced to turn off to reduce more the operation hours of the generator. Therefore, the power balance is given by the equation:

$$nP_{DG} = P_{load} + P_{op}' \quad (3.87)$$

Where: P_{op}' is the self consumed operating power when the hydrogen production process is OFF ($P_{op}' < P_{op}$).

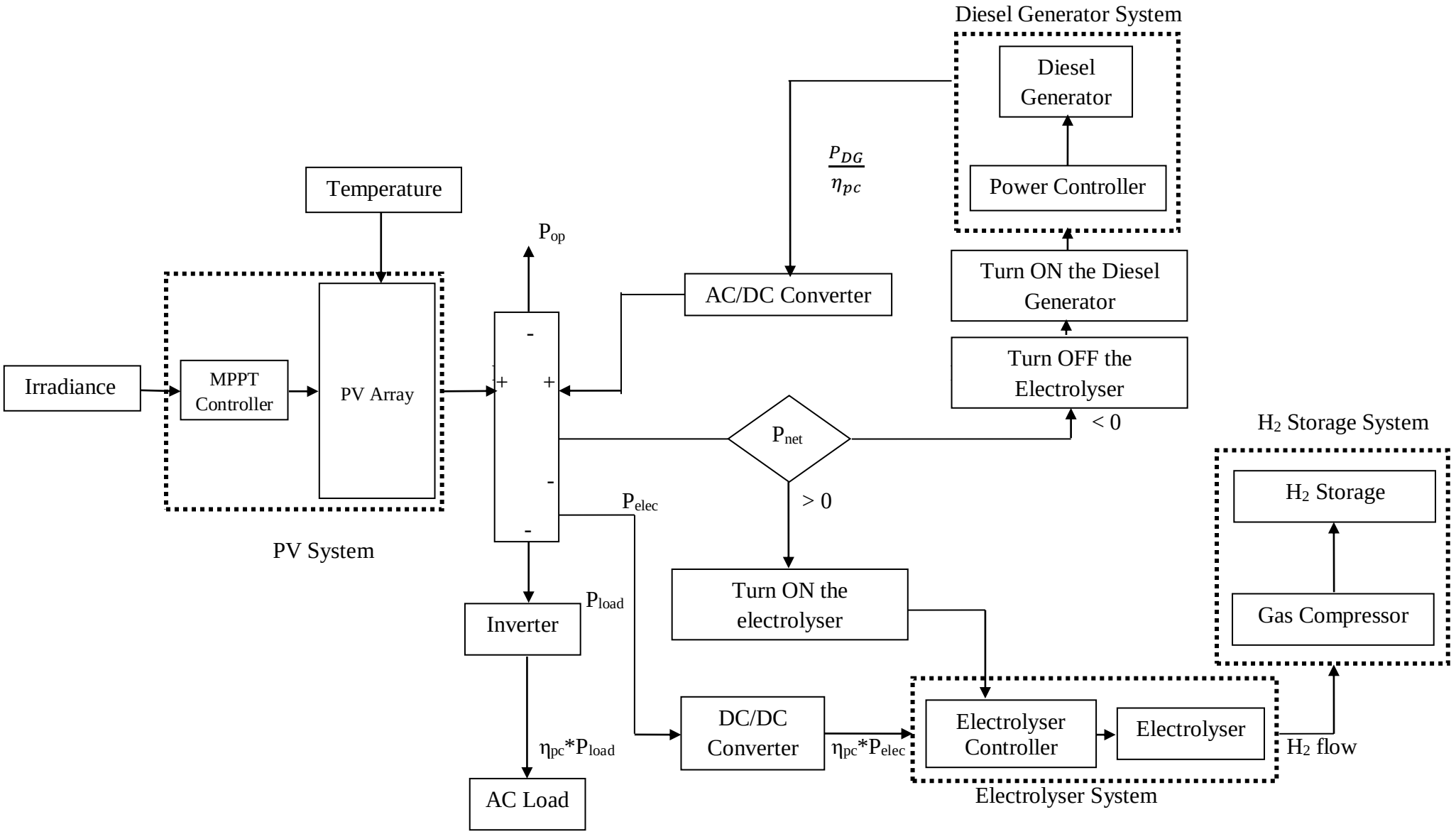

Figure 3.18: Hybrid power system control strategy diagram

3.4.1. Modes of Operation

The PV-Diesel-H_2 hybrid power system generates the operation points based on current photovoltaic, diesel generators, load conditions and actual limitations of the hydrogen sub-system. These limitations comprise the maximum and the minimum power consumption of the electrolyser ($P_{elec,max}$, $P_{elec,min}$), and the hydrogen tank maximum pressure ($p_{H2,max}$). The operating modes are summarized in the following table.

Table 5: The hybrid power system operation modes

Mode	Operating Conditions
Mode 1	• The output power from PV and the diesel generator (n=0, 1, 2 or 3) is higher than the load demand ($P_{PV} + nP_{DG} > P_{load}$). • High level of stored hydrogen ($p_{H2} \approx pH_{2,max}$). • High level energy consumption by the electrolyser ($P_{elec} \approx P_{elec,max}$).
Mode 2	• The output power from PV and the diesel generator (n=0, 1, 2 or 3) is higher than the load demand ($P_{PV} + nP_{DG} > P_{load}$). • The excess power fraction can be kept in the storage device.
Mode 3	• The output power from PV and the diesel generator (n=0, 1, 2 or 3) is higher than the load demand ($P_{PV} + nP_{DG} > P_{load}$). • The excess power can be retailed in the hydrogen storage.
Mode 4	• Emergency condition, no PV power due to a system fault or no solar energy (night times). • Only diesel generator supplies the required power. • Low level energy consumption by the electrolyser ($P_{elec} \approx P_{elec,max} \approx 0$).

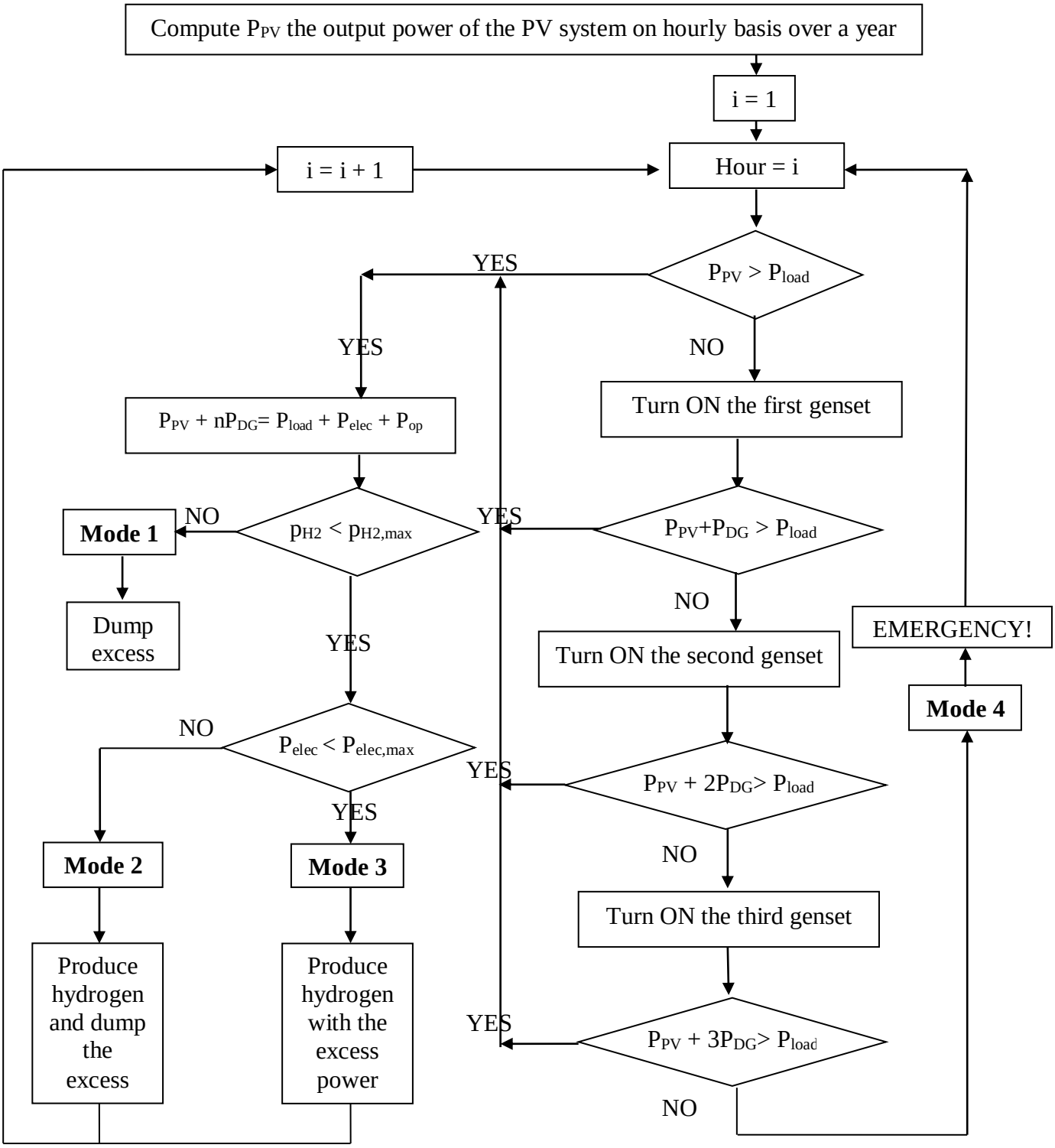

Figure 3.19: Power Management Strategy PMS of the system.

3.4.2. MPPT Control Algorithm

In this work, the Perturb and Observe P&O MPPT algorithm is used. The flow chart of such algorithm is shown in the following figure where ΔD is the incremental step of duty cycle in switching mode DC-DC converter that can be varied between 0 and 1. By controlling the converter duty cycle, the operating point is forced towards the PV array MPPT.

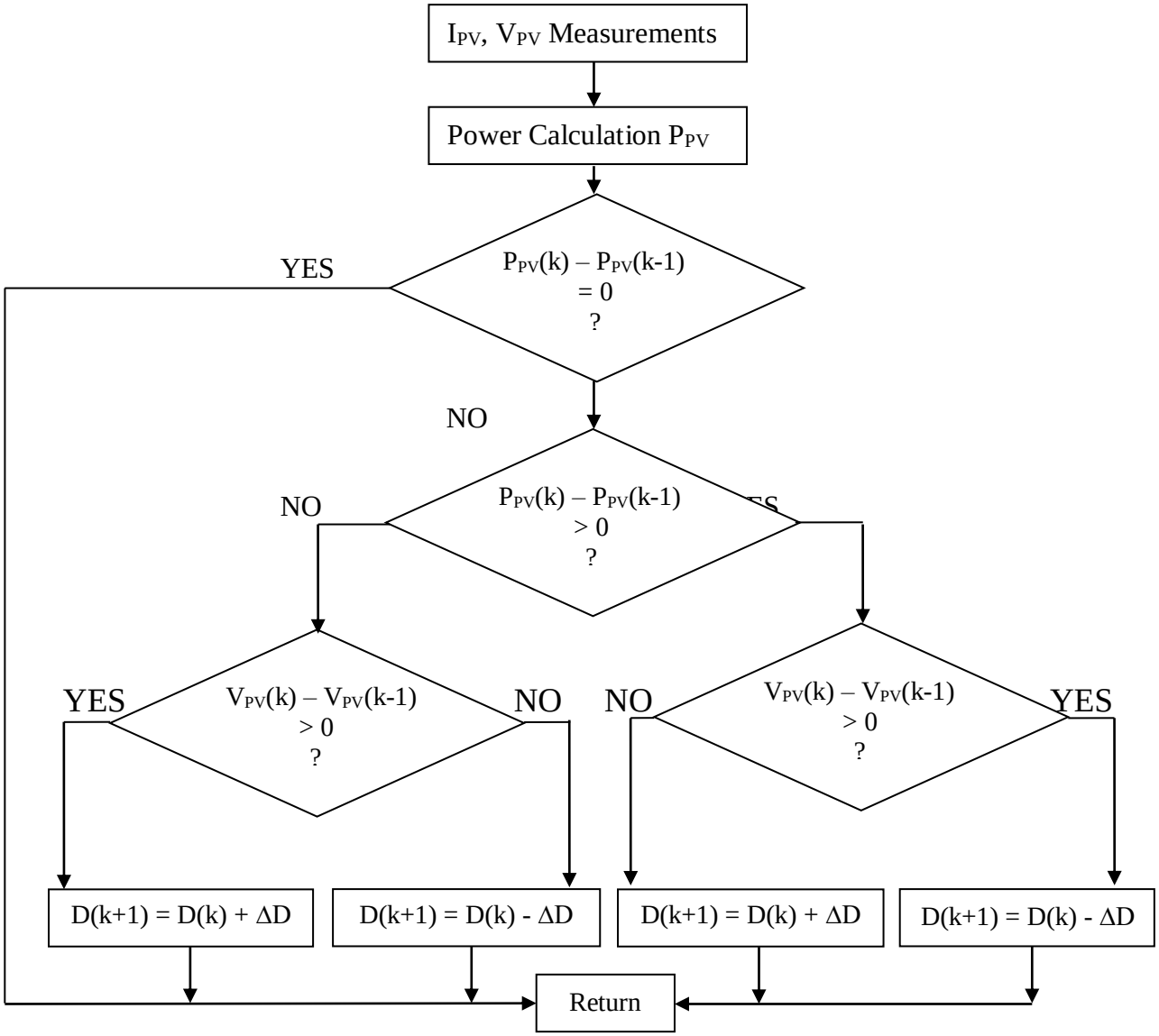

Figure 3.20: MPPT algorithm flowchart.

4.1. Introduction

In the previous chapter, the economic and the components models of the PV-Diesel-H_2 storage Hybrid Power System were described in detail. All the models are based on hourly values; they can be categorized as hourly model. In order to investigate the application of the proposed hybrid power system, this chapter presents a designed case study where Algeria is chosen.

4.2. Approach Procedure

After studying the different configurations, classifications and components selected for the PV-Diesel-H_2 storage Hybrid Power System, we propose the following procedure. The procedure relies on the steps below:

- STEP 1: Choosing the location for the project will fix all climatic parameters and allow us to derive the load profile.
- STEP 2: Simulating using HOMER Pro. Software.
  The ultimate goal of this study is to generate technically feasible, responsive solutions that verify the availability of resources. We will analyze different possible combinations of energy choices (solar panels, conventional energy, storage device...). This analysis will allow us also to make analyses of the technical criteria (the energy produced by each source, the fraction of renewable energy, the excess in energy, the stored hydrogen...), economic (the total Net Present Cost of the project, the Levelized Cost of Energy) and the greenhouse gases emissions.
- STEP 3: Optimizing using HOMER Pro.
  The aim of this step is to find optimal system based on different decision variables by filtering out the unfeasible solutions generated from the previous step and sorting a list of hybrid power systems that meet the need of the power load by searching for the lowest Net Present Cost.
- STEP 4: Conducting sensitivity analyses
  We will define all of the minimum renewable fraction and the annual average solar radiation to be our sensitivity parametric variables. Then, we will conduct some sensitivity analyses to show the effect of these parametric variables on the project's technical and economical feasibility.

4.3. Case Study Presentation

4.3.1. Economical Data

In HOMER, some economical data have to be defined before starting the simulation. These data are:

- The annual real interest rate: 3.75%. [89]
- The expected inflation rate: 4.00% [90]
- The project life time: 25 years.

4.3.2. Geography and Climate Description

The case study for this thesis is a remote area in Wilaya of Adrar which is the second largest province located in the western south of Algeria. The area of this province covers 427,968 km^2 which represents 18% of the total area of the country. It is divided into 28 communes or districts and each commune

contains a certain number of cities and villages called K'sars. Among the K'sars, Boukazine, which is located in Commune of Talmine (north-west of the main Commune Adrar), is selected for this research. The region of Adrar has a hot desert climate according to Kppen climate classification BWh. Winters are mild with average temperature around 14 °C. Summers are very hot; the temperature can reach its maximum of 51°C. Rainfall is very light and intermittent, and summers are dry [91]. Many sites in Adrar, which are isolated and the distance between them is far way, are not connected to the grid. Thus, this leads to think of hybrid systems for generating electricity for the people living in this region.

Table 6: The geographical coordinates and climate type classification in Boukazine.

Site	Area (km^2)	Latitude	Longitude	Altitude (m)	Climate
Adrar	427,968	29°18' North	0°8' West	258	BWh

Source: Wikipedia.

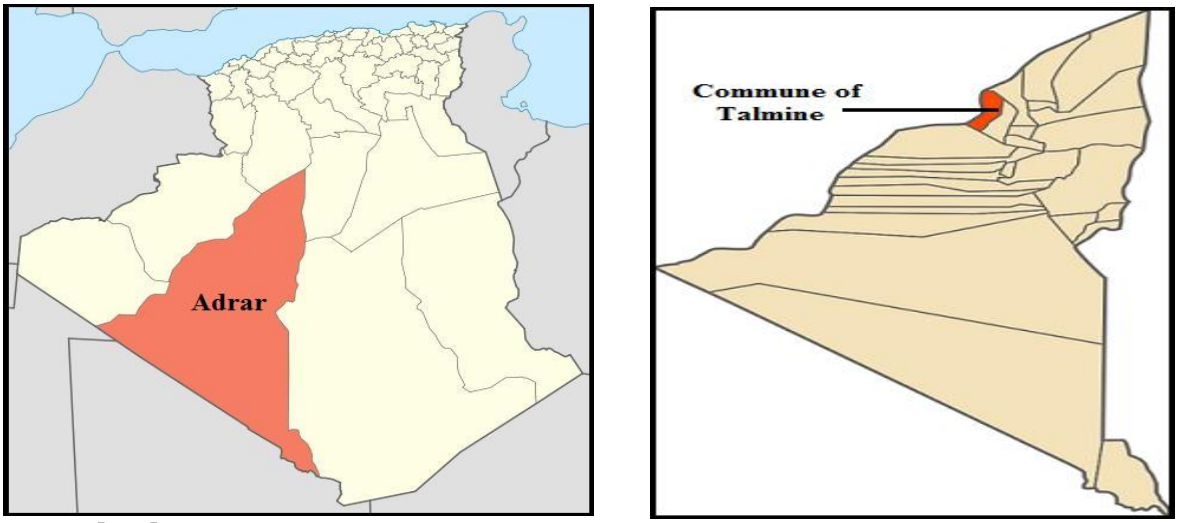

Source: [105].

Figure 4.1: Map of Wilaya of Adrar, Algeria.

Boukazine was selected as a case study due to several factors:

- Boukazine represents one of the most remote areas in Algeria which is far away from the nearest point of transmission line.
- Electricity in the region of Adrar and in the south of Algeria is provided by Isolated Grids IG. This kind of grids is electrical network, which can operate autonomously, is powered by a power plant (mainly diesel and gas turbines). Isolated Grids can facilitate the integration of renewable energy.
- The renewable sources mainly solar are widely distributed in this region and they are abundant throughout the year.
-

In this work, the simulation is done in Pavilion G15 HP computer with Intel® Core™ i3 @ 1.90 GHz, 4Go Installed RAM and 64 bits operating system. When HOMER Pro. is launched, it starts with HOMER Home screen. Here, we can choose the project location by clicking by clicking on the map or by entering the name of the location in the search box. We can also enter the project's name, author and description. The home screen contains also four key inputs: the discount rate, the inflation rate, the maximum annual capacity shortage and the project lifetime. The ribbon is organized into six tabs: load, components, resources, project, system and help. However, the HOMER interface is organized into: design, results and library.

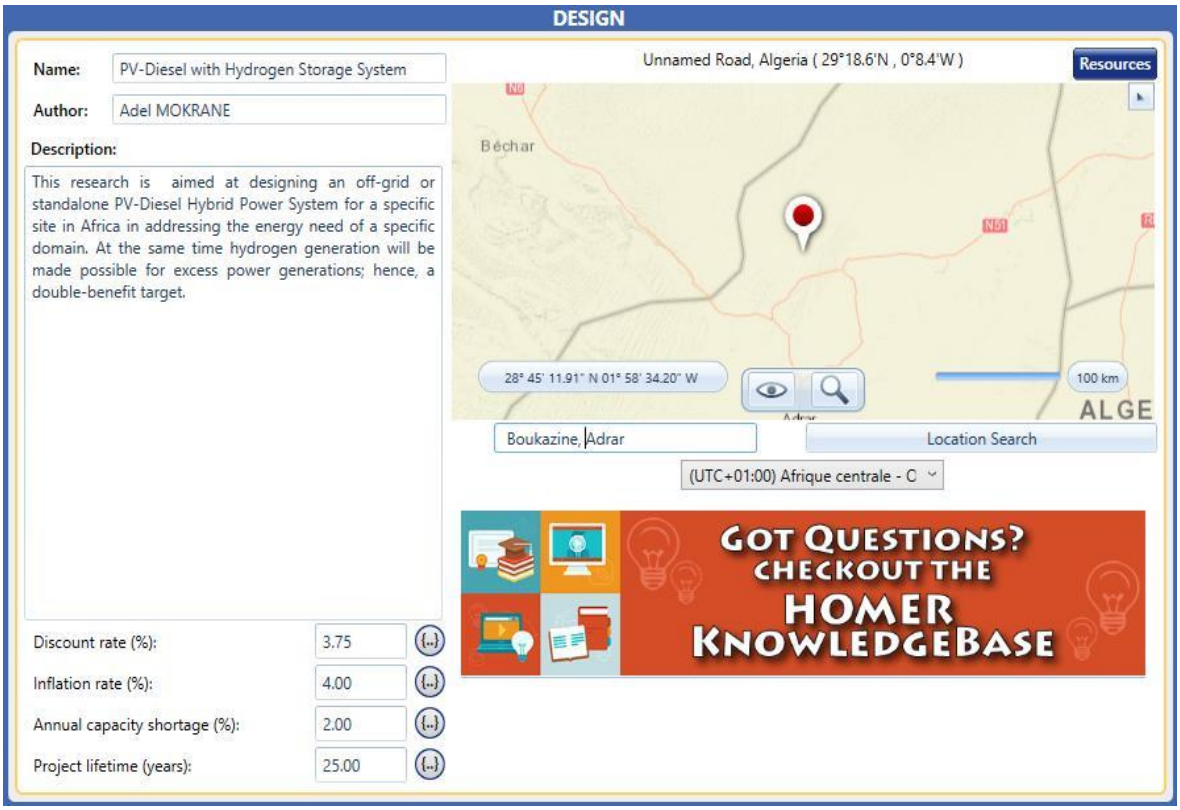

Figure 4.2: HOMER home screen.

4.3.3. Load Profile of Single Household

In this research, the hybrid power system is for providing electricity for fifteen (15) households. But first, we should obtain the load profile of a single household. In order to derive the household's load profile, which has not had electricity before, it is required to understand the conditions of the people living in Boukazine, Adrar. Other factors may play important roles in the load such as lifestyle of the people, the family income and capacity of purchasing electrical appliances. No data on energy consumption are available. Therefore, to derive the load profile of a single household, we referred literature review of load profiles available on internet of several remote area electrification projects realized in developing countries. A survey in the chosen village will be needed to collect data on energy consumption. However, existent surveyed data are unavailable. In addition, some assumptions are taken in consideration:

- ✓ The household accommodates a medium income family.
- ✓ The family consists of six (6) people as maximum according to the average occupancy of a single household in Algeria published by The National Agency for the Promotion and Rationalization of the Use of Energy APRUE [92].
- ✓ Since the village is located in a hot region, the peak load is recorded in summer due to the use of air conditioner.

The load profile of a single household in the village of Boukazine is presented in table below. The table shows the maximum load demand that can be registered during summer period (June to August). Thus, the energy consumption increases during that period and reaches 12.53 kWh/day. This increase is due to the use of air conditioning systems, and such consideration is taken into account in this study

Table 7: Daily load estimation for a single Household in Boukazine, Adrar.

Service	Space	No. in use	Power (W)	Total Power (W)	Hours/ Day	Day [Wh]	Night [Wh]
Lighting	Rooms	2	40	80	5		400
	Lounge	2	40	80	2		160
	Corridor	1	22	22	3		66
	Bathroom	1	22	22	3		66
	Toilet	1	20	20	1		20
	Kitchen	1	20	20	5		100
	Outdoor	1	40	40	2		80
Appliances	TV	1	80	80	5	160	240
	Satellite Receiver	1	20	20	5	40	60
	Lap-top	1	60	60	5	300	
	Air conditioner	1	1000	1000	4	3000	1000
	Radio	1	10	10	2	20	
	Refrigerator	1	300	300	21	4,500	1,800
	Cell Phones	2	5	10	2	20	
	Water Pump	1	500	500	1	500	
Subtotal Peak Load						**8,540**	**3,992**
Maximum Household Daily Load						**12,532 Wh/Day**	
15 Households Daily Load						**187.98 kWh/Day**	

Based on the Figure 4.3 below, which represents the annual evolution of the load curve of one of the Isolated Networks installed in the south of Algeria, an Excel sheet of 24 hours data is used in order to calculate the household's hourly load power (See Appendix A).

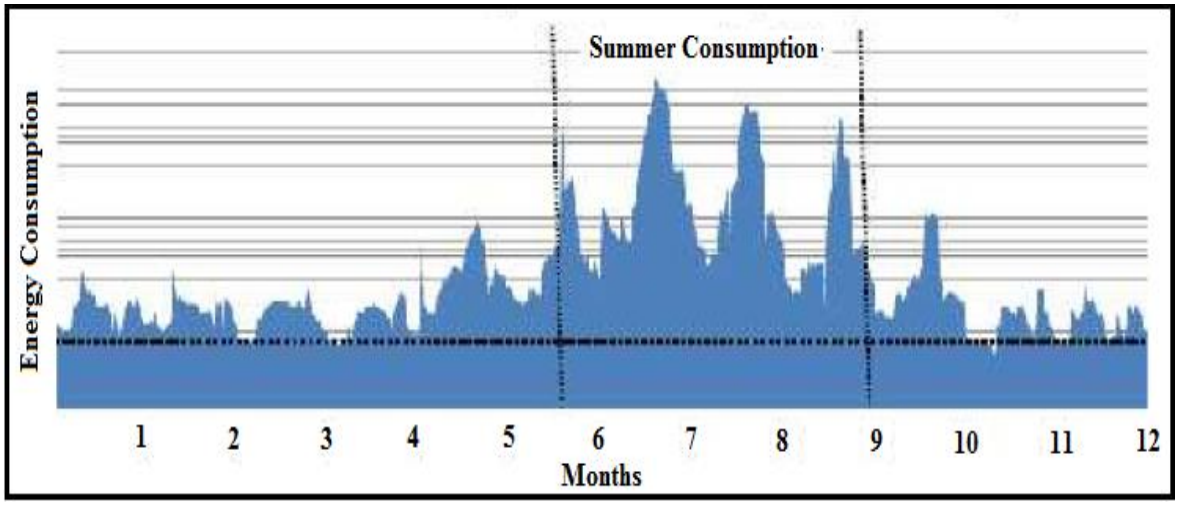

Figure 4.3: Annual evolution of the load curve of an Isolated Network (2013) [93].

The resulting monthly energy demand of a single household is shown in the following figure.

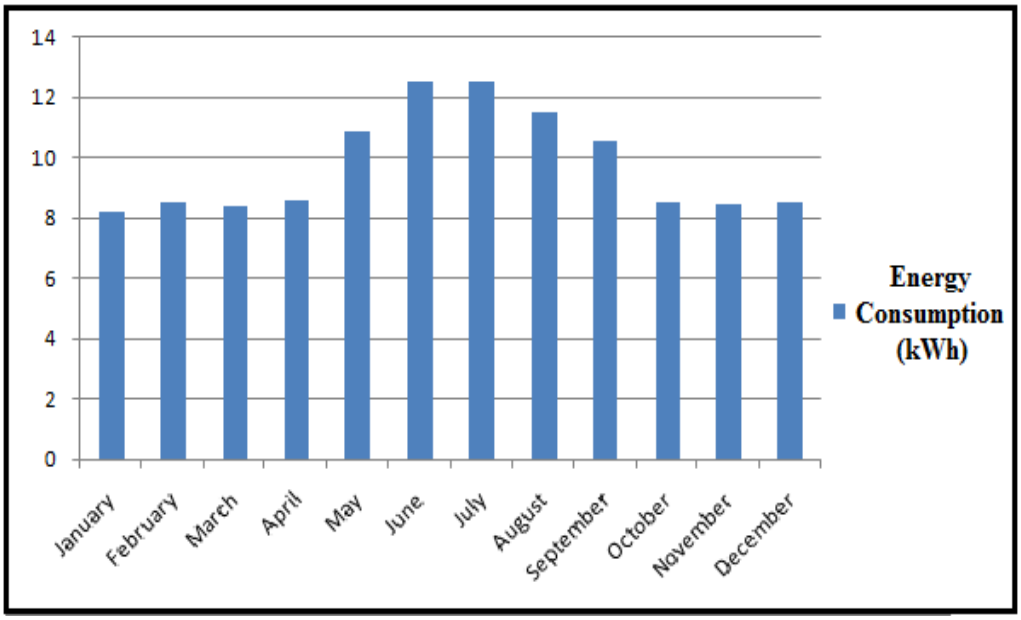

Figure 4.4: Monthly energy consumption variations.

Figure 4.5 below shows the load profile of one day in summer and another day in winter. It shows that the peak load occurs in the summer day and reaches 1.91 kW. The load experiences mainly three peaks: the first one occurs in the morning (6am to 7am) as a result of using light and preparing the breakfast, the second one in the midday where generally people come back from home for lunch and use some electric facilities (phone and laptop charging, air conditioner, water pump…), and the third one start before 7pm as it is the time most people finish their work, resulting the use of some electric facilities like radio, light, TV.

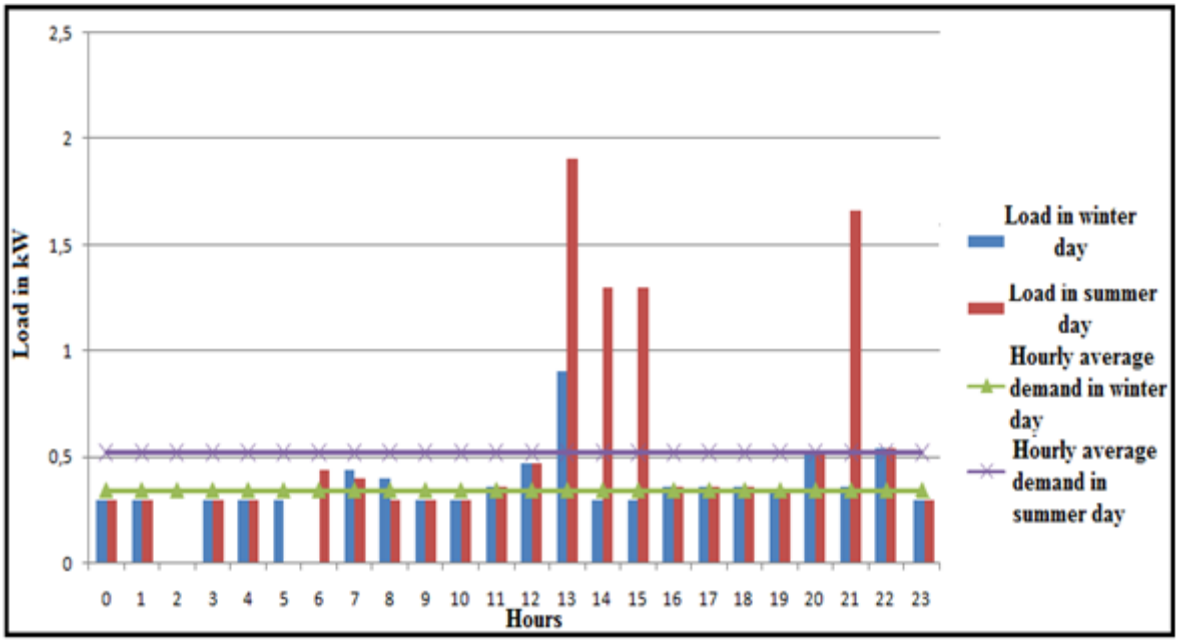

Figure 4.5: The load demand in a summer and winter day.

A new plan is required in order to get the monthly and annual profile for 15 households. This can be done in Excel by copying the monthly hourly load demand of single household to new linked cells and multiplying by 15 households supplied by the system (see appendix A).

The monthly hourly load profile for the 15 households created in Excel can be used to create synthetic load from that profile. Since we do not have more details of the load profile, so we have to approximate what the load looks like. The synthetic load is a fast method created by HOMER to produce a load that can be relatively realistic. Figure 4.6 below shows an overview of the load which is created (without random variability specifications). The daily profile window for January, that covers the 24 hour energy consumption for the 15 household, appears. In addition, the diagram of the seasonal profile demonstrates the monthly profile load over a year. The random variability inputs are changed to 10% for the day-to-day variability and 15% for the time-step variability (See Figure 4.7). The purpose of these two variables is that they allow us to add some randomness to the load data to make it more realistic. At the bottom, we can see the scaled annual average energy consumption per day which is 145.44 kWh/day and a peak load of 39.8 kW. The load factor, which is the ration between the average load power and the peak load, is calculated to be 0.15.

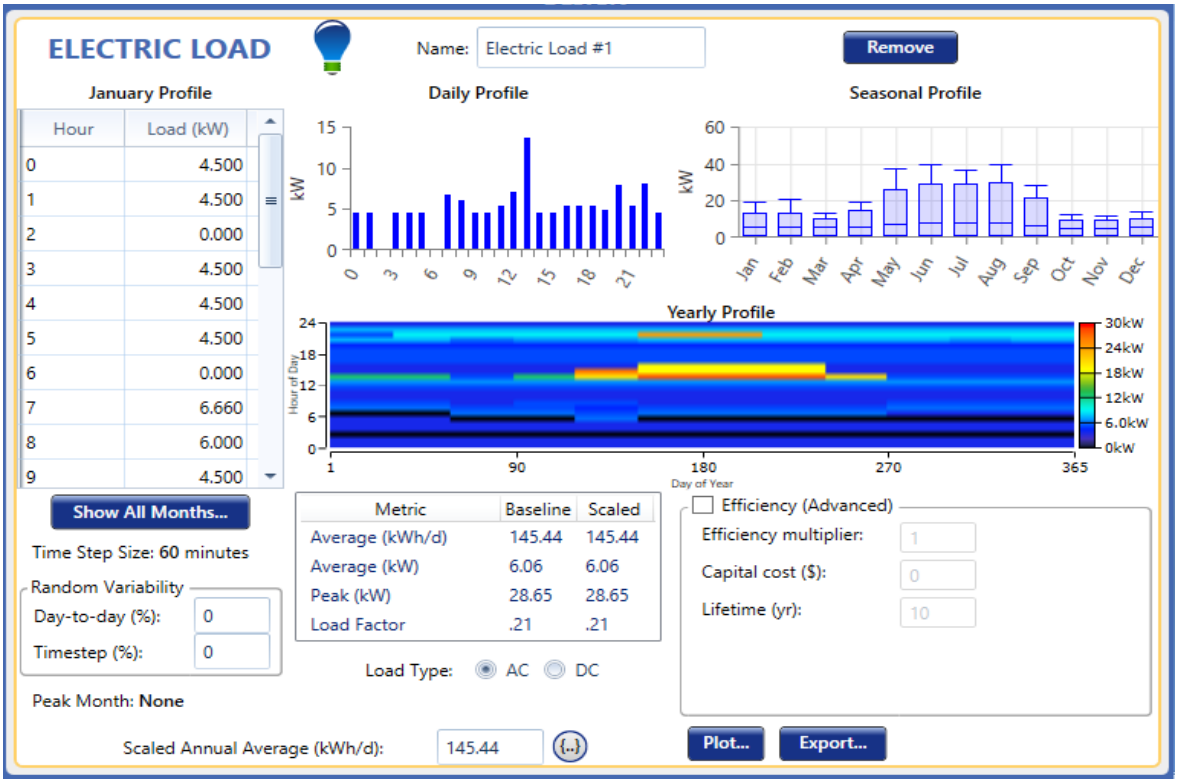

Figure 4.6: Primary load of the 15 households imported to HOMER (without random variability specifications).

Figure 4.7: Primary load of the 15 households imported to HOMER (with random variability specifications).

One of the plots which HOMER can create from the data entered is the yearly profile known as a D-map. A D-map is a visualization of the entire year's electric load starting from midnight Monday, January 1st. The time of days is represented on the y-axis and the day of the years are located on the x-axis. By pointing the mouse at any particular point on the D-map, we can see the specific electrical load at that time step.

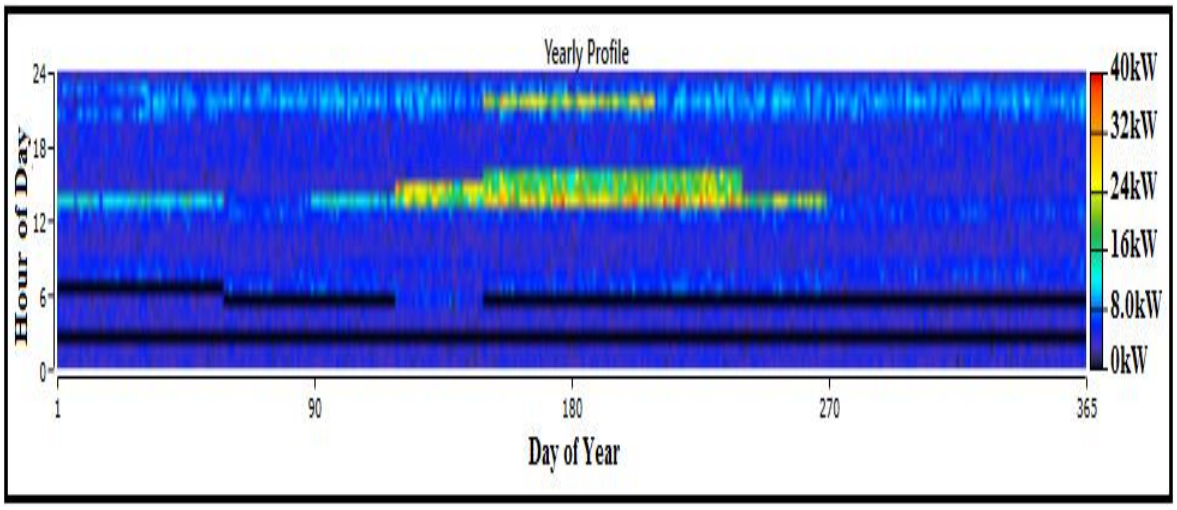

Figure 4.8: Yearly load profile of the 15 households.

Using the HOMER Plot button, the daily load profile can be plotted as shown below.

Figure 4.9: Daily load profile for a year.

4.4. System Design and Simulation

The previous section aim was to define all of the economical data, the location and the 15 households load profile. However in this section, the aim is to define the detail system design using HOMER Pro., including the selection of the different components that build up the system. This involves defining the technical specifications and costs (investment cost and O & M costs, replacement cost) of each component of our energy system.

4.4.1. Diesel Generator Selection

Homer Pro offers a multitude of genset choices with different types of fuels. When selecting a generator, first, it is important to determine its rated power, and then choose the type of fuel (diesel, gasoline or natural gas ...), finally determine the requirement to include the selected generator in all configurations or configure it just as a backup device only.
In this study, the diesel generator considered can be found in HOMER library. It is denoted as Generic 10kW Fixed Capacity Genset. Two other gensets are added to the design to have in total three gensets.

Table 8: Diesel generator operating assumptions.

Diesel Genset Assumptions	***Value***
Minimum Load ration	30%
Lifetime	15,000.00 Hours
Fuel curve intercept	0.480 L/hr
Fuel curve slope	0.286 L/hr/kW

The cost of commercially available diesel generator may vary from 250 to 800 USD/kW. For larger units per kW, the cost gets lower. The diesel generator economical specifications are summarized by the following table.

Table 9: The economical specifications of the selected generator.

Diesel Generator	
Capital Initial Cost	4,000 USD
Replacement Cost	4,000 USD
O&M Cost	0.3 USD/op.hour
Fuel Price (Diesel)	0.20 USD/L

The following figure represents the technical specifications of our diesel generator.

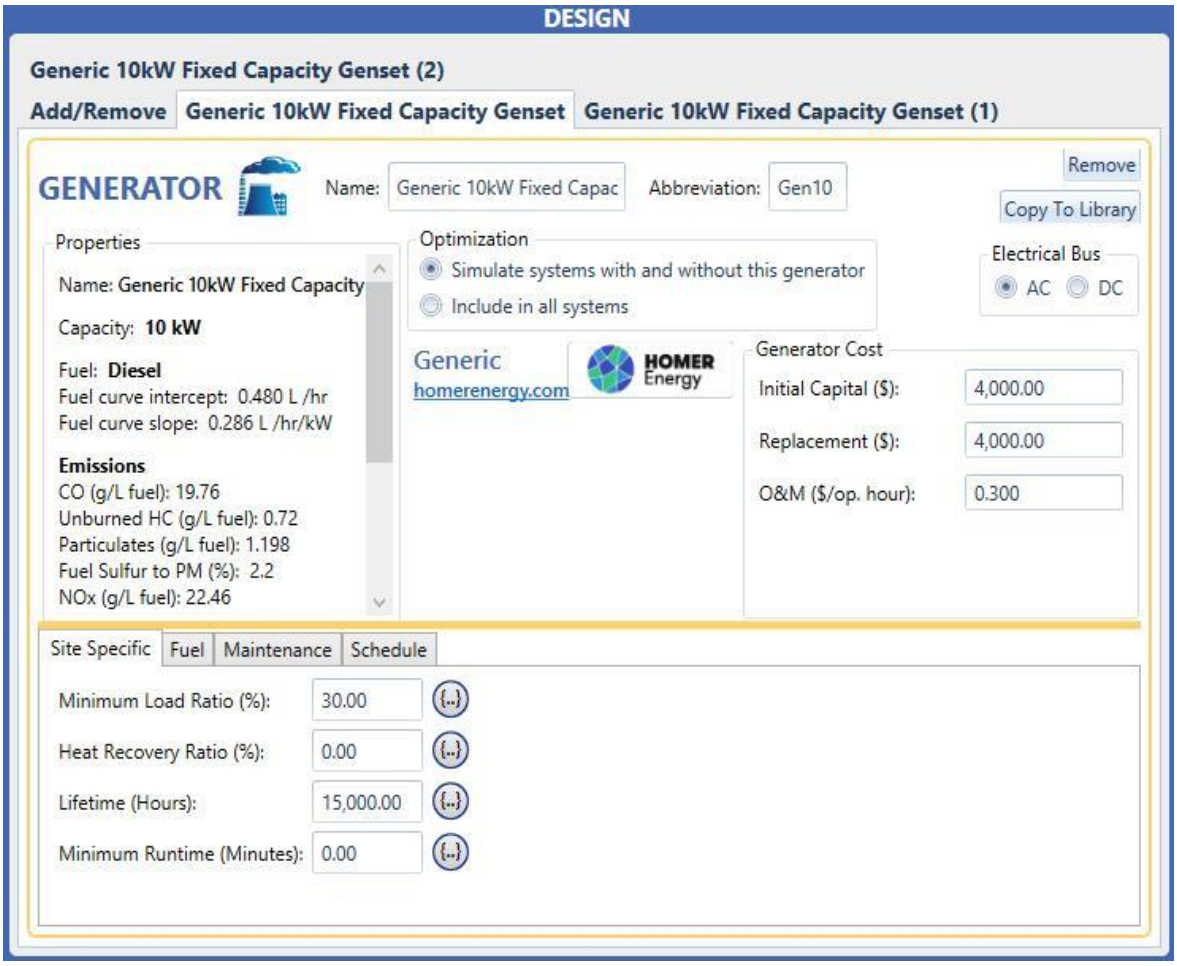

Figure 4.10: The technical specifications of the diesel generator.

The diesel generator fuel curves have been provided by HOMER as shown below.

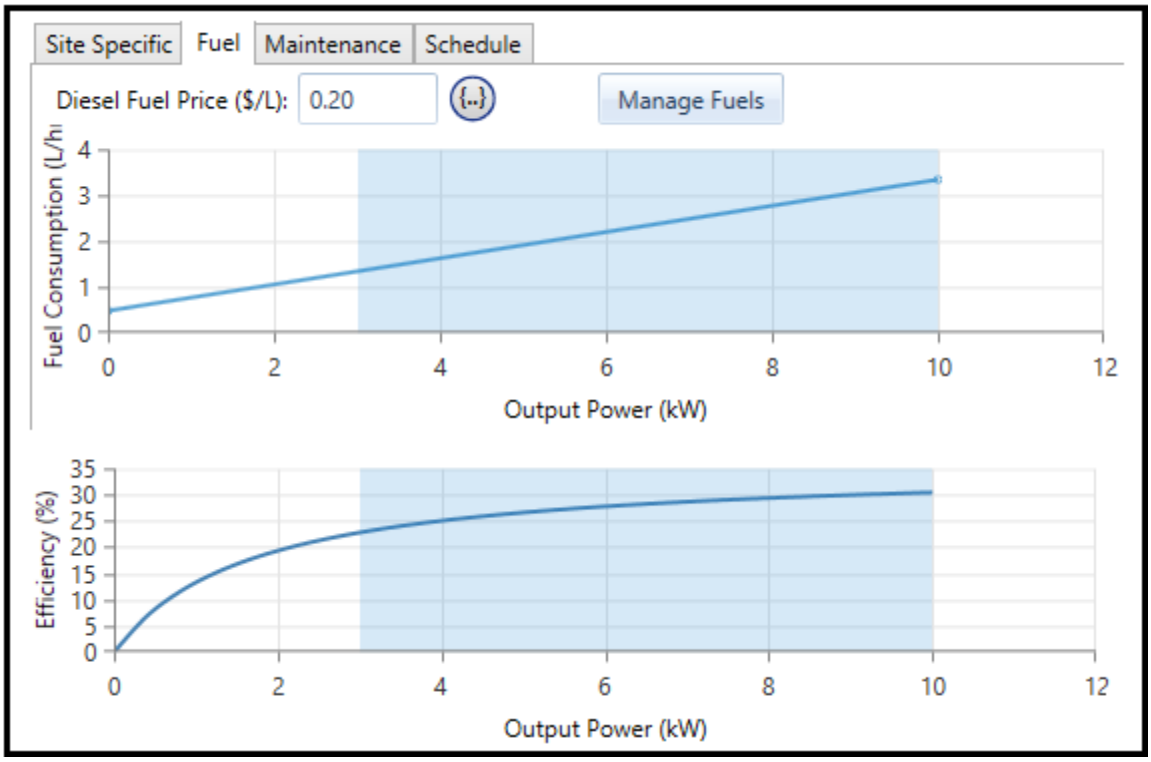

Figure 4.11: HOMER-generator fuel curves.

4.4.2. PV Module Selection

4.4.2.1. Technical and Costs Specifications

In our case study, the generic solar PV panel is selected for our system since it better represents the lowest option in the PV market. In addition, it does not have size dimensions built into it; therefore, it allows us not to estimate the amount of land needed for installing the PV panels. The technical assumptions are summed up in the following table.

Table 10: Solar PV panel technical specifications.

Photovoltaic Module	
Lifetime	25 years
Derating Factor	80%
Efficiency at STC conditions	13%
Ground Reflectance	36% [94]
Temperature Coefficient	-0.5 %/°C
Nominal Operating Temperature	49°C
Tracking System	No tracking/fixed slope at 29.3°
MPPT included in solar system?	YES
MPPT Efficiency	96%

As it can be seen in the above table, the converter, which contains an MPPT, is included in the PV solar system. Hence, the PV generator in such case is connected to the DC bus bar.

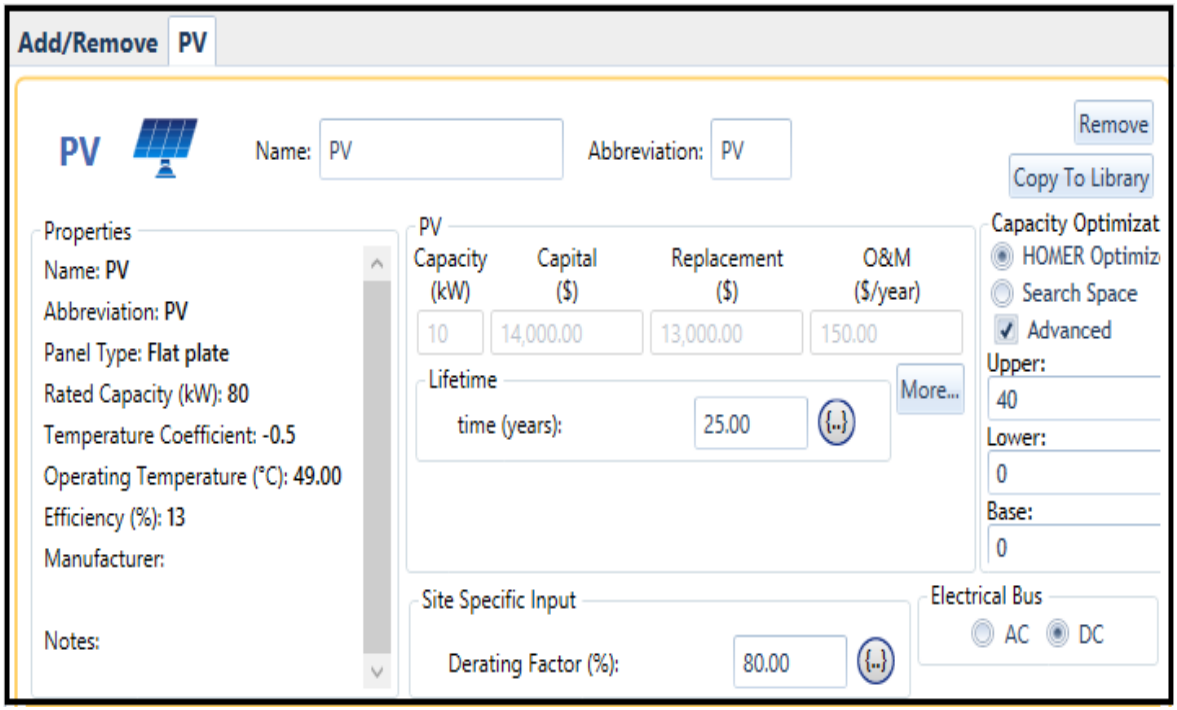

Figure 4.12: Solar PV module specifications.

According to the International Renewable Energy Agency IRENA Report [95], the capital cost may vary from 1,050 USD to 4,550 USD/kW. In our case study, the capital cost and replacement cost are 1,400 USD/kW and 1,300 USD/kW, respectively. The O&M cost is practically very small 15.0 USD/kW/year. The different assumed costs for the PV system and their curves are shown in the figure below.

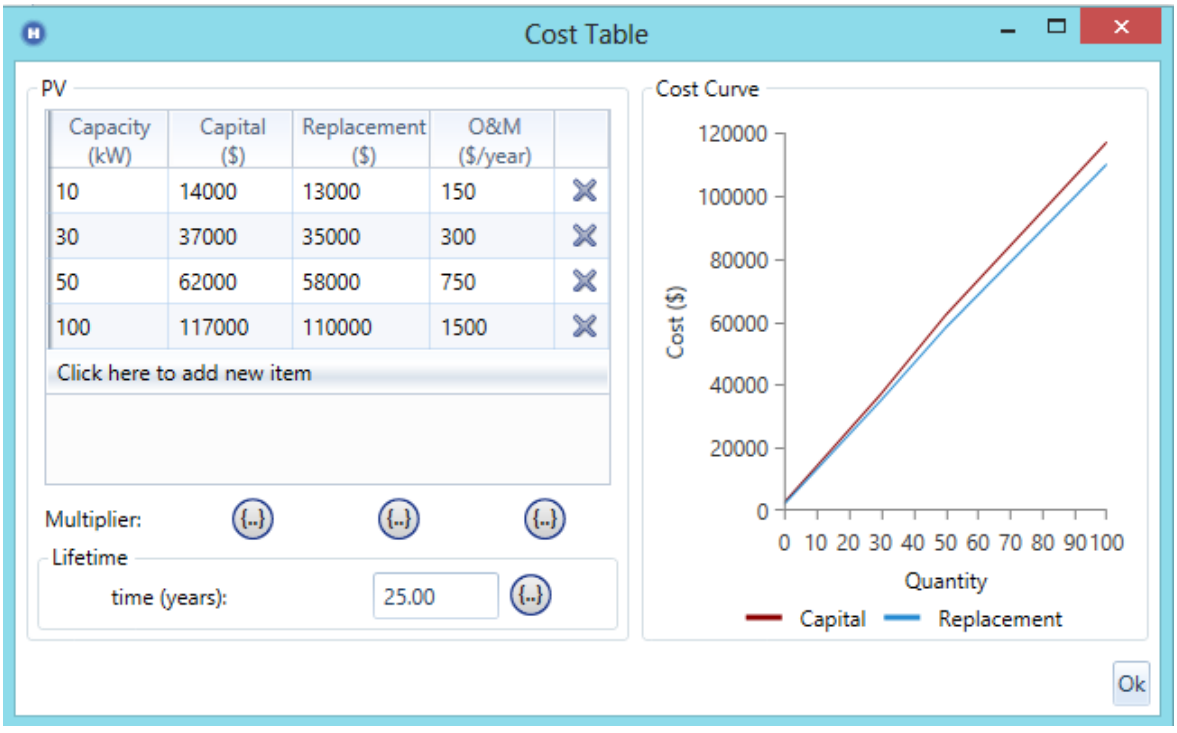

Figure 4.13: Solar PV module costs assumptions.

The solar PV HOMER model of the converter is shown in the figure below. We consider several quantities for HOMER to use in the system optimization.

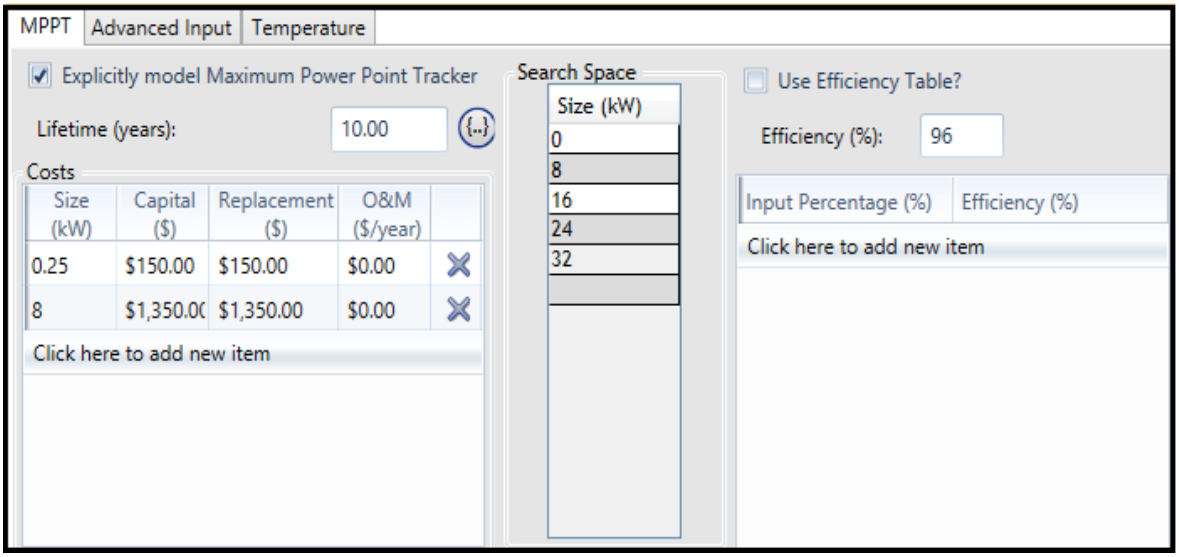

Figure 4.14: Solar PV HOMER inverter model.

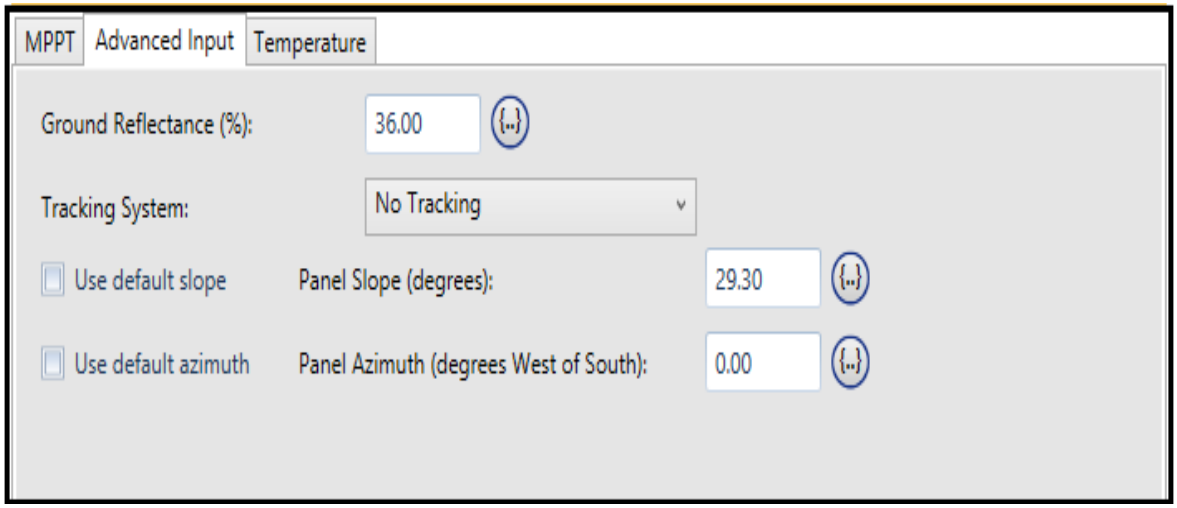

Figure 4.15: Solar PV HOMER: advanced input tab.

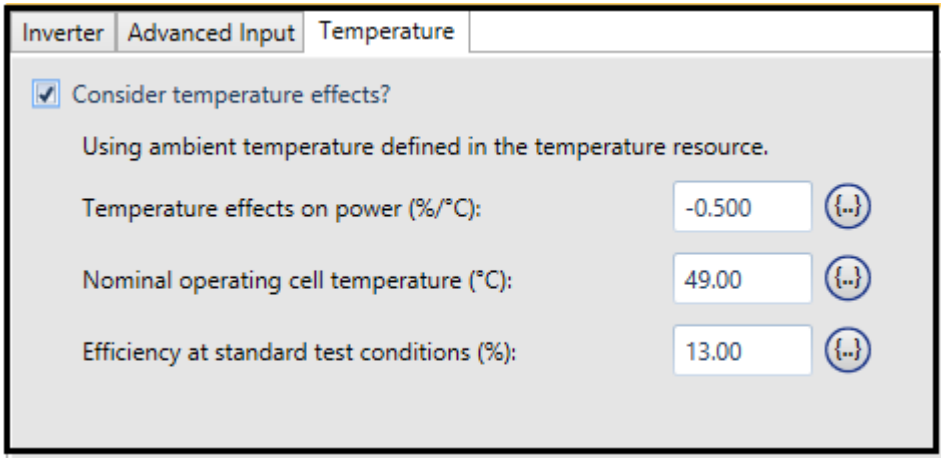

Figure 4.16: Solar PV HOMER: temperature tab.

4.4.2.2. Climatic Data Evaluation

Before sizing our PV system, we will first analyze the solar resource potential available and the monthly temperatures in Boukazine, Adrar. The climatic data for this study is obtained from Meteonorm 7.2 software. This latter can generates accurate and representative global climatic data for any place on earth. Meteonorm asks for the site's specification (latitude and longitude) inputs which are 29°18'17" North and 0° 31'27" West, respectively. The azimuth and the inclination have also to be specified: 0° and 29.3° respectively. The Peak Sun Hour PSH parameter represents the irradiation on the horizontal plane; it is the number of hours that the irradiation would be at a peak level of 1000 W/m^2.

The period of the radiation data is from 1991 to 2010, however for the temperatures from 2000 to 2009. The different climatic data are summed up in the following table.

Table 11: Horizontal and tilted radiations including the average temperature.

	Global Horizontal Irradiance GHI [kWh/m^2]	Solar Radiation on tilt angle [kWh/m^2]	PSH [h]	Average Temperature [°C]
January	141	214	5.4	12.9
February	146	194	5.2	16.2
March	202	236	6.5	21.4
April	221	226	7.4	25.3
May	241	222	7.8	30.5
June	240	212	8.0	35.2
July	245	219	7.9	38.2
August	225	221	7.3	37.2
September	192	211	6.4	33.1
October	166	207	5.4	27.5
November	139	201	4.6	19
December	127	199	4.1	14.4
Annual	2282	2561		-
Average	190.4	213.4	6.3	25.9

Meteonorm has the ability to generate many data in graphical or tabular form. The data are: solar irradiance (monthly and daily), temperature (monthly and daily), precipitations, and insolation duration. These data can be monthly or daily.

For our case, the different data are presented graphically as shown in Appendix A.

After analyzing the data of the solar radiations generated by Meteonorm, we observe that:

- ✓ July has the sunniest month with an average monthly radiation of 245 kWh/m^2 (an average daily radiation of 7.90 kWh/m^2).
- ✓ December, in contrast, has the lowest radiations with 127 kWh/m^2 (an average daily radiation of 4.09 kWh/m^2).

The average Global Horizontal Irradiance and the average temperature data, which are used to calculate the output power of the PV array, are input manually to HOMER Pro. This can be done by clicking the "Solar GHI" icon in the resource tab of the HOMER's navigation ribbon. Consequently, HOMER calculates the clearness index from the solar radiation data. The following figure shows this step.

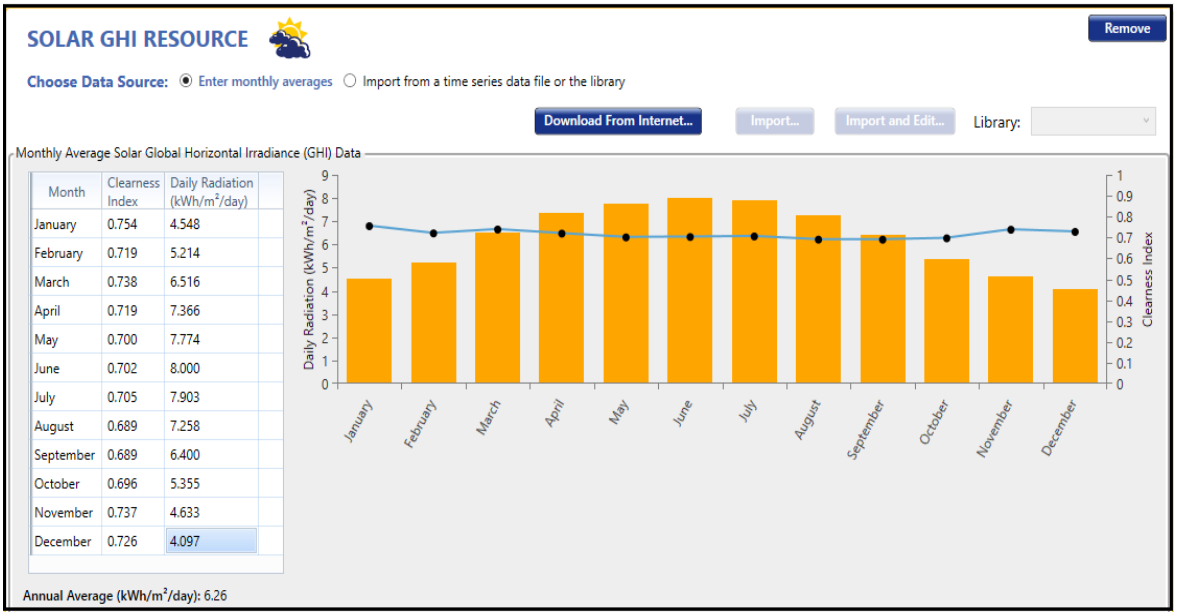

Figure 4.17: Global Horizontal Irradiance in Boukazine.

Figure 4.18: Entered temperature data to HOMER.

4.4.2.3. PV System Sizing

This part of the methodology includes manual calculations; it will not affect the simulation part. Its aim is to show how to design a PV power system as an off-grid system to supply the households. The total energy load $E_{loadtotal}$ is given by the following equation:

$$E_{loadtotal} = \frac{E_{load}}{\eta_{BOS}} \quad (4.1)$$

Where: E_{load} is the daily load profile calculated for the 15 households.
η_{BOS} is the Balance Of the System efficiency estimated to be 72%.

The power required to accommodate the load is given by:

$$P_{PV} = \frac{E_{loadtotal}}{PSH} \quad (4.2)$$

For our case, the daily load profile is calculated to be 187.98 kWh/day and the PSH for December is 4.1 h. Hence, the power needed is found to be 64 kW_p.

4.4.3. Electrolyzer Selection

According to the IEA Technology Roadmap for Hydrogen and Fuel Cells [96], the costs of alkaline electrolysers are estimated to be in the range of 850 USD/kW and 1500 USD/kW. It is expected that these costs would reduce in the coming 10 years with the improvement in alkaline technology, control systems and power electronics.

In our analysis, a 1 kW system is associated with 1200 USD capital, 1000 USD replacement and 0 USD/year maintenance. The alkaline electrolyser lifetime is considered as 10 years with an efficiency of 73%.

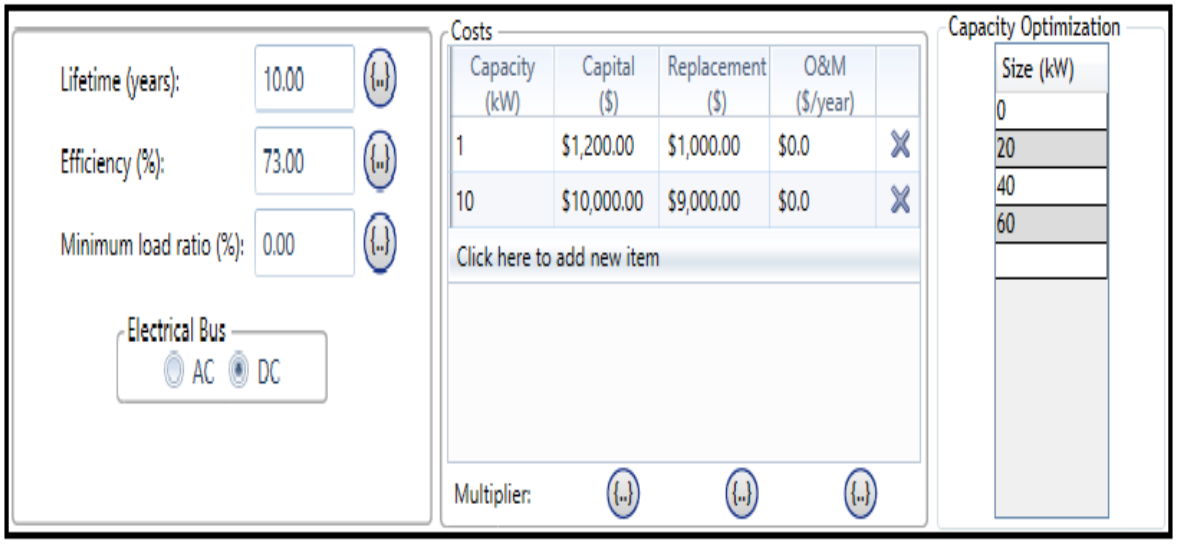

Figure 4.19: HOMER electrolyzer specifications.

4.4.4. Hydrogen Tank Selection

Hydrogen tank is sometimes included in the electrolyzer model. However, it is not the case with our model. Cost of tank with 1kg capacity is estimated to be 1000 USD. The replacement and the O&M costs are assumed to be 800 USD and 15 USD, respectively. The following figure shows the HOMER input tab of the hydrogen tank.

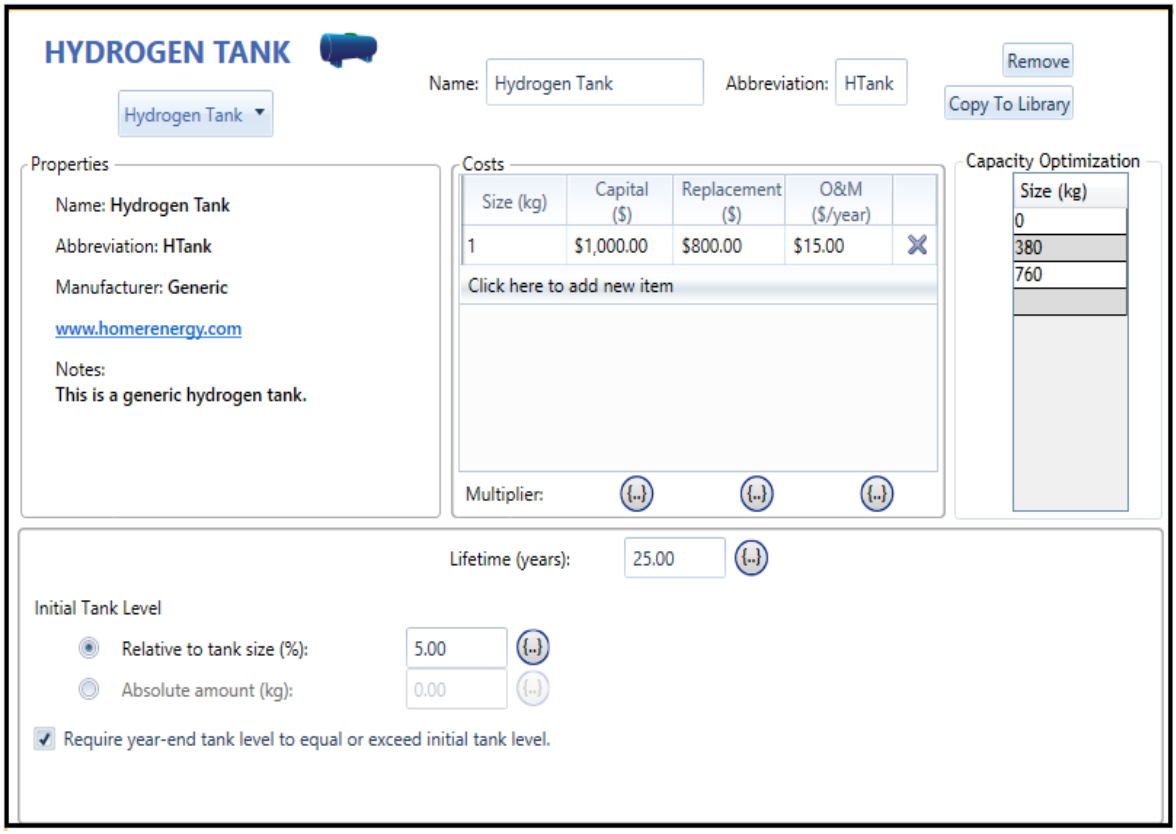

Figure 4.20: HOMER hydrogen tank specifications.

4.4.5. Converter selection

In order to convert the DC voltage to an AC voltage or vice versa, we must use an inverter. This letter makes it possible to compensate for power failures, to stabilize the electrical voltage and to eliminate electrical noise. HOMER Energy Pro. offers several inverter technologies according to the power system type; we can find grid-tied inverter that can connect the PV DC to the AC grid and bidirectional inverter that can connect between PV generator and/or batteries and the AC load.

In our case, we select a converter that can be found in the HOMER Pro. library. It has the name of Leonics MTP-413F. It has a lifetime of 10 years, inverting efficiency of 96% and rectifying efficiency of 94%. It is designed mainly for hybrid power system combining solar with diesel and other renewable resources.

Table 12: The inverter specifications.

Generic Converter	
Capital Cost	600 USD/kW
Replacement Cost	600 USD/kW
O&M Cost	0 USD/year
Lifetime (years)	10
Efficiency	96%

The bidirectional inverter properties and cost specifications are shown in the figure below.

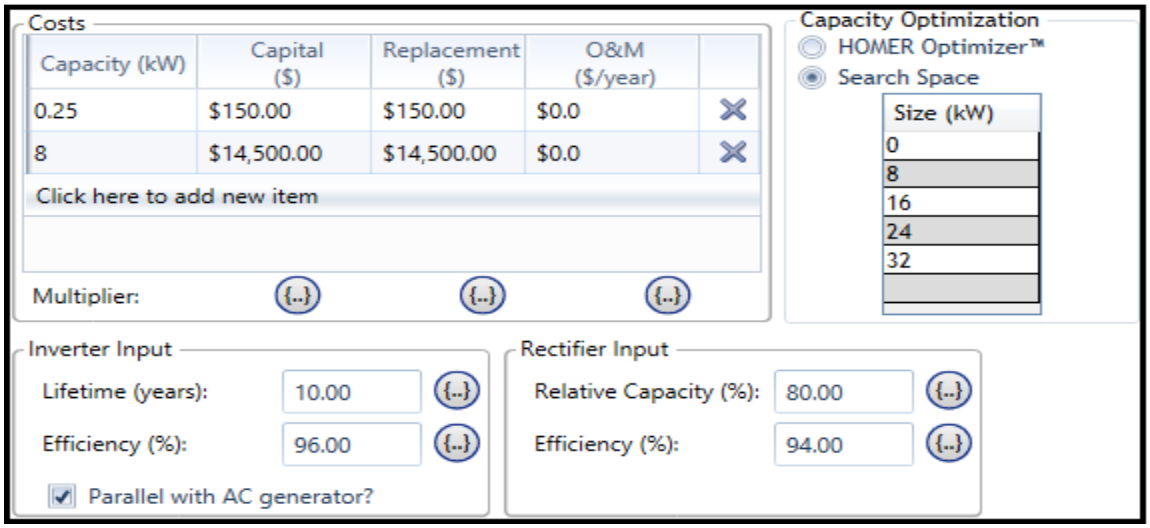

Figure 4.21: HOMER specifications for the inverter.

4.4.6. Dispatch Strategy

In hybrid power system, the only dispatchable energy source is the diesel generator. Since renewable energy sources are known with their intermittency and they cannot be controlled by the user, it must be used when available to satisfy the load or to produce hydrogen. The diesel generator has to turn ON to supply the load in case the renewable energy system is not able to supply the load. Therefore, using a genset is crucial in hybrid power systems to meet the load in a controlled manner to improve the system availability. Nevertheless, it is rather complicated to control the operation of the genset because of several aspects like the energy conversion efficiency which is very low.

HOMER Pro. can model two dispatch strategies: the Load following and the Cycling Charge. In Load Following strategy, the genset runs when needed and generates only the required power that cannot be generated by the renewable sources. In Cycling Charge strategy, the genset runs when needed and operates at its full capacity and the excess energy is sent to the electrolyzer to produce hydrogen.

In our case, the two strategies are considered for simulation. The controller that HOMER Pro. can only use one of the two. Generally, the cost assumptions of HOMER controller are left just as they are.

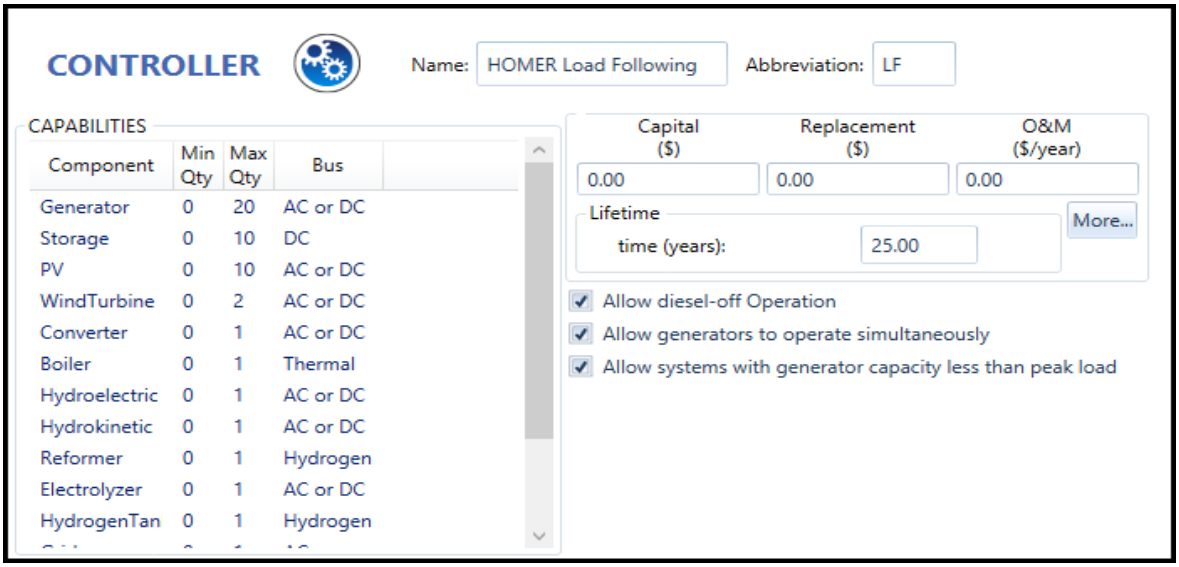

Figure 4.22: HOMER specifications for the controller.

The configuration shown in the figure below depicts the proposed system that consists of the PV generator, the converter, the diesel generator, the electrolyser with its hydrogen storage tank.

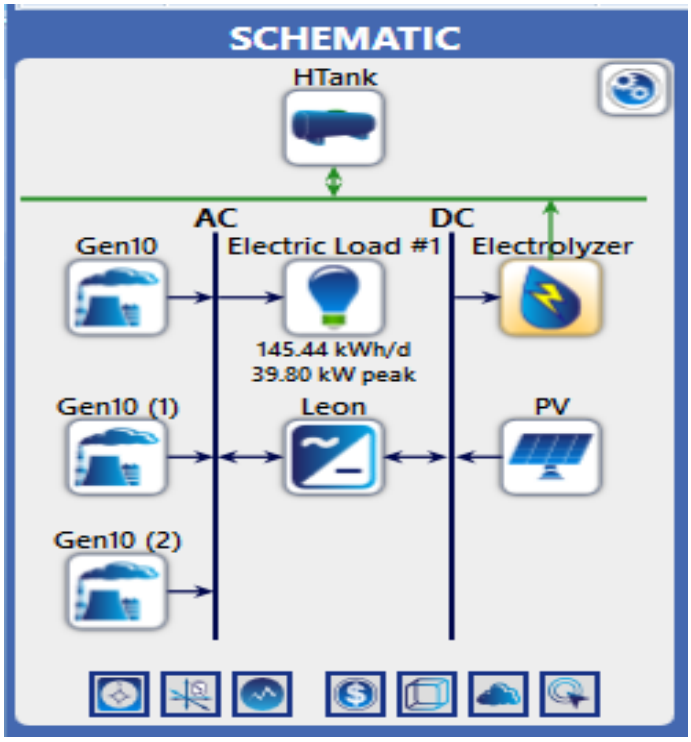

Figure 4.23: HOMER system configuration.

In order to find the optimal system, we need to consider several combinations of different hybrid system components' capacities. Hence, we provide a wide range of capacities to HOMER Pro. The larger the number of inputs, the higher time the simulation takes. The figure below, which can be accessed through the Search Space tab, tabulates the different values of all optimization variables. HOMER Pro. simulates the set of all possible combinations of these parameters.

Leon Capacity (kW) ☐ Optimizer	Electrolyzer Capacity (kW)	Gen10 Capacity (kW)	Gen10 (1) Capacity (kW)	Gen10 (2) Capacity (kW)	HTank Capacity (kg)	PV DC Capacity (kW)	PV Size (kW) ☑ Optimizer
0	0	0	0	0	0	0	0
8	20	10	10	10	380	8	40
16	40				760	16	
24	60					24	
32						32	

Figure 4.24: HOMER search space variables.

4.5. Sensitivity Analysis Variables

The factors that restrained or could enhance investment in renewable energy sector are analyzed through the sensitivity assessment. One of the most important advantages of HOMER is its ability to simulate full-year operating conditions and compare changes in feasibility by varying one variable. This will help us to assess how certain circumstances will affect our power system technically and economically.

HOMER Pro. uses the sensitivity analysis to reveal how changes in the inputs may affect the design and the system feasibility. In order to analyze the system design sensitivity to some defined factors, different scenarios have been proposed depending on:

- ✓ A range of minimum renewable fraction,
- ✓ The availability of renewable energy sources.

The two proposed factors can be referred to as keys factors for system designing. The first factor has been chosen because Algeria plans to increase the share of renewable power to reach 40% by the end of 2040. in the country's energy production mix. However, the second factor has been selected because the unpredictability of renewable sources is a constraint for the system design. The table below gives the sensitivity variable considered.

Table 13: Ranges tested of sensitivity variables.

Sensitivity Variable	Values.
Minimum renewable fraction (%)	0, 20, 40.
Average annual irradiance ($kWh/m^2/day$)	6.26, 4.10 (worst case in December)

4.6. Uncovered Factors

There were several factors that were not considered in our simulation process either for simplicity sake or HOMER finds difficulties to account for them. Extra costs, such as land acquisition, were left out mainly due to the remoteness of the region considered. It was supposed that land would be widely available in the vicinity of the village. Hence, the load data of the specific selected site and variables would be required before the feasibility of the project could be validated.

Another factor is the remoteness of the selected region. This could also lead to troubles with the labor supply for the system construction and long-term maintenance. It was supposed that such costs would be consistent throughout the project lifetime.

Furthermore, multiple renewable energy sources were not covered for example solar and wind despite that they have been realized to be more economic. The weather data are taken by approximating them to other data in sites that are around. The solar data are more reliable since the intensity of the solar energy will not change, however; wind data are harder to get because they change with region topography.

5.1. Introduction

The aim of this chapter is to show all the results of the simulation that has been done in the previous chapter.

5.2. HOMER Pro. Simulation Results and Analysis

HOMER Pro. software simulates the system operation by performing energy balance calculations in each hourly step throughout the year. For each hourly step, HOMER Pro, compares the electric load demand with the energy that is provided by the different energy sources. After that, it calculates the energy flows from and to each system component. HOMER Pro. carries out these energy balance calculations for each system configuration that needs to be considered. Then, it determines the feasible systems ranked on the basis of the NPC; system that can satisfy the load demand under some specified condition. After that, the software estimates the different costs of installing and operating the system over the project lifetime.

In our case, lots of simulations have been performed by HOMER Pro. to find out the most optimized and cost effective configuration of the hybrid power system considering all of the system components, their sizes and their costs assumptions. 14,604 solutions were simulated where 9,858 were feasible and 4,557 were infeasible due to the capacity shortage constraint. HOMER Pro. gives the overall optimization results. They are displayed in form of list of different system configurations ranked according to the increasing NPC of the project. The different sizes of the system components, which are considered during the HOMER Pro. simulations, can be checked. The PV generator considered output power ranges from 0kW to 40.0kW. However, the other components' sizes are all considered during the simulation. The Load Following is the only strategy used by HOMER Pro. The optimum overall system which is the one that can provide electricity at lowest price is ranked first. This system is build up by three generators of 10kW capacity resulting an NPC of $236,723 and a LCOE of $0.137/kW.
Figure 5.1 below gives the both the AC primary load (in orange) and the AC primary load served (in green) throughout the year. The difference between with these two loads is represented by the curve in black. The curve in black is referred to as the unmet electrical load which could happen because the power generated by the system was not sufficient to supply the load.

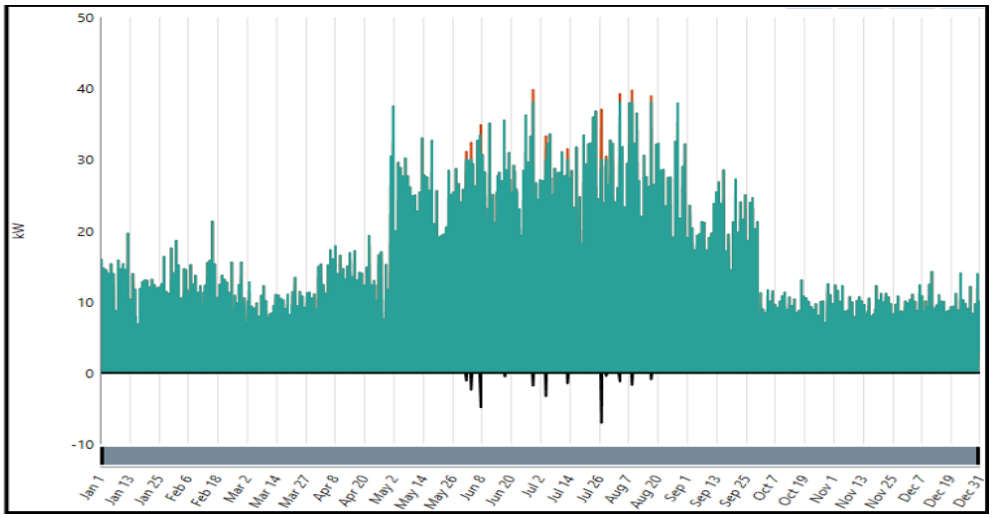

Figure 5.1: The AC primary load (orange), the AC primary load served (green) and the unmet electrical load (black)

Figure 5.2 depicts the global solar radiation power that is received by the tilt PV generator. It can be seen clearly that the highest solar radiation happens in summer (in July); it reaches 1.14 kW/m^2.

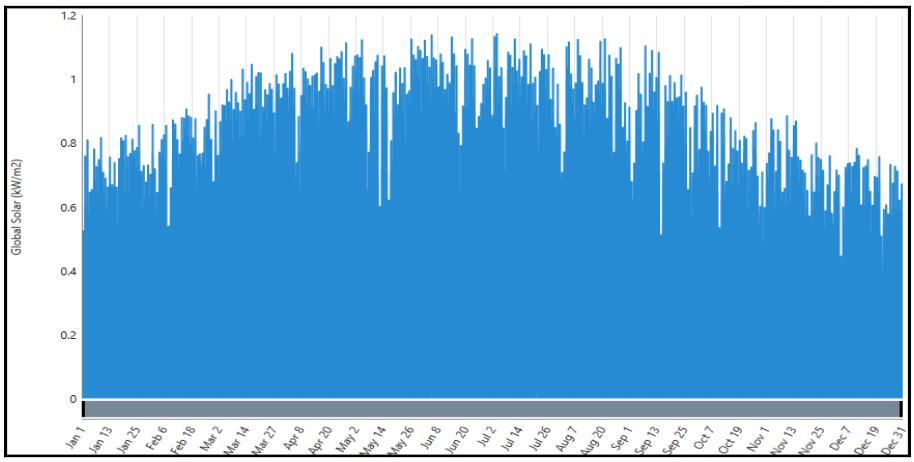

Figure 5.2: Global solar radiation power.

5.3. Optimization Results

After simulating all of the possible system configurations, HOMER Pro. displays a list of categorized optimization results. The categorized optimization list shows the least-cost system of each type. It enables us to compare the system category with other system category alternatives. Figure 5.3 gives the categorized optimization results and shows the most cost effective configuration of each system type. As in the overall optimization result, HOMER Pro. considers the system type of three diesel generators as the optimum one.

Export...

Optimization Results

Left Double Click on a particular system to see its detailed Simulation Results.

Categorized Ove

Architecture																Cost		
							PV (kW)	PV-MPPT (kW)	Gen10 (kW)	Gen10 (1) (kW)	Gen10 (2) (kW)	Electrolyzer (kW)	HTank (kg)	Leon25 (kW)	Dispatch	COE ($)	NPC ($)	Operating cost ($/yr)
									10.0	10.0	10.0				LF	$0.173	$236,723	$8,711
							21.7	16.0	10.0	10.0				8.00	LF	$0.181	$245,883	$7,496
							21.7	16.0	10.0		10.0			8.00	LF	$0.181	$245,883	$7,496
							21.7	16.0		10.0	10.0			8.00	LF	$0.181	$245,883	$7,496
							21.7	16.0	10.0	10.0	10.0			8.00	LF	$0.182	$249,319	$7,474
									10.0	10.0	10.0	20.0		8.00	LF	$0.235	$320,966	$10,647
							21.7	16.0	10.0	10.0		40.0		8.00	LF	$0.251	$340,238	$9,628
							21.7	16.0	10.0		10.0	40.0		8.00	LF	$0.251	$340,238	$9,628
							21.7	16.0		10.0	10.0	40.0		8.00	LF	$0.251	$340,238	$9,628
							21.7	16.0	10.0	10.0	10.0	40.0		8.00	LF	$0.251	$343,674	$9,607
									10.0	10.0	10.0		380		LF	$0.559	$763,774	$14,411
							21.7	16.0	10.0	10.0		20.0	380	8.00	LF	$0.605	$820,309	$14,265
							21.7	16.0	10.0		10.0	20.0	380	8.00	LF	$0.605	$820,309	$14,265
							21.7	16.0		10.0	10.0	20.0	380	8.00	LF	$0.605	$820,309	$14,265
							21.7	16.0	10.0	10.0	10.0	20.0	380	8.00	LF	$0.602	$823,745	$14,244
									10.0	10.0	10.0	20.0	380	8.00	LF	$0.621	$848,017	$16,347
							21.7	16.0	10.0	10.0			760	8.00	LF	$0.959	$1.30M	$18,896
							21.7	16.0	10.0		10.0		760	8.00	LF	$0.959	$1.30M	$18,896

Figure 5.3: HOMER categorized optimization solutions.

Firstly by taking a look at the categorized optimization results above, we can see that several system type, which can supply the load demand, are found. However, not all these systems do that fully; some of the system types cannot produce power for the electric load. Consequently, the unmet electrical load becomes higher. Secondly, it can be seen also that some system types have only either an electrolyzer or a hydrogen tank. These system are economically feasible but practically not since, in reality, the electrolyzer and the hydrogen tank are needed both at the same type for efficient production and storage of hydrogen. Thirdly, hydrogen can be produced by using the PV generator and either two or three generators. In our case, we are interested in the system type that considers the PV generator, the three generators, the inverter, the electrolyser and the hydrogen tank. Such system type uses a PV generator output power of 21.7kW, a 16kW MPPT-converter, three 10kW diesel generators, 20kW electrolyzer, hydrogen tank of 380kg and an inverter of 8.00 kW. The Load Following strategy is adopted in this system. The total Net Present cost NPC is found to be $823,744 and a LCOE of $0.602/kW. The eco-technical analysis results can be accessed by double click on the corresponding system type.

5.3.1. Economical Analysis Results of The PV/Diesel/Electrolyzer with Hydrogen Tank

The cost summary of our system includes all of the components capital, replacement, operating and maintenance, fuel and salvage costs. Fuel costs are only due to the diesel used in the three gensets. The salvage cost is the cost remaining in a component of the system at the end of the project lifetime. The table below sums up all of the costs stated before.

Table 14: Cost summary of the PV/Diesel/Electrolyzer with hydrogen tank.

Component	Capital ($)	Replacement ($)	O&M ($)	Fuel ($)	Salvage ($)	Total ($)
Electrolyzer	19,777.78	37,095.68	0.00	0.00	- 9,499.14	47,374.32
Genset 1	4,000.00	41,330.74	47,172.51	61,338.54	- 3,575.45	150,273.56
Genset 2	4,000.00	4,188.99	6,052.31	7,008.56	- 2,959.48	18,290.38
Genset 3	4,000.00	0.00	1,292.50	1,533.74	- 3,065.68	3,760.55
Hydrogen Tank	380,000.00	0.00	147,051.11	0.00	0.00	527,051.11
Leonics Inverter	14,500.00	30,068.24	0.00	0.00	- 7,699.61	36,868.62
PV	27,416.67	0.00	6,127.13	0.00	0.00	33,543.80
MPPT-Converter	2,588.71	5,368.13	0.00	0.00	- 1,374.62	6,582.22
System	456,283.15	118,051.77	207,695.50	69,888.35	- 28,174.08	**NPC = 823,744.59**

The different outflows and inflows through the entire project lifetime can be displayed in HOMER Pro. either in tabular or graphical form. Figure 5.4 below gives the nominal cash flow outputs of the considered system type components. Here we can see that the electrolyzer and the Leonics converter replacements occur each ten (10) years. Nevertheless, the diesel generators replacements occur for the genset 1 and 2 within the project life time. The diesel gensets 3 replacements does not occur because the hours of operation was declared before to be 15,000 hours which is large than the operation hours

of these generators in our case study. The capital cost for our project is estimated to be $456,283. The share of the hydrogen tank only represents 83% of the total capital cost.

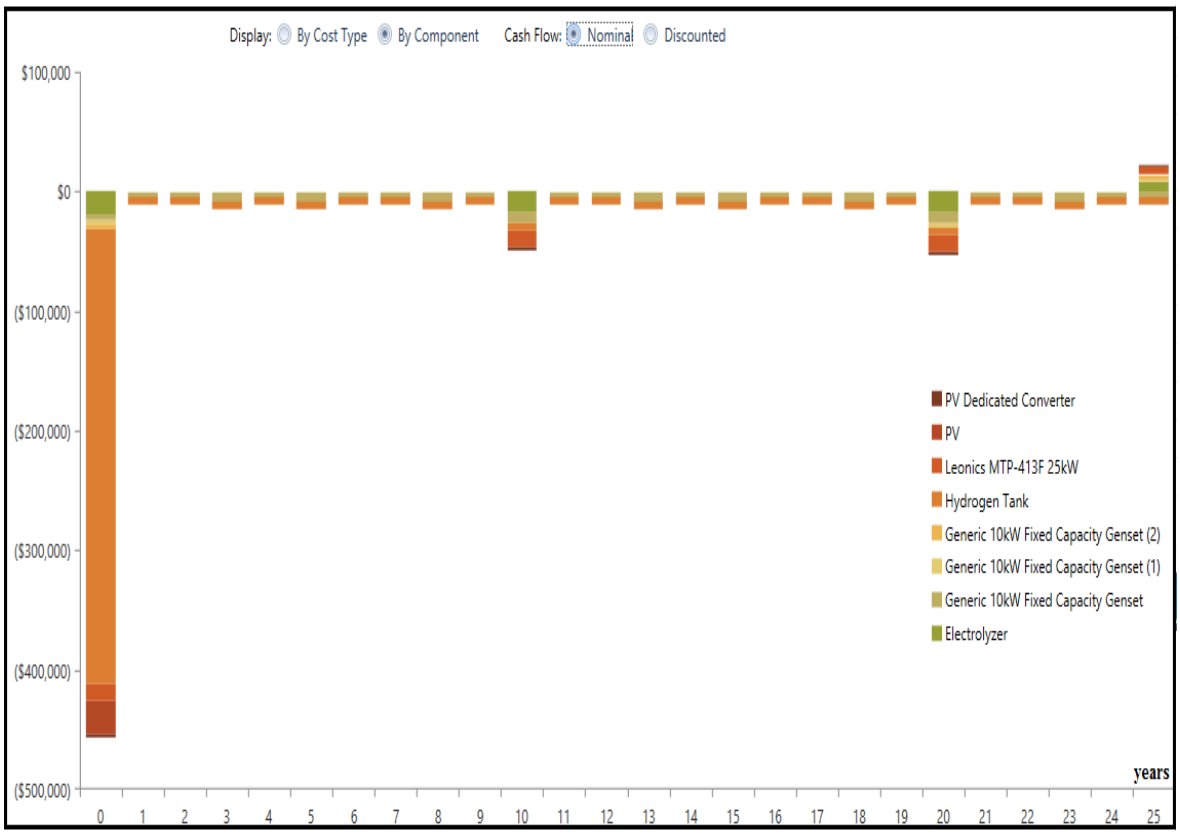

Figure 5.4: Project nominal cash flow by components.

5.3.2. Technical Analysis Results of The PV/Diesel/Electrolyzer with Hydrogen Tank

5.3.2.1. Electrical Power Production

The electrical tab in HOMER Pro. reveals several variable for the considered system type. In our case study, the unmet electric load (happens when the load demand exceeds the supply) is found to be 26.7kWh/yr which represents only 0.0503% of the annual AC primary load 53,060 kWh/yr. The energy produced by the different system's power sources and their shares are shown in the following table. The PV generator produces the highest percentage of 51.3% of the total annual energy generation. As stated by the table, the capacity shortage of this system is 0.188% which is very small resulting only 10 hours of load shedding during the entire year due to the incapability of generating enough power to satisfy the load.

Table 15: Energy produced by the different energy sources and their shares.

Production	kWh/yr	%
PV	37,354	51.24
Genset 1	31,342	43.0
Genset 2	3,437	4.72
Genset 3	759	1.04
Capacity shortage	-	0.188

The monthly average electric production from each of the system components in the hybrid power system is given in Figure 5.5. Here we can see that the largest percentage of the power is produced by the PV generator system especially in months of November, December, January, February, March and April. On the other hand, the power generated by the PV generator is relatively small during the period of May to October. Hence, the diesel generators have to generate much more power during the same period (May-October). As it can be seen in the figure, the contribution of the diesel generators in power production is considerably high that period. This implies that the diesel gensets are needed to supply more power to satisfy the peak demand.

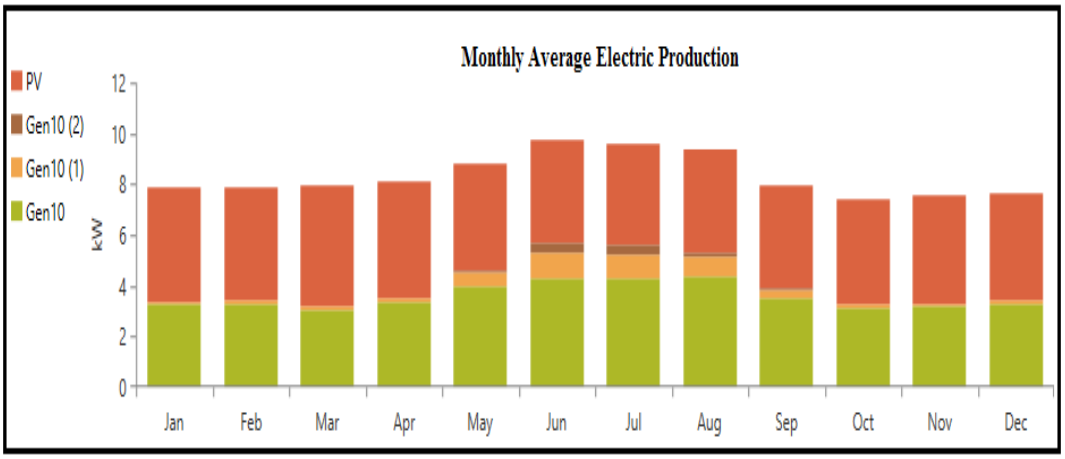

Figure 5.5: Monthly average electric production by the power source.

5.3.2.2. PV System Size Results

The PV tab shows the operation characteristics of the PV generator. The capacity factor of the PV system is 19.7% which is relatively low. Other characteristics are summarized in table 16. Figure 5.6 depicts the D-map of the PV output throughout the whole year.

Table 16: PV system characteristics.

Quantity	Value	Units
Rated Capacity	21.7	kW
Total Production	37,354	kWh/yr
Hours of Operation	4,383	Hrs/yrs
Levelized Cost	0.0416	$/kWh

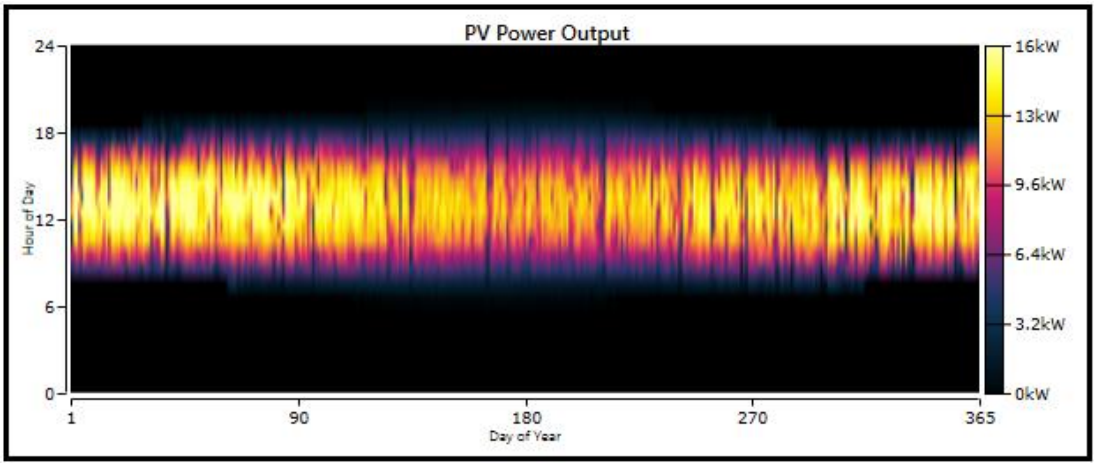

Figure 5.6: PV power output.

According to the HOMER Pro. simulations above, it has been found that the optimal hybrid configuration, which can supply the load and produce hydrogen at lower cost, contains PV arrays with a size of 21.7kW. The PV arrays generate DC electricity; they are connected to the DC bus bar. They can be divided into two arrays. In our case, we are going to use an MPP converter that has a range of 230-400V and a PV module that has a capacity of 210W and a voltage of 24.6V. Hence, 13 solar modules can be connected in series to adjust the array output voltage. Since an 11kW PV system requires 52 PV modules, they can be arranged into 4 strings each containing 13 series connected PV modules.

5.3.2.3. Conventional Power Production

The different diesel generators tabs show the operation conditions of the fuel-based power system. Table 17 below sums up the characteristics of the three gensets specified by HOMER Pro. However, Figures 5.7, 5.8 and 5.9 show the different gensets power output using D-map form. We can see clearly that the first diesel generator runs for longer hours since it operates during the nights to meet the load demand. However, it operates also during the day in case where the PV generator cannot supply power to satisfy the load. The two other gensets (2 and 3) are mainly used to compensate the system containg the PV generator and the genset 1. Genset 1 and 2 have fewer hours of operation and their purpose is to solve a higher load demand whenever it occurs. Genset 3 can be used as the "last hope" for the system to operate and solve any unpredictable peak demand that may happen at any time of the year.

Table 17: Diesel generator system characteristics.

Quantity	Genset 1	Genset 2	Genset 3	Units
Hours of Operation	6,095	782	167	Hrs/yr
Electrical Production	31,342	3,437	759	kWh/yr
Fuel Consumption	11,888	1,358	297	L
Fuel Energy Input	116,993	13,366	2,925	kWh/yr
Mean Electrical Efficiency	26.8	25.7	26.0	%
Fixed Generation Cost	0.663	0.663	0.663	$/hr
Marginal Generation Cost	0.0572	0.0572	0.0572	$/kWh

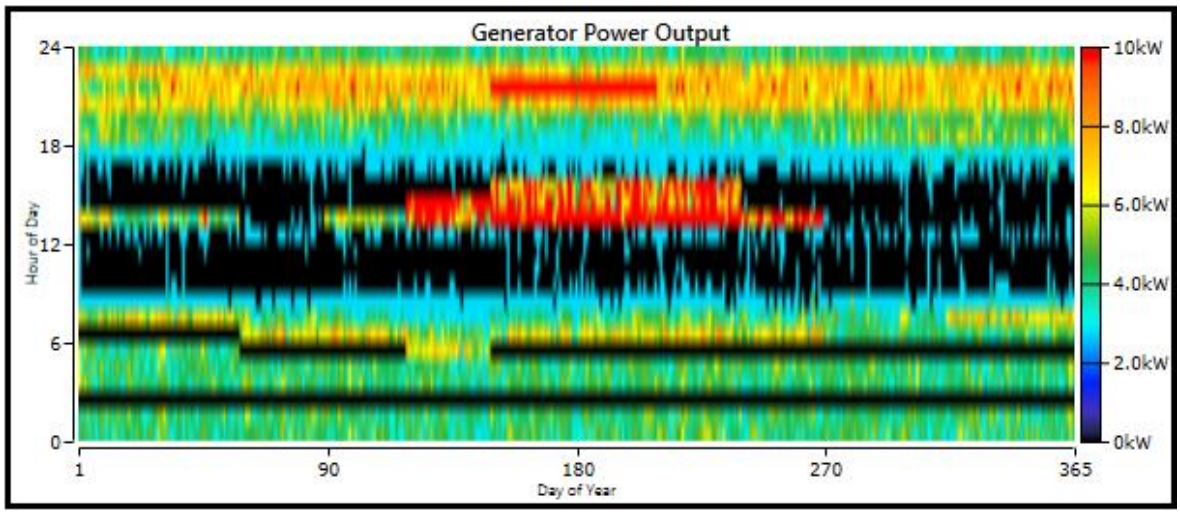

Figure 5.7: Diesel generator 1 power output.

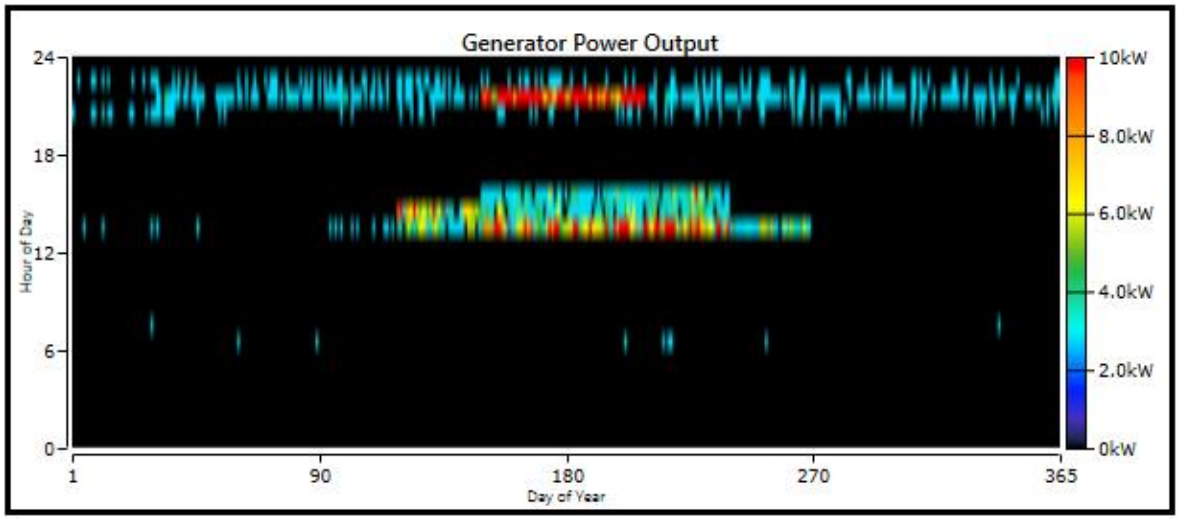

Figure 5.8: Diesel generator 2 power output.

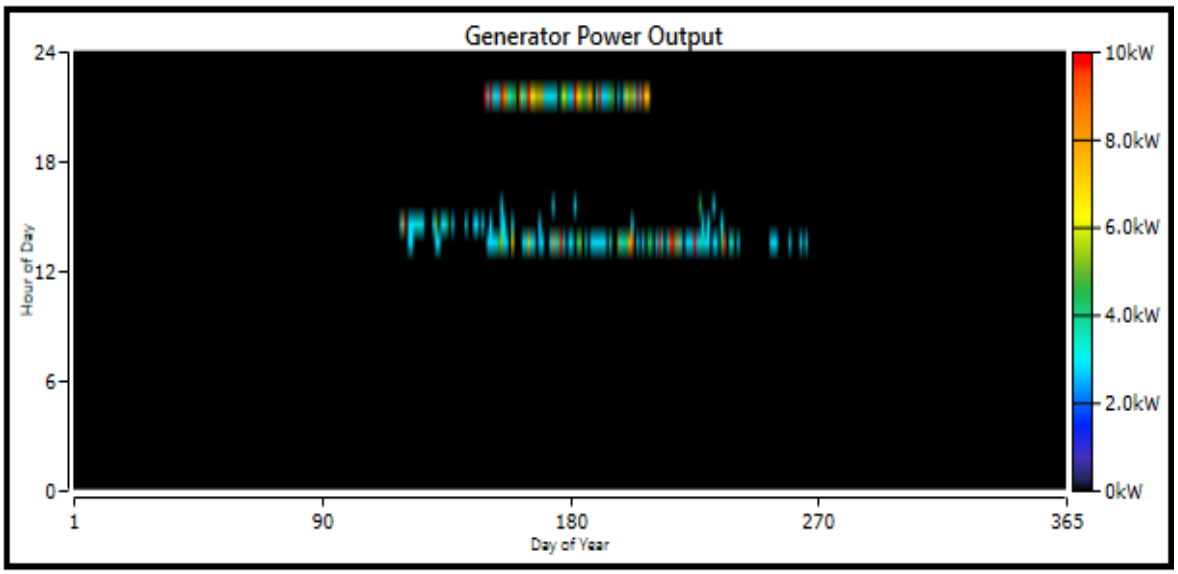

Figure 5.9: Diesel generator 3 power output.

- **Replacing the Three Diesel Gensets with a 30kW Diesel Genset**

The hybrid power system in our study consists of three diesel generators with each rated capacity of 10kW resulting a total capacity of 30kW. The three diesel gensets can be replaced by a single diesel genset having a rate capacity of 30kW, capital and replacement cost of $8,500. As shown in the Table 18 below, it can be seen that the PV system design size increase to reach 30.0kW with an electricity production share of 46.5%. As a result, the cost of energy and the total NPC increase to reach 0.668 $/kWh and $914,266, respectively. However, the electricity production share of the 30kW genset is 53.5%. As a result, the CO_2 emissions increase considerably to reach 63,258 kg/yr. Using a single genset of 30kW capacity leads to have a full hydrogen tank in only 5 months. Because of the excess in energy produced by the 30kW genset, the hydrogen production continues even during the night time in contrast to the case where we have 3 diesel gensets. Consequently, there exists an electricity excess of 28,750kWh/yr.

Table 18: Comparison when using three 10kW gensets and only one 30kW genset.

Quantity	3, 10kW Gensets	30 kW genset	Units
PV system size	21.7	30.0	kW
Share of PV	51.2	46.5	%
Share of gensets	48.8	53.5	%
LCOE	0.602	0.668	$/kWh
Total NPC	823,744	914,266	$
CO_2 emissions	35,386	63,258	Kg/yr
Electricity excess	0	28,750	kWh/yr

5.3.2.4. Fuel Consumption

The total fuel consumed by the three genset can be calculated resulting 13,545 liters of diesel. Hence, the average fuel consumed per day and the average fuel consumed per hour are calculated by HOMER: 37.1L/day and 1.55L/h, respectively. Figure 5.10 below shows the D-map of the fuel consumption throughout the year.

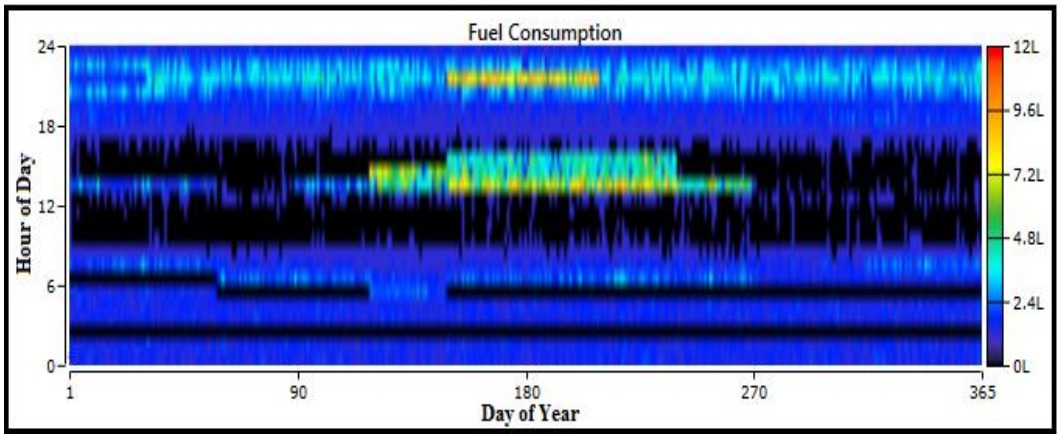

Figure 5.10: Fuel Consumed by the three gensets.

5.3.2.5. Power conversion System

The converter tab reveals the operation conditions of the electrical conversion system (inversion and rectification). It includes many quantities. Some of these quantities are summarized by Table 19. The D-map of the output power of both the inverter and the rectifier is shown in Figure 5.11. It can be seen that inversion happen mostly during day times (5am to 8pm). During this period, the Leonics converter inverts the DC power that is produced by the PV generator. On the other hand, rectification occurs during night times in only few hours with less power compare to the inversion process.

Table 19: Power conversion system characteristics.

Quantity	Inverter	Rectifier	Units
Capacity	8	6.4	kW
Hours of Operation	4,374	75.0	h/yr
Energy Out	17,545	21.3	kWh/yr
Energy In	18,280	22.7	kWh/yr
Losses	731	1.36	kWh/yr

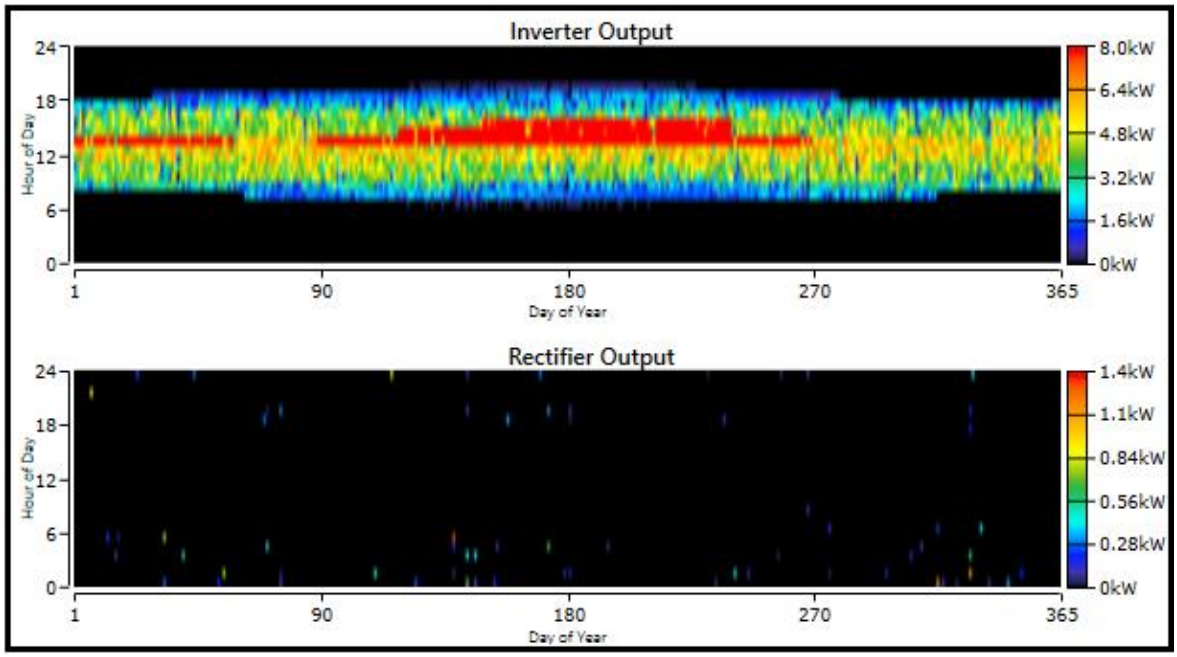

Figure 5.11: The inverter and the rectifier power output.

5.3.2.6. Electrolyzer Hydrogen Production

In the electrolyzer tab, several quantity values are tabulated. Table 20 below shows some of these values. Figure 5.12 gives the D-map of the input power to the electrolyzer. It can be seen that the maximum input power can attain 12kW and this happens usually during winter. However in summer, the input power of the electrolyzer is low. This is mainly because the hybrid system priority is to satisfy the load. In case of peak load, the electrolyzer input power turns to be zero. The hydrogen production output by the electrolyzer is depicted by Figure 5.13. Hydrogen is produced with large amounts generally in winter days. A maximum production rate of 0.25 kg/h can be reached in February. However in summer days, the maximum production rate of 0.17 kg/hr can be reached in June.

Table 20: Electrolyzer system characteristics.

Quantity	Value	Units
Rated Capacity	20.0	kW
Mean input	2.18	kW
Total input energy	19,099	kWh/yr
Capacity Factor	10.9	%
Hours of operation	3,973	h/yr
Total production	353	Kg/yr

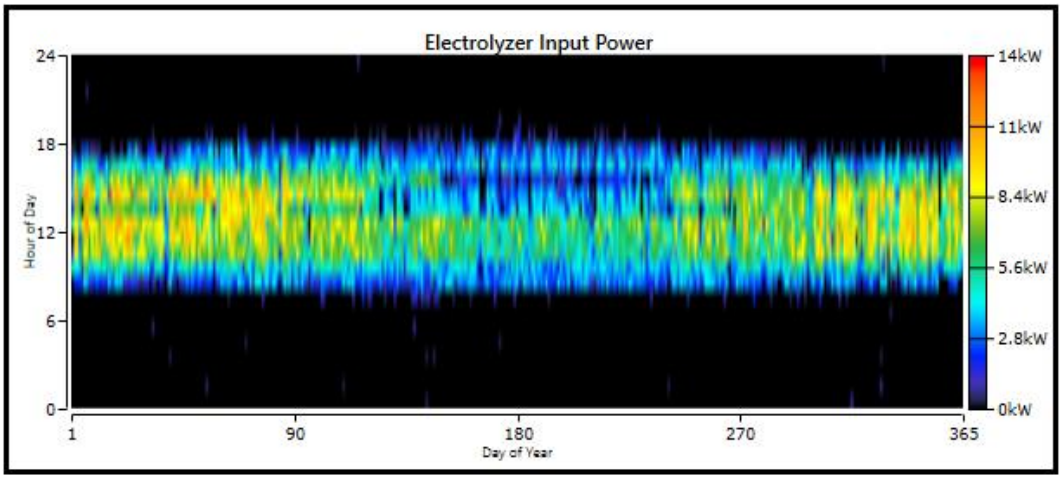

Figure 5.12: The yearly electrolyzer input power.

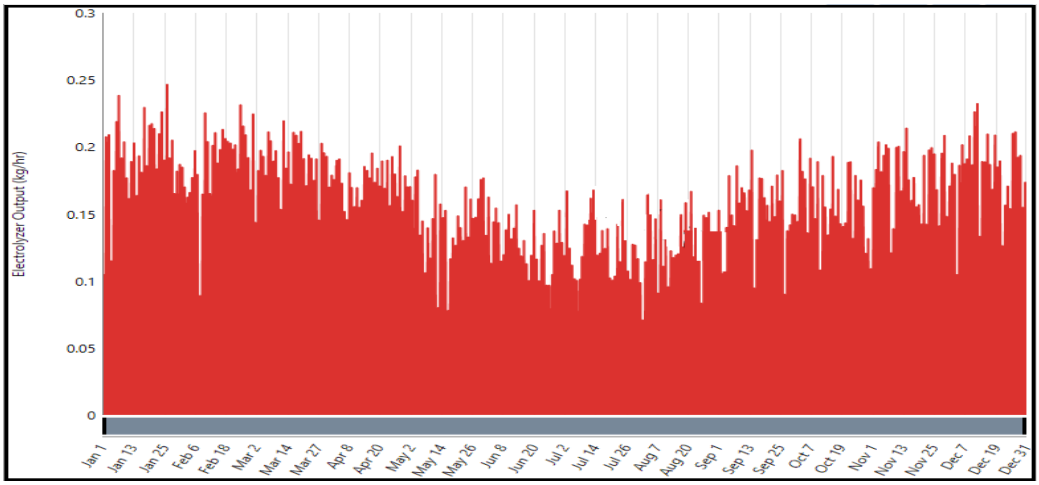

Figure 5.13: The yearly hourly electrolyzer hydrogen production.

5.3.2.7. Hydrogen System Production

The hydrogen quantity produced by the electrolyzer (353 kg) is sent directly to the hydrogen tank that contains initially a quantity of hydrogen of 19.0 kg. The energy storage capacity is found to be 12,667 kWh and the tank autonomy, which the ration of the energy storage capacity and the average electric load (6.06 kW in our case), is calculated to be 2,090 hours. Figure 5.14 shows the development in the hydrogen tank level through the entire year.

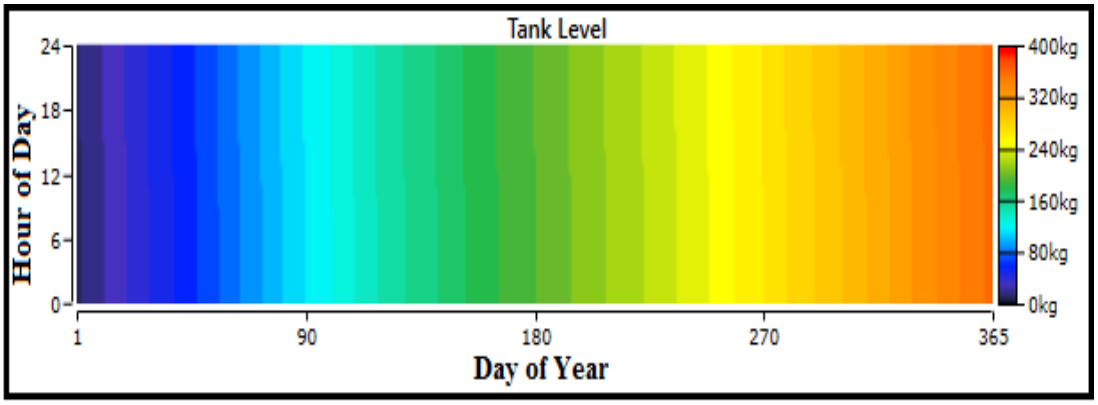

Figure 5.14: The hydrogen tank level.

5.3.3. CO_2 Emissions

5.3.3.1. System Optimization without Considering the CO_2 Emissions Effect

In our case study, solar power cannot be the sole source of electricity in a stable based-load; however, it can reduce the utilization of conventional power sources. There are many types of emissions related to electricity generation. The main emission is the CO_2 emission which is considered in this thesis. CO_2 is the largest component of the emissions from electricity generation systems which use conventional power sources.

The amount of CO_2 generated by the diesel generators is 35,386 kg. In this section, the cost penalty of the pollutant emissions is not accounted. Further analysis is done in the next section.

5.3.3.2. System Optimization Considering the CO_2 Emissions Effect

When designing a renewable power project, it is crucial to account the environmental benefits. Many countries around the world make many efforts to mitigate the climate change by taking severe decisions to reduce the Greenhouse Gases GHG emissions. One of these decisions is implementing policies in industries that produce GHG emissions. In many countries (mainly developed one), these industries are charged for each ton of GHG emission in order to change their behaviors to reduce these gases. Although there is no such direct charging mechanism for GHG emissions, however it is worth to design a system by taking into consideration the emissions costs.
The CO_2 price per ton varies from country to another. In our case study, we assume a value of $19.7 per ton similar to the CO_2 European emission allowances [97]. A comparison between the two cases (with and without considering the emissions) can be established using the table 21 which summarizes the main techno-economical parameters. An increase of 2.2% can be recorded in both the Net Present Cost and the LCOE.

Table 21: Comparison between systems with and without emission consideration.

Quantity	Without emission consideration	With emission consideration	Units
PV design size	21.7	26.0	kW
PV Production Share	51.3	55.8	%
Total Production	72,898	78,258	kWh/yr
Fuel Consumption	13,543	13,160	L
Gensets Hours of Operation	7043	6794	Hr
NPC	823,744	841,454	$
LCOE	0.602	0.615	$/kWh

5.4. Sensitivity Analysis

5.4.1. HOMER Pro. Sensitivity Analysis Results

According to the results obtained from Meteonorm software on the solar radiation, the average annual daily solar radiation was found to be 6.26 kWh/m^2/day. In addition, the minimum monthly daily solar radiation was 4.10 kWh/m^2/day. Sensitivity analysis is conducted for the annual average solar

radiation. Figure 5.15 shows the sensitivity plot for varying the renewable fraction and the average annual solar radiation in the ranges mentioned before. The whole plot is blue which implies that the optimal system type is the same for all the variables considered in this analysis. Hence, the optimal system type is Genset 1/Genset 2/ PV with LCOE ranges between 0.173 and 0.223$/kWh.

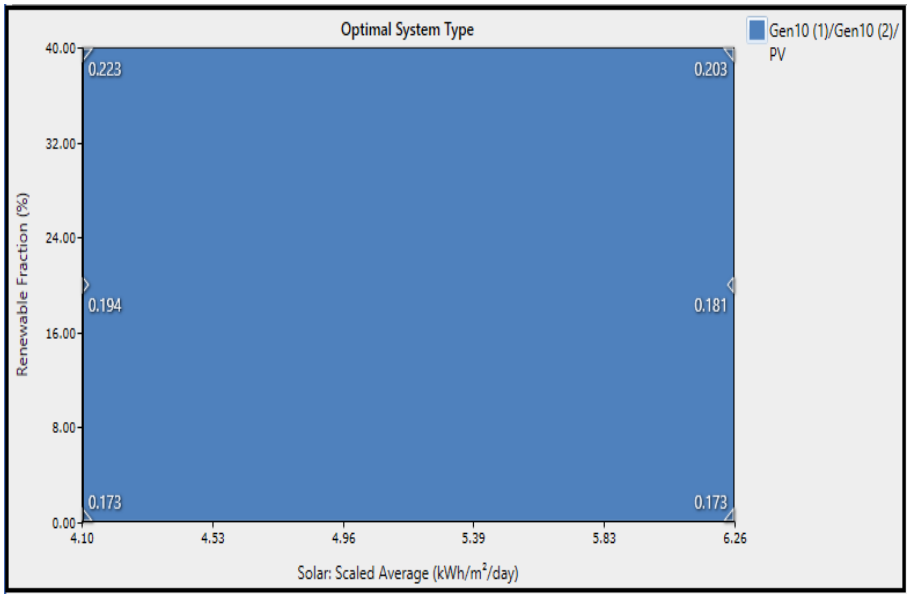

Figure 5.15: Optimal system type at different solar radiation and renewable fraction.

In this section, we only focus on the results relating to our PV-Diesel/Electrolyzer with hydrogen storage hybrid system. The values for this sensitivity variable are: 0%, 20%, and 40%. These are the three different scenarios to be taken in consideration:

- ✓ In the first case, these are no constraints on the renewable share (0%).
- ✓ In the second case, the share of renewable is aligned with the Algerian strategy tha establishes 20% of the energy production by renewable by 2025.
- ✓ In the third case, the share of renewables may reach 40% by 2040 according to the Algerian plans.

For a fixed average annual solar radiation at 6.26 kWh/m^2/day, we vary the minimum renewable fraction to be equal to 0% then 20% and finally 40%. The results of the considered hybrid system are observed:

- For a minimum renewable fraction of 0%, the results are the same as shown by the different figures given in the simulation section above since the average annual solar radiation has not been changed (6.26 kWh/m^2/day):

The winning system type: Conventional fueled system
PV system size: 21.7 kW
NPC: $823,744
LCOE: 0.602$/kWh
Maximum renewable fraction: 33.0%

- For a minimum renewable fraction of 20%, the results are similar to the previous case unless in the winning system type, in this case, it is the PV with the three gensets.
- For a minimum renewable fraction of 40%, the system configuration has changed resulting changes in the different components sizes as well as in the economical parameters:

The winning system type: PV + three gensets
PV system size: 40.0 kW
NPC: $863,683
LCOE: 0.631$/kWh
Maximum renewable fraction: 44.9%

For a fixed average annual solar radiation at 4.10 kWh/m^2/day, we do the same as previously. The results of the considered hybrid system are observed:

- For a minimum renewable fraction of 0%, the PV system design is increased. Consequently, the other components sizes as well as the economical parameters have increased.

The winning system type: Conventional fueled system
PV system size: 29.6 kW
NPC: $840,358
LCOE: 0.614$/kWh
Maximum renewable fraction: 31.3%

- For a minimum renewable fraction of 20%, the results are similar to the previous case with 0% renewable share unless in the winning system type, in this case, it is the PV with the three gensets.
- For a minimum renewable fraction of 40%, the system type is changed totally. The hybrid system in this case contains only two gensets instead of three. In addition, the PV system design size is increased to replace the size of the omitted genset.

The winning system type: PV + three gensets
PV system size: 40.0 kW
NPC: $878,073
LCOE: 0.646$/kWh
Maximum renewable fraction: 40.0%

5.4.2. Effect of Changes the Minimum Renewable Fraction and the Solar Radiation

The hybrid power system in our case contains all of the PV generator, diesel gensets, an electrolyzer and a hydrogen tank. The sensitivity analysis above yields a system type different from the system type considered in our case. Although this system is not the optimum configuration, it can still satisfy the load demand but with higher cost of energy. Figure 5.16 and Figure 5.17 illustrate how the energy cost (LCOE) and the NPC vary with the variation of the minimum renewable fraction and the average annual solar radiation.

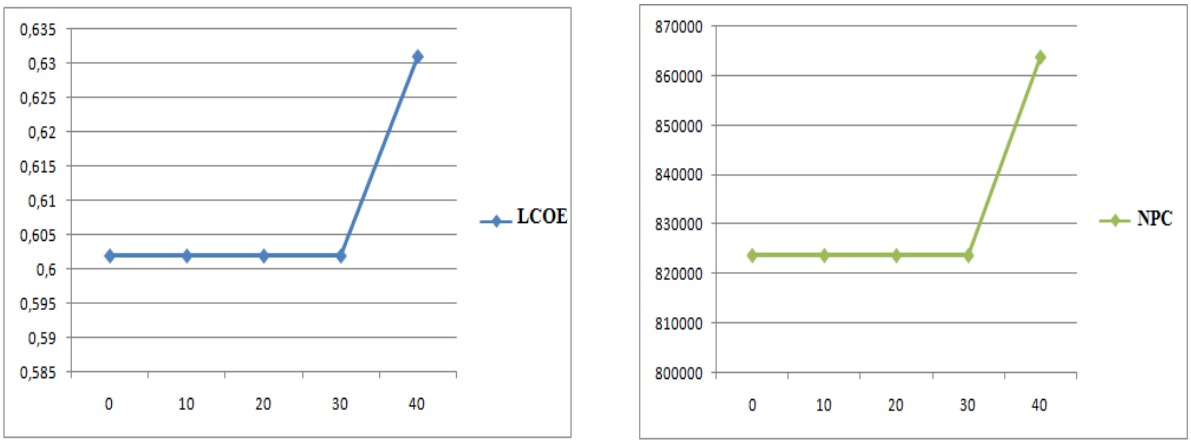

(a) (b)

Figure 5.16: (a) LCOE and (b) NPC at different minimum renewable fractions.

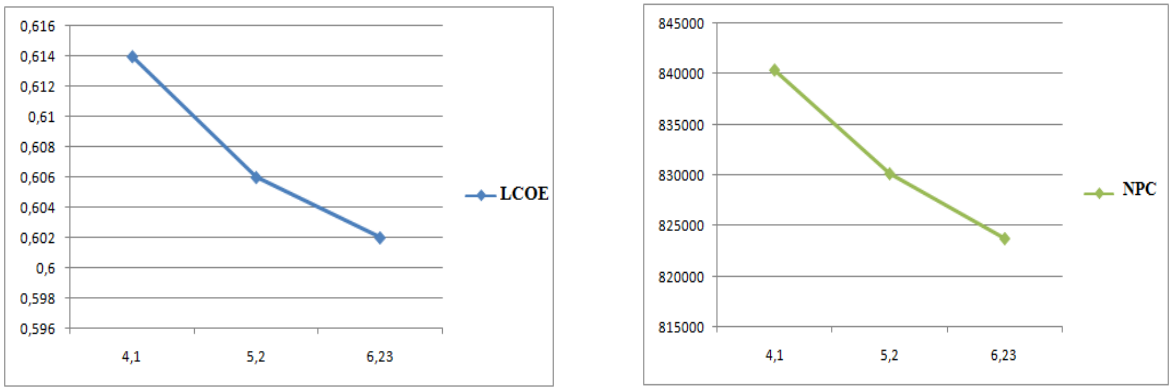

(a) (b)

Figure 5.17: (a) LCOE and (b) NPC at different annual average solar radiation.

According to Figure 5.16, we can see that both the LCOE and the NPC remain the same as the minimum renewable fraction increase from 0% to 30%. However, they increase when the minimum renewable fraction increase from 30% to 40%. The stability in both the LCOE and the NPC is explained by the constant PV system capacity (21.7kW). The considerable increase of LCOE and NPC (almost 5%) implies that the hybrid system compensates the power reduction of the diesel generators due to the increase in the PV generator capacity.

According to Figure 5.17, we can see that both the LCOE and the NPC decrease as the annual average solar radiation increases. The small drop in the NPC can be explained by the drop in the capacity of the PV generator. Hence, the capital, the replacement and the O&M costs drop as the capacity of the PV system decreases. Knowing that PV power output is proportional to the solar radiation; hence, a small change in the solar radiation does not vary the PV output power considerably. As a result, the effect of the energy cost is not significant as shown by Figure 5.17 (a) (within a range of 0.01 $/kWh) which is negligible.

The main objective of this thesis was to design, optimize and investigate an optimum size of a renewable-based hybrid power system that can generate electricity for a selected remote region in Algeria. In addition to electricity generation, hydrogen can be also produced from the excess of electricity whenever it exists and then stored in hydrogen tank. A rural village from Wilaya of Adrar called Boukazine comprising only 15 households (without including the public utilities and the small businesses) has been chosen for this analysis. The monthly hourly load consumption of these 15 households has been estimated based on information obtained from literature review. The procedure to create this average consumption profile was to estimate a consumption of a single household based on daily usage of electrical appliances. Then, a new plan to get the load consumption profile of any number of households was to multiply the single household consumption profile by a constant, fifteen (15) in our case. Then, the monthly hourly load consumption profile data were entered manually to HOMER Pro. and subjected to some random variability inputs to make them look more realistic. The average daily load consumption was 145.44 kWh/day and an approximate maximum demand of 39.8 kW has been observed mainly during midday between 11am to 3pm. The maximum demand occurred mainly in summer due to the long period use of the air conditioning systems. The variable daily load profile is depicted in Figure 4.7 has been assumed throughout the year. This load profile is severely impacted by both the seasonal variations and the day length. This latter varies significantly because the region of Adrar is located in the northern hemisphere far from the equator.

The region of Adrar receives abundance sunlight with an average annual solar radiation of 6.263 $kWh/m^2/day$. The solar data have been obtained for a software named Meteonorm which is able to generate accurate solar and temperature data for any place on Earth. In addition to solar resources, the region has the highest wind potential with 88% of the time the wind speed is above 3 m/s which yields a wind power that varies between 160 W/m^2 and 280 W/m^2 at a height of 10 m above the ground. Although the abundance of the wind potential, only solar technology has been selected in our project as the candidate resource for both electricity and hydrogen production in the hybrid power system except for the diesel genset. Not only the solar data were needed, but the capital, the operating and maintenance O&M and the replacement costs of the different system components have been identified using literature review of some organizations' websites and recent international reports done by laboratories like the National Renewable Energy Laboratory NREL. Afterward, simulations have been performed for large number of hybrid power system configurations. At the end of these simulations, the Net Present Cost NPC and the energy cost LCOE of each system configuration have been calculated for a project technical lifetime of 25 years in sake to find an option with the lowest cost.

The diesel only based power systems seem to be more economical thanks to their initial capital investments. Such systems can be installed with small capital investment when compared to renewable energy based hybrid power systems. Nevertheless, the conventional fueled systems have the highest lifetime cost due to their replacement costs and considerable O&M cost for fuels. On the other hand, hybrid systems require higher capital investments but lower O&M costs. The lifetime cost analysis, which can be done by comparing the different simulated system types cash flows, states that the conventional fueled technology is less economical than the renewable based hybrid system. The final decision on the optimum configuration selection has been taken based on several criteria. Meeting the load demand, the photovoltaic system maximum share in electricity production, the maximum hydrogen quantity produced and the system configuration with least NPC and LCOE were the main criteria considered that can help in the optimum configuration selection. According the simulation results, the optimum system configuration for both electricity and hydrogen generation was found to be:

PV capacity	21.7kW
MPPT converter	16.0kW
3 Diesel generator	10kW each
Inverter	8.00kW
Electrolyzer	20.0kW
Hydrogen tank	380 kg

The diesel generators were required to generate a total of 48.76% of the total system energy generation. Since there was no power source other than solar PV, the operations hours of the diesel gensets were find to be considerable. This was mainly in order to compensate the absence of solar energy during night times and solve the issue of peak load especially during summer. On the other hand, the solar PV generator produced 51.24% of the total system energy generation. Part of this energy was used by the electrolyzer to produce hydrogen where a total production of hydrogen of 353 kg/yr was recorded. The electrolysis process was performed mainly during day time (5am to 8pm). This is due to the existence of excess of electricity in that period. A 20.0kW rated capacity electrolyzer could reach a maximum input of power of 13.3kW. The maximum renewable fraction of the optimized hybrid system was found to be 33.0%. Hence, the diesel generators were required to supply 67% of the total load. HOMER Pro. estimated the capacity shortage to be only 0.188% which implies only 10 hours of power outage during a year. Homer Pro, does not take in consideration all of the region remoteness, the power interruptions due to the harsh environment or the shut downs for maintenance in the calculation of such parameter. Otherwise, the power outage hours would increase significantly.

The Load Following has been found as the optimal dispatch strategy. Under such strategy, the diesel genset produces enough power to satisfy the load whenever it is required. As a result, the system shortage capacity was lowered to be at its minimum (0.188%). The Cycle Charging dispatch strategy was excluded completely by HOMER Pro. because the hybrid system under this study did not contain any storage capacity like batteries. The HOMER Pro. simulations showed that the hours of operation of the diesel gensets 1, 2 and three were 6,095, 782 and 167, respectively. Hence for a project lifetime of 25 years, the lifetime operating hours of each diesel generator are 152,375, 19,550 and 4175, respectively. Consequently, the operating hours of both genset 1 and 2 throughout the entire project lifetime is higher than their lifetime operating hours which is 15,000 hrs. The diesel genset 1 was required to be replaced at least each 2 years. Genset 2 was required to be replaced in year 20. Genset 3 does not need to be replaced.

The HOMER Pro. simulation results revealed that the hybrid power system can supply electricity at a cost of energy of 0.602 $/kWh, which is almost nine (9) times the cost of energy from the national grid (0.07 $/kWh). From the sensitivity analysis, it has been demonstrated the system can meet the demand with higher energy cost when using greater minimum renewable fraction. On the other hand, there were no significant changes in the LCOE when considering the variations in the annual average solar radiations between 4.2 and 6.26 kWh/m^2/day. The lifetime cost analysis of the system has demonstrated that the project requires a capital investment of $456,283, where 83% of this capital cost represents only the capital cost of the hydrogen tank. The replacement and the O&M costs were estimated to be $118,051.55 and $207,695.50, respectively. The lifetime fuel and the salvage costs were found to be $69,888.35 and $28,174.00, respectively. Overall, the project NPC is worth $823,744.56.

The optimized hybrid power system uses three diesel generators than have a total hours operation of 7044 hours/years. The presence of this conventional technology yields a considerable emissions of pollutants mainly CO_2. Simulation results have been shown that the three diesel gensets can generate 35,386 kg of CO_2. The emission penalty was not taken into consideration in this work. However, further analysis has shown that the implication of such penalties may increase the system NPC and LCOE on one hand. On the other hand, the diesel generators hours of operation may be reduced; hence, reducing the fuel consumed. The quantity of the CO_2 emitted would be reduced if the system was integrated with a clean, efficient and emission-free power production technology like Fuel Cell which can be powered by the hydrogen produced locally.

One of the most important aspects of the considered hybrid power system is the presence of the hydrogen system. This latter can be seen as a renewable energy source and bountiful in supply. Hydrogen is a clean and non-toxic energy; it does not cause any harm to human health. This feature makes it the most preferred fuel compared to other sources of fuels. In addition, hydrogen energy is very efficient and hence an ideal fuel source for energy production than can be used for different applications. At national level, hydrogen technology can offer several benefits like diversifying the national energy mix.
The hybrid system in this project was able to produce a total weight of 353 kg of hydrogen. The Net Calorific Value (or the Low Heat Value LHV) and the Gross Calorific Value (or High Heat Value HHV) of hydrogen at a temperature of 25°C and a pressure of 1 atm are 119.93 MJ/kg and 141.88 MJ/kg, respectively. Thus, the energy that can be release by the total weight produced of hydrogen is 30,342.3 MJ (or 11,760.7 kWh) using the LHV and 50,083.6 MJ (or 13,912.2 kWh) using HHV. This huge energy can be used to supply the load of the 15 households considered in this study for at least 80 days without using the other sources of power (neither PV nor diesel generator) during that period.

The main purpose of this study was to find a techno-economic optimum size of an off-grid hybrid power system for electrifying a small village of 15 households in region of Adar, Algeria. The optimized hybrid power system can also produce hydrogen gas using the process of electrolysis of water and store it in a bulky hydrogen tank.

First, a literature review was conducted to identify a representative load consumption profile for the village containing only fifteen households. Furthermore, the possible renewable and non-renewable energy resources that can be used to generate electricity were identified by investigating the past data on the potentials related to such energy resources. This work focused on the solar energy potential; thus, weather data of the region were needed including annual variations of solar radiation and temperature. The hybrid system under this study contains different power production, conversion and storage technologies. The basic components were identified to assure reliable production and storage of energy. These system components are: the photovoltaic PV generator, the diesel generator, the converter, the electrolyzer and the hydrogen tank. An extensive research was made in order to determine their technical performances through the modelling of each of the considered system component. After that, HOMER Pro. was used to implement the techno-economic simulation and optimization resulting in a hybrid power system of 21.7 kW PV, three 10.0 kW diesel generators, 8.00 kW converter, 20.0 kW electrolyzer and 380 kg hydrogen tank. Afterward, the hybrid system was modeled to assess the different power management strategies which yielded the Load Following to be the optimum dispatch strategy. Finally, sensitivity analysis was conducted to study the effect of uncertainties in some selected variable on the system configuration design. Both the minimum renewable fraction and annual average solar radiation were selected in the "what if" analysis.

During the analysis of the results, many figures and graphs were presented in order to show the cost summary and the performance of the different system components. A focus was given to the system component operation and management when there was a power deficit or excess. The following conclusions could be drawn based on the different system analyzes:

- ✓ Solar energy resources in the region of Adrar bear excellent potential and cost-competitive against other renewables. However, stand-alone solar energy system cannot provide a continuous supply of power due to the solar resource intermittency. Hence, conventional fueled technology can be used to solve that intermittent nature.

- ✓ At present, hybrid power systems with hydrogen storage are not cost-competitive against both stand-alone conventional fueled system and grid utility power source. However, such storage system type offers the possibility to store safer, cleaner and more efficient energy to use it in other application for electricity generation and transportation, for instance.

- ✓ From the lifetime cost analysis, the estimated levelized cost of electricity LCOE has been found to be 0.602 $/kWh. It has been also that this cost increases either with the increase in the minimum renewable fraction of the decrease in the annual average solar radiations.

- ✓ The hybrid power system under this study emits a considerable quantity of pollutant mainly carbon dioxide gas. However, this emitted quantity is largely less than the quantity of pollutant emitted by the Isolated Grids networks that use mainly diesel or natural gas. The implication of the emission penalties in designing hybrid system may increase both the Net Present Cost and the cost of energy.

- ✓ The hydrogen quantity produced by the hybrid system under this study is considerable. This hydrogen gas would be converted to other forms of energy like electricity if the system was integrated with hydrogen power generation technologies like fuel cells or hydrogen combustion engine. This represents also a perfect solution for increasing the system renewable fraction and decreasing pollutant emissions. However, the lifetime cost of the whole system will increase significantly.

While this work has addressed the techno-economic optimal sizing of a hybrid power system for both generating electricity and producing hydrogen, it can be used as a basis for diverse future work. This latter may emphasize on different sides of the system:

- ✓ Regarding the system power management, further control system options could be developed for better production, conversion and storing of energy.

- ✓ Other renewable energy technologies like wind energy would be integrated with the existent energy (solar) owing to maximize the renewable fraction and minimize the carbon dioxide emissions.

- ✓ Biomass would be also an efficient solution to produce biofuels and take the place of the conventional fuel.

[1] International Energy Agency, "Energy Access Outlook 2017: From poverty to prosperity". World Energy Special Report, 2017. https://www.iea.org/publications/freepublications/publication/WEO2017SpecialReportEnergyAccessOutlook.pdf (accessed in March 2018).

[2] Bhattacharyya, SC, 2012, "Energy Access Programmes and Sustainable Development: A Critical Review and Analysis". Energy for Sustainable Development, 16(3): 260-71.

[3] Africa Renewable Energy Initiative AREI Framework, "A Framework for Transforming Africa Towards a Renewable Energy Powered Future with Access for All." October 2015. https://info.brot-fuer-die-welt.de/sites/default/files/blog-downloads/arei_brochure_eng-revised-24-11.15.pdf

[4] Karekezi, S., and Ranja, "Renewable Energy Technologies in Africa". An Energy Training Course Handbook, ZED Books Ltd. Oxford U.K, 1997.

[5] A. Boudghene Stambouli, Survey Report on "An Overview of Different Energy Sources in Algeria" United Nations, Index 382958, 2007 http://www.jeaconf.org/UploadedFiles/Document/db8b44dd-8036-47ef-a62a-080f35315daa.pdf

[6] Abou El-Maaty M. Abd El-Aal,"Modelling and Simulation of a Photovoltaic Fuel Cell Hybrid System''. PhD thesis at University of Kassel, April 2005.

[7] P. Hollmuller, J. Joubert, B. Lachal, and K. Yvon: Evaluation of a 5 kWp Photovoltaic Hydrogen Production and Storage Installation for a Residential Home in Switzerland, International Journal of Hydrogen Energy 25, 2000, pp. 97-109.

[8] Geovanni S, Orlando L, Rafeal P, Alberto S, Sebastian P. "Analysis of the Current Methods Used to Size a Wind/Hydrogen/Fuel Cell-Integrated System: A New Perspective". International Journal of Energy. 2010;34:1042-51.

[9] Michal Nachmany, Sam Frankhauser, Jana Davidoka, "A Review of Climate Change Legislation in 99 Countries", Climate Change Legislation in Algeria. http://www.lse.ac.uk/GranthamInstitute/wpcontent/uploads/2015/05/ALGERIA.pdf (accessed in March 2018).

[10] V.O. Lydia, S. Magyari, V. L. Adriaan, "Facts and Figures: Solar Energy 2017 Northern Africa". Solar PLAZA, 2017. https://static1.squarespace.com/static/5742da5ce3214003461529ef/t/5980bc67725e25d62c229720/1501609069176/Solar+Facts+%26+Figures+Africa+2017+-+Northern+1.0.pdf

[11] Energy & Mines Book 2007. www.mem-algeria.org (accessed in March 2018).

[12] CIA World Factbook, "Country Comparison: Area", Retrieved 17 January 2013. https://www.cia.gov/library/publications/theworldfactbook/rankorder/2147rank.html

[13] Ministry of Energy, "Electricité et Gaz". http://www.energy.gov.dz/francais/uploads/2016/Energie/electricite-gaz-maj.pdf

[14] International Energy Agency, "World energy balances", IEA World Energy Statistics and Balances (database), 2018.

[15] Ministry of Energy, "Bilan Energitique National 2016", Edition 2017. http://www.energy.gov.dz/francais/uploads/2017/Bilans_et_statistiques_du_secteur/Bilan-Energetique/Bilan_Energetique_National_2016_edition_2017.pdf

[16] Stambouli A. Boudghene, "Algerian Renewable Energy Assessment: The Challenge of Sustainability", Energy Policy 39 (2011) 4507–4519.

[17] Stambouli A. Boudghene, Koinuma H, "A primary Study on a Long-Term Vision and Strategy for the Realisation and the Development of the Sahara Solar Breeder Project in Algeria". Renewable and Sustainable Energy Reviews 2012;16:591–8.

[18] D. Dib, Y. Soufi, C. Benachiba, "Renewable Energy and Energy Efficiency Program in Algeria (Investigation and Perspectives)". Conference Paper: 7th International Conference and Exhibition on Ecological Vehicles And Renewable Energies, EVER2012, At Monaco. France.

[19] Ministry of Energy and Mines of Algeria, "Renewable Energy and Energy Efficiency Program", march 2011. https://portail.cder.dz/IMG/pdf/Renewable_Energy_and_Energy_Efficiency_Algerian_Program_EN.pdf

[20] Stambouli A. Boudghene, Z. Khiat, S. Flazi, Y. Kitamura, "A Review on the Renewable Energy Development in Algeria: Current Perspective, Energy Scenario and Sustainability Issues". Renewable and Sustainable Energy Reviews 16 (2012) 4445–4460.

[21] A. Ghezloun, A. Saidane, N.Oucher, "Actual Case of Energy Strategy In Algeria and Tunisia". Energy Procedia 74 (2015) 1561 – 1570.

[22] Zakaria Bouzid et al., "Overview of Solar Potential, State of the Art and Future of Photovoltaic Installations in Algeria". International Journal of Renewable Energy Research, Vol.5, No.2, 2015.

[23] B. Mahmah, F. Harouadi, H. Benmoussa, S. Chader, M. Belhamel, A. M'Raoui, K. Abdeladim, N.A. Cherigui and C. Etievant, "MedHySol: Future Federator Project of Massive Production of Solar Hydrogen", International Journal of Hydrogen Energy, Vol. 34, N°11, pp. 4922 – 4933, 2009.

[24] Driscoll, J., Benyoub,S.,RiddifordF.,2007. "CO2 sequestration in the In Salah Gas Project". International Conference on Integrated Sustainable Energy Resources in Arid Regions, Sub: Environment 2007, Abu-Dhabi,UAE.

[25] Yashwant Sawle, S.C. Gupta, Aashish Kumar Bohre, "PV-wind hybrid system: A review with case study". Cogent Engineering (2016), 3: 1189305.

[26] S. Goel and S. M. Ali, "Cost Analysis of Solar / Wind / Diesel Hybrid Energy Systems for Telecom Tower by Using HOMER," Int. J. Renew. Energy Res., vol. 4, no. 2, 2014.

[27] G. Deb, R. Paul, and S. Das, "Hybrid power generation system," Int. J. Comput. Electr. Eng., vol. 4, no. 2, pp. 141–144, 2012.

[28] Vladimir Lazarov, Gilles Notton, Zahari Zarkov, “Hybrid Power Systems with Renewable Energy Sources – Types, Structures, Trends for Research and Development”. Eleventh International Conference on Electrical Machines, Drives And Power Systems, ELMA 2015.

[29] F. Mavromatakis, G. Makrides, G. Georghiou, A. Pothrakis, Y. Franghiadakis, E. Drakakis and E. Koudoumas, "Modeling the Photovoltaic Potential of a Site," Renewable Energy, vol. 35, pp. 1387-1390, 7, 2010.

[30] Rohella RS, Panda SK, Das P. “Perovskite Solar Cell - A Source of Renewable Green Power”. International Journal of Scientific and Research Publications. 2015;7(5).

[31] M. G. Villalva, J. R. Gazoli and E. R. Filho, "Comprehensive Approach to Modeling andSimulation of Photovoltaic Arrays," Power Electronics, IEEE Transactions on, vol. 24, pp. 1198-1208, 2009.

[32] Andrej Cotar, et al. “Photovoltaic Systems, Commissioning party: IRENA- Istrian Regional Energy Agency”; January 2012. http://www.irena-istra.hr/uploads/media/Photovoltaic_systems.pdf

[33] Solomon Teklemichael Bahta, “Design and Analyzing of an Off-Grid Hybrid Renewable Energy System to Supply Electricity for Rural Areas (Case Study: Atsbi District, North Ethiopia)”, KTH School of Industrial Engineering and Management Energy Technology EGI-2013-115MSC EKV976, 2013.

[34] K. Ranabhat, L. Patrikeev, K. Andrianov, “An introduction to solar cell technology”. Journal of Applied Engineering Science 14(2016)4, 405 481-491.

[35] Miro Zeman, “Introduction to Solar Electricity," in SOLAR CELLS, TU Delft, pp. 1.1- 1.13.

[36] J. F. Baalbergen, "System Design and Power Management of a Generator-set with Energy Storage for a 4Q Drive," in Electrical Power Engineering, MSc: Delft University of Technology, October 2007.

[37] Aaron Marks, “Reducing Diesel Consumption with AHI Batteries,” AQUION ENERGY, Las Vegas, Nevada, pp. 1–6, 2014.

[38] Timothy A. Loehlein, “Maintenance is One Key to Diesel Generator Set Reliability,” 2007. http://cset.mnsu.edu/engagethermo/documents/Cummins%20Generator%20System%20Maintenance.pdf

[39] K.M. Iromi Udumbara Ranaweera, “Techno-Economic Optimum Sizing of Hybrid Renewable Energy System: Rural Electrification in Sri Lanka”, Master Thesis at Faculty of Engineering and Science – University of Agder, 2013.

[40] Solar Energy Research Institute, “Basic Photovoltaic Principles and Methods”, Colorado: Technical Information Office, 1982, pp. 1-67.

[41] Hartmut Wendt, "Electrochemical Hydrogen Technologies, Electrochemical Production and Combustion of Hydrogen". International Journal for Hydrogen Energy, ELSEVIER, 1990.

[42] Regine Reissner, Jan Vaes Seyed, Schwan Hosseiny, "RESelyser: System Concept for a combined RES-Electrolyser plant with optimised efficiency: Part 1 Review of electrolyser system with special emphasis on the HYSOLAR system", Project RESelyser, 2015.

[43] A. Uluoglu, "Solar-Hydrogen Stand-alone Power System Design and Simulations". Master Thesis, The Graduate School of Natural and Applied Sciences of Middle East Technical University, 2010.

[44] European Commission, "Hydrogen Energy and Fuel Cells: A Vision of Our Future", Special Report, EUR 20719 EN. http://www.fch.europa.eu/sites/default/files/documents/hlg_vision_report_en.pdf

[45] Menelaos Tamvakologos, "Hybrid Energy System in Power Plant". Master Thesis University of Strathclyde, 2010.

[46] VLEEM: "Final Report: Very Long Term Energy Environment Modelling", 2002. http://www.vleem.org/PDF/annex8-monograph-distribution.pdf

[47] J. O'M. Bockris; "Energy: the Solar-Hydrogen Alternative". Sydney: Australia and New Zealand Book Co., 1975.

[48] D. Stolten; "Hydrogen and fuel cells: Fundamentals, Technologies and Applications", World Hydrogen Energy Conference, p.875-877. - ISBN 978-3-527-32711-9, May 2010.

[49] Oystein Ulleberg, "Stand-alone Power Systems For the Future: Optimal Design, Operation & Control of Solar-Hydrogen Energy Systems", Ph.D. dissertation, Norwegian University, Trondheim, 1998.

[50] A.M. Osman Haruni, "A Stand-Alone Hybrid Power System with Energy Storage". Ph.D. dissertation, Centre of Renewable Energy and Power Systems (CREPS). University of Tasmania, 2013.

[51] Matouk M. Elamari, "Optimisation of Photovoltaic-Powered Electrolysis for Hydrogen Production for a Remote Area in Libya". Ph.D. dissertation, University of Manchester, 2011.

[52] Tilak, B, Lu, P, Colman, J. Srinivasan, "Electrolytic production of hydrogen", Plenum Press, New York, 1981.

[53] Decourt, B, Lajoie, B, Debarre, R, & Soupa, "The Hydrogen-Based Energy Conversion FactBook", The SBC Energy Institute, 2014. http://www.4is-cnmi.com/presentations/SBC-Energy-Institute_Hydrogen-based-energy-conversion_FactBook-vf.pdf

[54] Jose L. Bernal-Agust n, "Simulation and Optimization of Stand-alone Hybrid Renewable Energy Systems" Renewable and Sustainable Energy Reviews (2009) pp.2111–2118.

[55] Nandi SK, Ghosh HR. “Prospect of Wind-PV-Battery Hybrid Power System as an Alternative to Grid Extension in Bangladesh”. Energy. 2010;35(7):3040-7.

[56] Qinhao Zhang, “Maximum Power Point Tracking in Photovoltaic Systems Using Model Reference Adaptive Control”. Master Thesis, Swanson School of Engineering. University of Pittsburgh, 2012.

[57] Roberto Faranda, Sonia Leva, “Energy Comparison of MPPT Techniques for PV Systems”. WSEAS Transactions on Power Systems, 1996.

[58] A. Dolara, R. Faranda, and S. Leva, “Energy Comparison of Seven MPPT Techniques for PV Systems,” J. Electromagnetic Analysis & Applications, no. 3, pp. 152–162, Sep. 2009.

[59] T. Esram and P. Chapman, “Comparison of Photovoltaic Array Maximum Power Point Tracking Techniques,” IEEE Trans. Energy Convers., vol. 22, no. 2, pp. 439– 449, Jun. 2007.

[60] M. A. Gomes de Brito, L. Galotto, Jr., L. P. Sampaio, G. de Azevedo e Melo, and C. A. Canesin, “Evaluation of the Main MPPT Techniques for Photovoltaic Applications,” IEEE Trans. Ind. Electron., vol. 60, no. 3, pp. 1156–1167, Mar. 2013.

[61] Ramos Hernanz, JA., Campayo Martín, Zamora Belver, I, “Modelling of Photovoltaic Module”. International Conference on Renewable Energies and Power Quality ICREPQ, European Association for the Development of Renewable Energies, Environment and Power Quality (EA4EPQ). Spain 2010.

[62] K.Safia, L.Meriem, "Contribution de L'effet des OTC Sur Les propriétés des Cellules Solaires: Application aux Structures: p-Si/n-Zno:Al", Master thesis, University of Ferhat Abbas, Sétif, 2011.

[63] A. Abete, E. Barbisio, F. Cane and P. Demartini, "Analysis of photovoltaic modules with protection diodes in presence of mismatching," in Photovoltaic Specialists Conference, 1990., Conference Record of the Twenty First IEEE, 1990, pp. 1005-1010 vol.2.

[64] M. C. Alonso-García and J. M. Ruíz, "Analysis and Modelling the Reverse Characteristic of Photovoltaic Cells". Solar Energy Materials and Solar Cells vol. 90, pp. 1105-1120, 2006.

[65] J. A. Gow and C. D. Manning, "Development of a Photovoltaic Array Model for Use in Power-Electronics Simulation Studies," IEE Proceedings - Electric Power Applications, vol. 146, pp. 193-200, 1999.

[66] A. Kassis and M. Saad, "Analysis of Multi-Crystalline Silicon Solar Cells at Low Illumination Levels Using a Modified Two-Diode Model," Solar Energy Materials and Solar Cells, vol. 94, pp. 2108-2112, 2010.

[67] R. Chenni, M. Makhlouf, T. Kerbache, and A. Bouzid, "A Detailed Modeling Method for Photovoltaic Cells". Energy, vol. 32, pp. 1724- 1730, 2007.

[68] S. Silvestre and A. Chouder, "Effects of Shadowing on Photovoltaic Module Performance," Progress in Photovoltaics: Research and Applications, vol. 16, pp. 141-149, 2008.

[69] K. Ishaque, Z. Salam, and H. Taheri, "Accurate MATLAB Simulink PV System Simulator Based on a Two-Diode Model," Power Electronics vol. 11, p. 9, 2011.

[70] Y. El Basri, M. Bressan, L. Seguier, "A Proposed Graphical Electrical Signatures Supervision Method to Study PV Module Failures". Solar Energy 116 (2015) 247–256.

[71] K. h. Chao, S. Ho, M. Wang. "Modeling and Fault Diagnosis of a Photovoltaic System". Electric Power Systems Research 78 (2008), pp. 97-105.

[72] Ismail, M., Moghavvemi, M., & Mahlia, T. (2013), "Techno-Economic Analysis of an Optimized Photovoltaic and Diesel Generator Hybrid Power System for Remote Houses in a Tropical Climate". Energy Conversion and Management, 69, 163-173.

[73] John A. Duffie, William A. Beckman, "Solar Engineering of Thermal Processes". Fourth Edition Published by John Wiley & Sons, Inc., 2013.

[74] D. M. Tobnaghi, R. Madatov and d. naderi, "The Effect of Temperature on Electrical Parameters of Solar Cells," pp. 1-4, December 2013.

[75] J. W. BISHOP, "Computer Simulation of the Effects of Electrical Mismatches in Photovoltaic Cell Interconnection Circuits", Solar Cells, vol.25, pp 73-89, 1988.

[76] Guiseppe Marco Tina, "Simulation Model of Photovoltaic and Photovoltaic/Thermal Module/String under Non-uniform Distribution of Irradiance and Temperature". J. Sol. Energy Eng 139 (2), 021013, 2016.

[77] Md. Aminul Islam, "Power Management and Control for Solar-Wind-Diesel Stand-alone Hybrid Energy Systems". Master Thesis, Saint Mary's University, Halifax, Nova Scotia.

[78] Rodolfo DL, Jose LBA, "Multi-objective design of PV–wind–diesel–hydrogen–battery systems". Renewable Energy 2008; 33(12):2559–2572.

[79] Weldemariam. "Genset-Solar-Wind Hybrid Power System of Off-grid Power Station for Rural Applications". Electrical Power Engineering. Delft: Delft University of Technology, 2010.

[80] A. Ursa and P. Sanchis, "Static-Dynamic Modelling of the Electrical Behavior of a Commercial Advanced Alkaline Water Electrolyser," International Journal of Hydrogen Energy, vol. 37, no. 24, Dec. 2012.

[81] A. S. Tijani, N. A. B. Yusup, and A. H. A. Rahim, "Mathematical Modeling and simulation analysis of advanced alkaline Electrolyzer system for hydrogen production," Procedia Technology, vol. 15, pp. 798-806, 2014.

[82] Y. S. Kumara De Silva, "Design of an Alkaline Electrolysis Stack". Master Thesis, University of Agder, 2017.

[83] O. Ulleberg, "Modeling of Advanced Alkaline Electrolyzers: A System Simulation Approach". International Journal of Hydrogen Energy 2003; 28:21–33.

[84] E. Tzimas, C.Filiou, S.D. Peteves and J.-B. Veyret Petten, "Hydrogen Storage: State of The Art and Future Perspective", The Netherlands pp:15.

[85] J.M Smith, H C Van Ness, M M Abbott, "Introduction to Chemical Engineering Thermodynamics". The McGraw Hill Chemical Engineering Series, 7th edition, McGraw-Hill Higher Education, 2005.

[86] Ulleberg Ø., "Stand-Alone Power Systems for the Future: Optimal Design, Operation & Control of Solar-Hydrogen Energy Systems". PhD thesis, Norwegian University of Science and Technology, Trondheim, 1998.

[87] Tom Lambert, "Micropower System Modelling with HOMER". Mistaya Engineering Inc, National Renewable Energy Laboratory, 2006. https://www.homerenergy.com/documents/MicropowerSystemModelingWithHOMER.pdf

[88] Homer Energy. (2016). HOMER Pro Version 3.7 User Manual. Available at: https://www.homerenergy.com/pdf/HOMER_v3.7%20manual_updated-08-11.pdf (accessed : 23.04.2018).

[89] Trading Economics site, https://tradingeconomics.com/algeria/interest-rate (Accessed July 2018).

[90] International Monetary Fund, "Algeria". Staff Report for the 2014 Article IV Consultation, November 2014. https://www.imf.org/external/pubs/ft/scr/2014/cr14341.pdf

[91] National Oceanic and Atmospheric Administration, "Adrar Climate Normals, 1961-1991". Retrieved October 21st, 2016.

[92] The National Agency for the Promotion and Rationalization of the Use of Energy, "Consommation Energétique Finale en Algerie 2015". Edition 2017. http://www.aprue.org.dz./documents/PUBLICATION%20CONSOMMATION%20ENERGETIQUE%20FINALE%202015.pdf

[93] A. IDDA, S. BENTOUBA, ''Perspectives de l'Energie Solaire Photovoltaïque pour le remplacement du Diesel dans les Réseaux Isolés du Sud Algérien'', Conference Paper, 1st International Symposium on Hydrocarbons, Energies and Environment, University of Ouargla, Algeria, 2014.

[94] J. A. Coakley, "Reflectance and Albedo, Surface". In Encyclopedia of Atmospheric Sciences; Holton, J.R., Ed.; Academic Press: Oxford, UK, 2003; pp. 1914–1923. http://www.curry.eas.gatech.edu/Courses/6140/ency/Chapter9/Ency_Atmos/Reflectance_Albedo_Surface.pdf

[95] IRENA, "Renewable Power Generation Cost 2017". International Renewable Energy Agency, 2018.

[96] IEA. 2015a. Technology Roadmap for Hydrogen and Fuel Cells, OECD/IEA, Paris, France. https://www.iea.org/publications/freepublications/publication/TechnologyRoadmapHydrogenandFuelCells.pdf. (Accessed July 2018).

[97] Business Insider, https://markets.businessinsider.com/commodities/co2-emissionsrechte (Accessed July 2018).

[98] https://kids.britannica.com/students/assembly/view/52522

[99] https://www.electricaltechnology.org

[100] www.cleanenergyreviews.info

[101] http://www.pveducation.org

[102] www.pvpmc.sandia.gov

[103] http://www.itacanet.org

[104] http://www.alternative-energy-tutorials.com

Appendix A

Month	Daily Load (kWh)	Hours																						Hourly Average Demand
		0	1	2	3	4	5	6	7	8	9	10	11	12	13	14	15	16	17	18	19	20	21	22	23	
January	8,232	0,3	0,3	0	0,3	0,3	0,3	0	0,444	0,4	0,3	0,3	0,36	0,47	0,91	0,3	0,3	0,36	0,36	0,33	0,532	0,364	0,542	0,3	0,3513333333
February	8,532	0,3	0,3	0	0,3	0,3	0,3	0	0,444	0,4	0,3	0,3	0,36	0,47	0,91	0,3	0,3	0,36	0,36	0,33	0,532	0,664	0,542	0,3	0,3638333333
March	8,412	0,3	0,3	0	0,3	0,3	0	0,444	0,4	0,3	0,3	0,3	0,36	0,97	0,41	0,3	0,3	0,36	0,36	0,33	0,412	0,664	0,542	0,3	0,3588333333
April	8,592	0,3	0,3	0	0,3	0,3	0	0,444	0,4	0,4	0,3	0,3	0,36	0,47	0,91	0,3	0,3	0,36	0,36	0,33	0,492	0,664	0,542	0,3	0,3663333333
May	10,872	0,3	0,3	0	0,3	0,3	0,444	0,36	0,34	0,4	0,3	0,3	0,36	0,47	1,41	1,8	0,3	0,36	0,36	0,33	0,492	0,644	0,542	0,3	0,4613333333
June	12,532	0,3	0,3	0	0,3	0,3	0	0,444	0,4	0,3	0,3	0,3	0,36	0,47	1,91	1,3	1,3	0,36	0,36	0,33	0,532	1,664	0,542	0,3	0,5305
July	12,532	0,3	0,3	0	0,3	0,3	0	0,444	0,4	0,3	0,3	0,3	0,36	0,47	1,91	1,3	1,3	0,36	0,36	0,33	0,532	1,664	0,542	0,3	0,5305
August	11,532	0,3	0,3	0	0,3	0,3	0	0,444	0,4	0,3	0,3	0,3	0,36	0,47	1,91	1,3	1,3	0,36	0,36	0,33	0,532	0,664	0,542	0,3	0,4888333333
September	10,532	0,3	0,3	0	0,3	0,3	0	0,444	0,4	0,3	0,3	0,3	0,36	0,47	1,41	1,8	0,3	0,36	0,36	0,33	0,532	0,664	0,542	0,3	0,4471666667
October	8,532	0,3	0,3	0	0,3	0,3	0	0,3	0,444	0,4	0,3	0,3	0,36	0,47	0,41	0,8	0,3	0,36	0,36	0,33	0,532	0,664	0,542	0,3	0,3638333333
November	8,492	0,3	0,3	0	0,3	0,3	0	0,3	0,444	0,4	0,3	0,3	0,36	0,47	0,41	0,8	0,3	0,36	0,36	0,33	0,492	0,664	0,542	0,3	0,3621666667
December	8,532	0,3	0,3	0	0,3	0,3	0	0,3	0,444	0,4	0,3	0,3	0,36	0,47	0,41	0,8	0,3	0,36	0,36	0,33	0,532	0,664	0,542	0,3	0,3638333333
Average daily load	9,777																								

Monthly hourly estimated load profile of a single household.

Month	Daily Load (kWh)	Hours																						
		0	1	2	3	4	5	6	7	8	9	10	11	12	13	14	15	16	17	18	19	20	21	22	23
January	123,48	4,5	4,5	0	4,5	4,5	4,5	0	6,66	6	4,5	4,5	5,4	7,05	13,65	4,5	4,5	5,4	5,4	5,4	4,95	7,98	5,46	8,13	4,5
February	127,98	4,5	4,5	0	4,5	4,5	4,5	0	6,66	6	4,5	4,5	5,4	7,05	13,65	4,5	4,5	5,4	5,4	5,4	4,95	7,98	9,96	8,13	4,5
March	126,18	4,5	4,5	0	4,5	4,5	0	6,66	6	4,5	4,5	4,5	5,4	7,05	6,15	4,5	4,5	5,4	5,4	5,4	4,95	6,18	9,96	8,13	4,5
April	128,88	4,5	4,5	0	4,5	4,5	0	6,66	6	6	4,5	4,5	5,4	7,05	13,65	4,5	4,5	5,4	5,4	5,4	4,95	7,38	9,96	8,13	4,5
May	163,08	4,5	4,5	0	4,5	4,5	6,66	5,4	5,1	6	4,5	4,5	5,4	7,05	21,15	27	4,5	5,4	5,4	5,4	4,95	7,38	9,66	8,13	4,5
June	187,98	4,5	4,5	0	4,5	4,5	0	6,66	6	4,5	4,5	4,5	5,4	7,05	28,65	19,5	19,5	5,4	5,4	5,4	4,95	7,98	24,96	8,13	4,5
July	187,98	4,5	4,5	0	4,5	4,5	0	6,66	6	4,5	4,5	4,5	5,4	7,05	28,65	19,5	19,5	5,4	5,4	5,4	4,95	7,98	24,96	8,13	4,5
August	172,98	4,5	4,5	0	4,5	4,5	0	6,66	6	4,5	4,5	4,5	5,4	7,05	28,65	19,5	19,5	5,4	5,4	5,4	4,95	7,98	9,96	8,13	4,5
September	157,98	4,5	4,5	0	4,5	4,5	0	6,66	6	4,5	4,5	4,5	5,4	7,05	21,15	27	4,5	5,4	5,4	5,4	4,95	7,98	9,96	8,13	4,5
October	127,98	4,5	4,5	0	4,5	4,5	0	4,5	6,66	6	4,5	4,5	5,4	7,05	6,15	12	4,5	5,4	5,4	5,4	4,95	7,98	9,96	8,13	4,5
November	127,38	4,5	4,5	0	4,5	4,5	0	4,5	6,66	6	4,5	4,5	5,4	7,05	6,15	12	4,5	5,4	5,4	5,4	4,95	7,38	9,96	8,13	4,5
December	127,98	4,5	4,5	0	4,5	4,5	0	4,5	6,66	6	4,5	4,5	5,4	7,05	6,15	12	4,5	5,4	5,4	5,4	4,95	7,98	9,96	8,13	4,5
Average daily load	146,655																								

Monthly hourly estimated load profile of the 15 households.

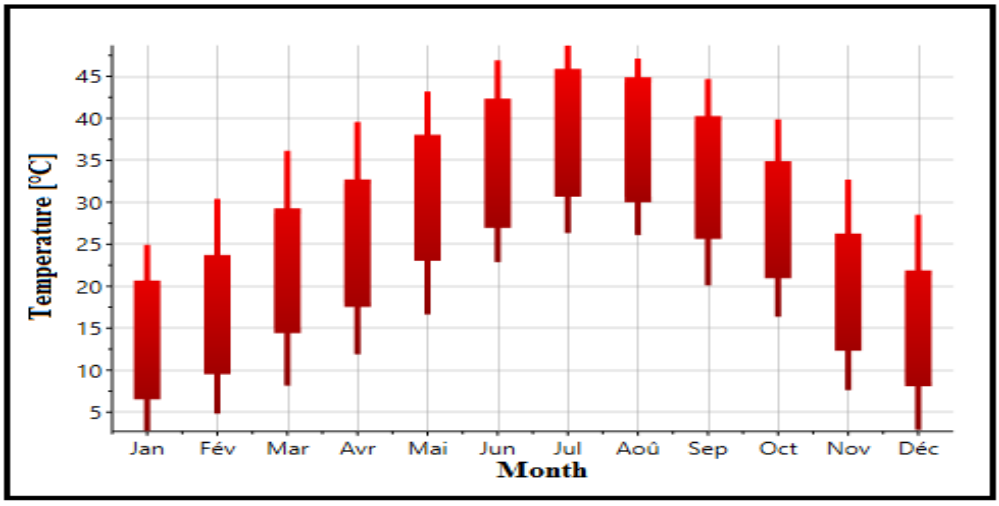

Monthly temperature data generated by Meteonorm.

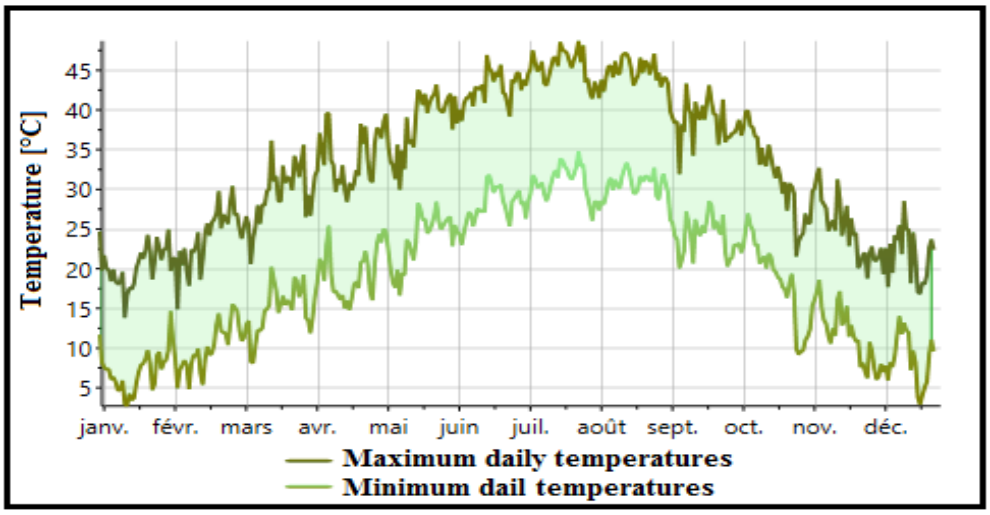

Daily temperature data generated by Meteonorm.

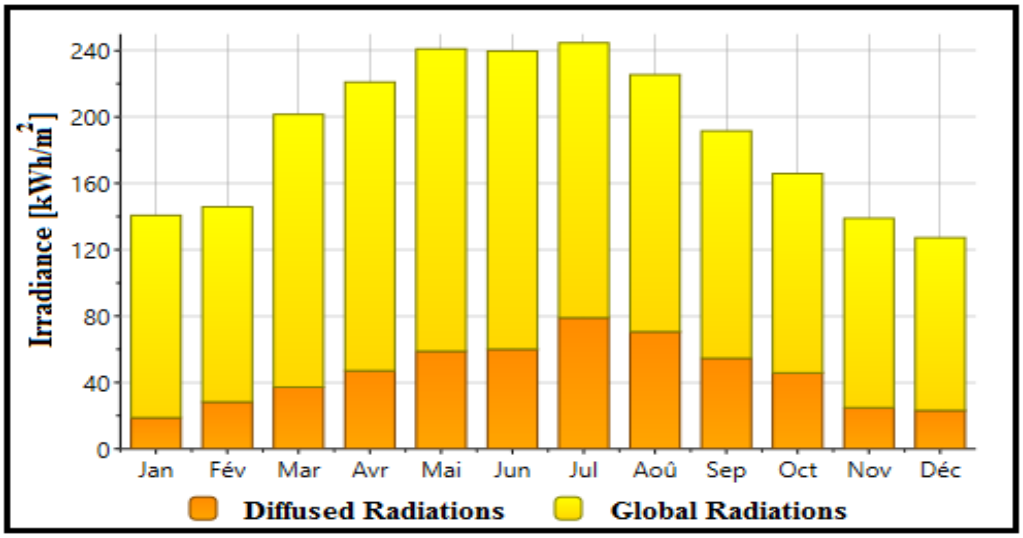

Monthly solar radiation data generated by Meteonorm.

Daily global solar radiation data generated by Meteonorm.

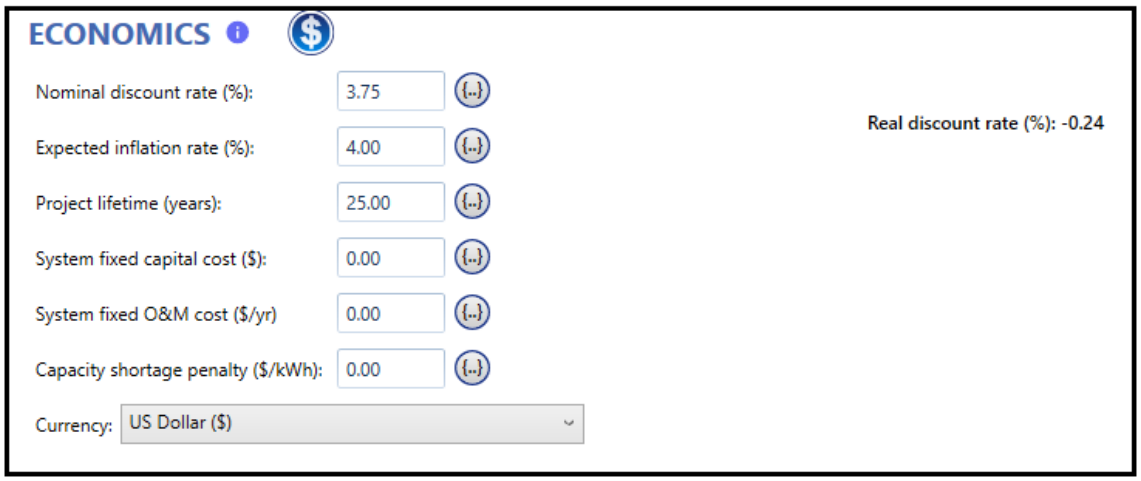

The Project Economics

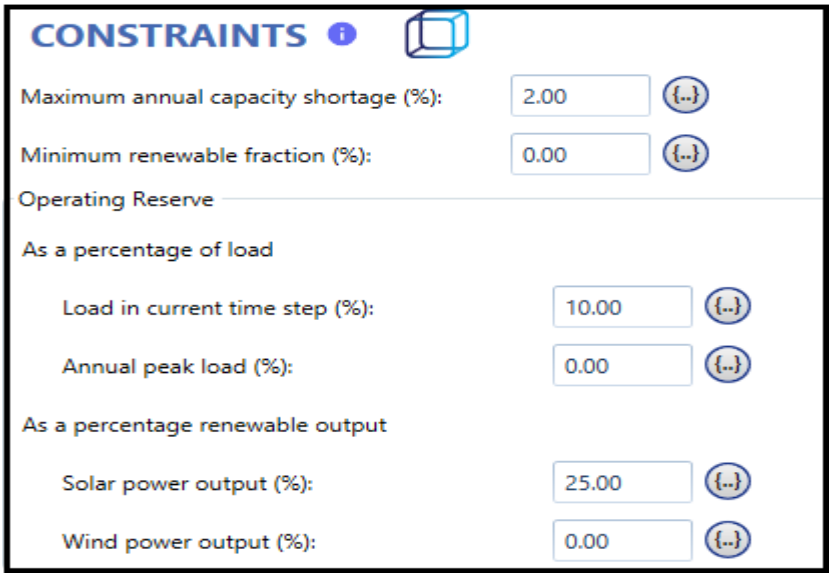

The Project Constraints